# Performance Investigation of Solar and Wind Energy Hybridized Water Pumping System for Potato Irrigation- a Case of Samira Village

**Kemer Hussien Dinsa**

**A Thesis Submitted to the department of Thermal and Aerospace Engineering, School of Mechanical, Chemical and Materials Engineering, Presented in partial fulfillment of the requirement for the degree of Master of Science in Thermal Engineering**

**Office of Graduate Studies**
**Adama Science and Technology University**

**Adama, Ethiopia**

**August, 2021**

# Performance Investigation of Solar and Wind Energy Hybridized Water Pumping System for Potato Irrigation - a Case of Samira Village

**Kemer Hussien Dinsa**

**Advisor: Dr. Addisu Bekele**

**A Thesis Submitted to the department of Thermal and Aerospace Engineering, School of Mechanical, Chemical and Materials Engineering, presented in partial fulfillment of the requirement for the degree of Master of Science in Thermal Engineering**

**Office of Graduate Studies**

**Adama Science and Technology University**

**Adama, Ethiopia**

**August, 2021**

# DECLARATION

I hereby declare that this Master Thesis entitled “Performance Investigation of Solar and Wind Energy Hybridized Water Pumping System for Potato Irrigation - a Case of Samira Village” is my original work. That is, it has not been submitted for the award of any academic degree, diploma or certificate in any other university. All sources of materials that are used for this thesis have been duly acknowledged through citation

| _____ | _____ | _____ |
|---|---|---|
| Name of the student | Signature | Date |

# RECOMMENDATION

I, the advisor of this thesis, hereby certify that I have read the thesis entitled "Performance Investigation of Solar and Wind Energy Hybridized Water Pumping System for Potato Irrigation - a Case of Samira Village" prepared under my guidance by Kemer Hussien submitted in partial fulfillment of the requirements for the degree of Master of Science in Thermal Engineering.

Therefore, I recommend the submission of revised version of the thesis to the department following the applicable procedures.

| _____ | _____ | _____ |
|---|---|---|
| Advisor | Signature | Date |

# APPROVAL PAGE

I, the advisor of the thesis entitled “Performance Investigation of Solar and Wind Energy Hybridized Water Pumping System for Potato Irrigation - a Case of Samira Village” and developed by Kemer Hussien; hereby certify that the recommendation and suggestions made by the board of examiners are appropriately incorporated into the final version of the thesis.

| | | |
|---|---|---|
| Advisor | Signature | Date |

We, the undersigned, members of the Board of Examiners of the thesis by Kemer Hussien have read and evaluated the thesis entitled “Performance Investigation of Solar and Wind Energy Hybridized Water Pumping System for Potato Irrigation - a Case of Samira Village” and examined the candidate during open defense. This is, therefore, to certify that the thesis is accepted for partial fulfillment of the requirement of the degree of Master of Science in Thermal Engineering.

| | | |
|---|---|---|
| Chairperson | Signature | Date |
| Internal Examiner | Signature | Date |
| External Examiner | Signature | Date |

Finally, approval and acceptance of the thesis is contingent upon submission of its final copy to the Office of Postgraduate Studies (OPGS) through the Department Graduate Council (DGC) and School Graduate Committee (SGC).

| | | |
|---|---|---|
| Department Head | Signature | Date |
| School Dean | Signature | Date |
| Office of Postgraduate Studies, Dean | Signature | Date |

# ACKNOWLEDGEMENT

First and foremost, I want to thank the Almighty Allah for giving me the patience, fortitude, and wisdom to finish this work.

Then, I would want to convey my heartfelt appreciation to Dr. Addisu Bekele, my advisor, for his unwavering professional advice and support throughout my job. I appreciate his assistance in personal problems as well as his useful advice on my career. To me, he was much more than an academic advisor.

Last but not least, I would want to express my gratitude to all of my friends for their unconditional support during my studies (especially, Genemo N. and Gebi B.).

I owe a huge debt of appreciation to my parents (particularly my father and mother) for their consistent support and encouragement throughout my years of study from elementary to higher education, as well as during the process of researching and writing my thesis. I would not have been able to fulfill my ambition without their help, and I am grateful for their constant support.

# ABSTRACT

*Arsi is one of the biggest areas of land where agriculture is the major sector, and seasonal reliance limits the sector's output. The presence of several river basins demonstrates the area's irrigation potential. The use of hybridized wind and solar energy water pumping technology for irrigation is a creative and long-term solution to this problem. The adoption of this technique can result in several advantages, including increased production by reducing reliance on rainfall and improved farmer living conditions. Performance investigation of solar and wind energy hybridized water pumping system for potato irrigation- a case of Samira in Arsi zone is presented in this study. The system was created with the geography of the location and local metrological data in consideration. The hybridized wind and solar energy system were designed to be capable of irrigating a hectare-sized potato field with a daily water need of 68$m^3$ and a total dynamic head of 91m.*

*CROPWAT is used to calculate the crop's water requirements, while HOMER is used for optimization, simulation, sensitivity, and economic analysis. The amount of energy consumed to pump water is more than the amount of water required by the users, according to the findings.*

*After optimizing using the HOMER software, a solar and wind energy hybridized system with the specifications 10kW PV, 7BWC Excel-s, 20kW converter, Total net present cost (NPC)* $111,598.50 *and Levelized cost of energy (COE) $0.00978/kWh is selected for the Samira village, Munessa woreda, which has an irrigation problem that is dependent on the season is chosen. The site's water requirement is 68$m^3$/day, which can be readily met by building two systems for the community. There is surplus electrical power from the installed hybrid system that is utilized for other purposes by utilizing a battery, and there is also excess water that we use for other purposes. So, while our goal is to tackle the irrigation water problem, the system also solves other issues.*

*Keywords: Sensitivity analysis, Renewable hybrid system, electric franklin pump, Hybrid*

# TABLE OF CONTENTS

**CONTENTS**

ACKNOWLEDGEMENT ..... i
ABSTRACT ..... ii
TABLE OF CONTENTS ..... iii
LIST OF FIGURE ..... vii
LIST OF TABLE ..... viii
LIST OF SYMBOLS AND NOMENCLATURE ..... ix
ABBREVIATION ..... x
GREEK SYMBOLS ..... xi
CHAPTER 1 ..... 1
INTRODUCTION ..... 1
1.1 Background of the study ..... 1
1.1.1 Solar photovoltaic water pumping system ..... 3
1.1.2 Wind powered water pumping system ..... 5
1.1.3 Hybridized solar photovoltaic and wind energy for water pumping ..... 6
1.2 Statement of the problem ..... 7
1.3 Objective of this thesis ..... 7
1.4 Theoretical /conceptual framework ..... 8
1.5 Scope ..... 8
1.6 Significances of the study ..... 8
CHAPTER 2 ..... 9
LITRATURE REVIEW ..... 9
2.1 Hybrid Energy water pumping systems ..... 9
2.2 Basics of wind energy ..... 10
2.2.1 Energy extracted from the wind ..... 10
2.2.1.1 Rotor swept area ..... 11
2.2.1.2 Air density ..... 11
2.2.2 Wind speed distribution ..... 12
2.2.2.1 Weibull probability distribution ..... 12
2.3 Photovoltaic power system ..... 13

2.3.1 Global Irradiation on Horizontal Surface ..... 13
2.4 Works linked to performance investigation of solar and wind energy hybridized water pumping system ..... 15
CHAPTER 3 ..... 20
METHODOLOGY ..... 20
3.1 Process model ..... 20
3.1.1 Data sources and collection method ..... 20
3.2 Water source ..... 22
3.2.1 River flow rate ..... 22
3.3 Crop water requirement ..... 24
3.3.1 Reference crop evapotranspiration ..... 26
3.3.2 Determination of irrigation water requirement:-using CROPWAT software . 26
3.4 Potatoes water requirement ..... 28
3.4.1 Net depth application of water ..... 30
3.4.2 Irrigation frequency at peak water requirement ..... 30
3.4.3 Irrigation scheduling ..... 32
3.4.3.1 Gross depth of water application ..... 32
3.5 Preliminary system capacity ..... 33
3.5.1 Design flow rate of the system ..... 33
3.5.2 Water storage sizing ..... 33
3.5.3 Selection and sizing of piping material ..... 34
3.6 Hydraulics of drip irrigation system ..... 35
3.6.1 Determining lateral total length ..... 36
3.6.2 Total discharge required ($T_{ds}$) ..... 37
3.6.3 Head loss in the mainline ..... 38
3.6.4 System layout design for drip irrigation system ..... 40
3.7 Performance characteristic of piping system ..... 41
3.7.1 Static head of the system ..... 41
3.7.2 Head loss due to friction ..... 42
3.8 Water pumping technology ..... 45
3.8.1 Types of water pump ..... 46
3.8.2 Working point ..... 47

3.8.3 Power of pump ..... 48
3.8.4 Cavitation ..... 49
3.8.4.1 Net positive suction head (NPSH) ..... 49
3.8.5 Solar insolation and PV panel location and wind velocity data ..... 51
3.8.6 Calculation of solar radiation based on the data given in a monthly average solar sunshine hour ..... 52
CHAPTER 4 ..... 55
HYBRID ENERGY SYSTEM MODELLING WITH HOMER ..... 55
4.1 Simulation ..... 56
4.2 Optimization ..... 58
4.3 Sensitivity analysis ..... 58
4.4 Physical modelling ..... 59
4.5 Loads ..... 59
4.6 Economic modelling ..... 60
4.7 HOMER software steps for wind and solar PV hybridized energy water pumping system for irrigation ..... 63
4.7.1 Create a question that HOMER can help you to answer ..... 63
4.7.2 Create HOMER file ..... 63
4.7.3 Build schematic ..... 63
4.7.4 Enter load detail ..... 64
4.7.5 Cost data and size specifications of each component ..... 66
4.7.5.1 Solar PV size and cost ..... 66
4.7.5.2 Wind turbine size and cost ..... 67
4.7.5.3 Converter size and cost ..... 72
4.7.6 Renewable energy resources assessment ..... 72
4.7.6.1 Solar energy resource ..... 73
4.7.6.2 Wind energy resource ..... 75
4.8 Add sensitivity analysis ..... 76
CHAPTER 5 ..... 78
RESULTS AND DISCUSSION ..... 78
5.1 Optimization results ..... 78
5.1.1 PV system ..... 78

5.1.1.1 Cost of PV system ..... 78
5.1.1.2 Electrical production of PV alone ..... 79
5.1.2 Hybrid wind and solar energy system ..... 80
5.2 Examine sensitivity analysis ..... 82
5.2.1 Cost summary ..... 84
5.2.2 Electrical production summary ..... 85
5.2.2.1 PV system electrical production ..... 86
5.2.2.2 Wind turbine: BWC Excel-s electrical production ..... 87
5.2.2.3 Converter ..... 88
5.2.2.4 Emission ..... 88
CHAPTER 6 ..... 89
CONCLUSION AND RECCOMENDATION ..... 89
6.1 Conclusions ..... 89
6.2 Recommendation and Future work ..... 89
REFERENCES ..... 91
APPENDIX ..... 98
Appendix A: Schedule 40 PVC Pipe Dimensions and Pressure Rating ..... 98
Appendix B: Friction Factor as a Function of Reynolds Number and Relative Roughness for Round Pipes the Moody Chart ..... 99
Appendix C: KL Values of Different Fittings ..... 100
Appendix D: Atmospheric Pressure at Different Altitudes ..... 101
Appendix E: Mollier Diagram ..... 102

# LIST OF FIGURE

Figure 1. 1: map of Arsi zone (Oromia Region Administrative Map, 2017) ..... 2
Figure 1. 2:block diagram of a stand-alone PV water pumping system (Bonsa, 2013) ..... 3
Figure 1. 3:photovoltaic cells, modules and Arrays (Svarc, 2021) ..... 4
Figure 1. 4:basic operation of photovoltaic system (Photovoltaic Cell - Energy Education, 2018) ..... 5
Figure 1. 5:components and working of a wind pump (Aized et al., 2019) ..... 6
Figure 3. 1 Process podel…….. 20
Figure 3. 2 Width and Length representation of river ..... 23
Figure 3. 3 determination of reference evapotranspiration of the farm site (Samira) ..... 27
Figure 3. 4 Simulated irrigation water requirement (for one irrigation season) ..... 28
Figure 3. 5 crop water requirements for potato (for one irrigation season) ..... 29
Figure 3. 6 schematic layout of the Gravity Drip Irrigation System ..... 41
Figure 3. 7 static head of the system ..... 42
Figure 3. 8 selected pump curve ..... 47
Figure 3. 9 system working point ..... 48
Figure 4. 1:relationship between simulation, optimization and sensitivity analysis ("Optimization of Hybrid Renewable Energy System Using Homer," 2019)……...56
Figure 4. 2:average monthly deferrable loads ..... 65
Figure 4. 3:the power curve of the selected wind turbine ..... 71
Figure 4. 4:the graph of the average daily radiation with respect to clearness index of the site ..... 75
Figure 4. 5: the graph of average monthly wind speed for Samira ..... 76
Figure 5. 1:cost summary of PV system alone……..79
Figure 5. 2:the monthly average electric production of the PV ..... 80
Figure 5. 3:shows the optimal system type as the demand and global solar radiation increase ..... 83
Figure 5. 4:cost summary of hybrid solar and wind energy system alone ..... 84
Figure 5. 5:shows the monthly average electric production of the system ..... 86

# LIST OF TABLE

Table 2. 1:the representative date of the month according to (Duffie et al., 1994) ..... 14
Table 3. 1 the time taken by floater to travel 10m ..... 24
Table 3. 2 total available water (Pereira et al., 2015) ..... 29
Table 3. 3 water holding capacity of agricultural soils (Olorunfemi et al., 2016) ..... 31
Table 3. 4 farm irrigation efficiency for different climate ..... 32
Table 3. 5 typical spacing of emitters of 2 & 4 L h-1 discharge for different soil texture (Kifle & Gebretsadikan, 2016) ..... 37
Table 3. 6 constants of friction loss equations (Source: G. Allen, 1996) ..... 39
Table 3. 7 common pipe materials ..... 43
Table 3. 8 average wind speed of the site ..... 51
Table 3. 9 the representative date of the month (Duffie et al., 1994) ..... 53
Table 3. 10 monthly average solar sun shine hour and calculated solar radiation in kwh/m2day for the Semira village ..... 54
Table 4. 1:average monthly deferrable loads of the Samira village ..... 65
Table 4. 2:the cost of the PV per kW ..... 67
Table 4. 3:the size of PV array to be considered during the simulation of the systems ..... 67
Table 4. 4:the cost of the wind turbine per 10kW ..... 70
Table 4. 5:the size of wind turbine to be considered during the simulation of the systems 70
Table 4. 6:the power extracted from selected wind turbine ..... 71
Table 4. 7:the cost of the converter with 25% tax and transportation addition from (AIMS POWER, 2020) ..... 72
Table 4. 8:the size of the converter should take into account while optimizing systems ..... 72
Table 4. 9:the average daily radiation for each of the 12 months ..... 74
Table 5. 1:net present Cost analysis for PV system alone ..... 79
Table 5. 2:the summary of the PV system alone and PV-wind hybrid system ..... 81
Table 5. 3:shows the summary of the NPC of hybridized solar and wind energy ..... 84
Table 5. 4:annualized Costs of hybrid solar and wind energy system ..... 85
Table 5. 5:shows the % of the PV and wind turbine for the productions and consumptions of the deferrable load ..... 85
Table 5. 6:shows the property of the selected PV ..... 86
Table 5. 7:shows the property of the selected wind turbine ..... 87
Table 5. 8:shows the property of the Converter selected ..... 88
Table 5. 9:shows the Emission from the systems ..... 88

# LIST OF SYMBOLS AND NOMENCLATURE

| SYMBOL | NAME | UNITS |
|---|---|---|
| $A_n$ | Cross section area | $m^2$ |
| $A_r$ | Area of Rotor | $m^2$ |
| Dn | Depth point | M |
| $d_r$ | Relative distance | M |
| $D_r$ | root zone depth | M |
| H | soil water holding capacity | mm/m |
| $h_f$ | friction losses in suction side pipework | M |
| $P_0$ | Mechanical power | W |
| $P_a$ | Air pressure | Pa |
| $p_h$ | hydraulic power | W |
| Q | Flow rate | $m^3/s$ |
| T | Temperature | $^oC$ |
| $T_{ds}$ | total lateral discharge | l/h |
| $V_I$ | Cut-In Wind Speed | m/s |
| $V_O$ | Cut-Out Wind Speed | m/s |

# ABBREVIATION

| | |
|---|---|
| FAO | Food and Agriculture Organization |
| DC | Direct current |
| PV | Photovoltaic |
| AC | Alternate current |
| PV/WT | Hybrid PV and wind energy |
| NPC | Net present cost |
| COE | Cost of energy |
| $ | Dollar |
| KWh | Kilo watt hour |
| NMSA | National Metrology Services Agency |
| PVWP | Solar water pumping |
| TDH | Total dynamic head |
| NASA | National Aeronautics and Space Administration |
| CSA | Cross section area |
| ET | Evaporation and transpiration |
| IWR | Irrigation water requirement |
| TAW | Total available water |
| NPSH | Net Positive Suction Head |
| $R_a$ | extraterrestrial radiation |

| | |
|---|---|
| NREL | National Renewable Energy Laboratory |
| CRF | capital recovery factor |
| F | Darcy friction factor |
| $R_e$ | Reynolds number |
| K | friction factor |
| $Z_r$ | effective rooting depth |
| $\Theta_{FC}$ | Field capacity |
| P | Depletion fraction, |
| TNPC | Total net present cost |
| CSA | Cross sectional area |
| AWV | Average wind velocity |
| MPPT | Maximum power point tracking |
| W/PV WP | Wind and solar PV hybrid energy water pumping |

# GREEK SYMBOLS

| | |
|---|---|
| $\delta$ | Sun declination angle [$^o$] |
| $\varepsilon$ | Emissivity [-] |
| $\Theta_Z$ | Zenith angle [$^o$] |
| $\rho_w$ | Density of water [kg/m$^3$] |
| $\rho_a$ | Density of air [kg/m$^3$ ] |
| $\zeta$ | Stefan Boltzmann constant [W/m$^2$ .K$^4$ ] |

| | |
|---|---|
| $\Phi$ | Latitude of location[$^{o}$ ] |
| $\varepsilon$ | Emissivity |
| $\Omega$ | Solar hour angle [$^{o}$] |
| $\eta$ | Efficiency |
| $\varepsilon_r$ | relative roughness |

# CHAPTER 1

# INTRODUCTION

## 1.1 Background of the study

Improving the agricultural sector is critical for a country's growth. This can be accomplished by reducing the agricultural sector's seasonal reliance, which implies that daily water supply through various mechanisms is needed. According to Ethiopia's Central Statistical Agency, the country's total projected population is 100 million people, with 85 percent of the population living in rural areas and relying on subsistence agriculture (agribusiness) (| FAO | Food and Agriculture Organization of the United Nations, 2012). Despite the fact that agriculture is the most important industry, rain-fed agriculture covers the majority of Ethiopia's cultivated land. Water is a driving force for the transportation of nutrients in various plants and plays an important role in photosynthesis and cooling by transpiration. As a result, for optimal crop production, adequate soil moisture availability in the crop root zone is important. Precipitation provides available soil moisture for crops, which is then consumed by evapotranspiration or crop water use. As a result, an irrigation system used to provide water for irrigation should be developed.

Irrigation is one of the well-established methods on numerous farms. It is practiced on various levels around the world. It allows the diversification of crops while increasing crop yields. Subsequently, the pumps are used as a means of delivering water to the farm, various systems are engaged for this purpose and classified depending on energy input as manually driven pumps, combustion engine driven pumps, and solar/wind-powered pumps.

In Ethiopia, many agricultural practices depend on rainfall. Even those areas which have irrigation system uses manually driven pump which is inefficient to cover large farmlands which in turn results in the reduction of production. Some other irrigation system uses a combustion engine to drive the pump which results in higher running cost and additional maintenance and repair expenses (Hussein, 2019). Besides that, it results in environmental pollution. Therefore, by employing renewable energy sources wind and solar hybridized powered irrigation system not only improves the efficient use of energy, but also reaches the off-grid rural farm areas.

While considering the development of one's country, energy is one of the key points. Hybrid wind and solar energy water pumps are most often applied when utility power is not readily available. In Ethiopia, about 73.44 percent of the population lives without access to electricity (World Bank Annual Report, 2015). The site selected for this work is also a rural area without access to electricity found in Oromia Region, the specific area is Samira.

Samira is a small rural area in the East Arsi zone found at 24Km from the electric Power from Kersa and 65Km from Shashamane city. With a geographical coordinates of latitude 7.20592 and longitude 38.60801. Samira is well known for the production of sugarcane and potato. Though Samira has been endowed with the Teji River, a lack of suitable mechanisms for utilizing water efficiently and at the appropriate time has a negative impact on agricultural production.

Teji River is a tributary of the Lagano, located in East Oromia, Arsi zone in Samira village. It flows year-round with sufficient capacity. Lakeda, Damu, and Itica are feeder rivers of major size. Other minor tributaries also contribute a considerable size of water. The river flows west through Damu, then it meets with Lagano.

Figure 1. 1: map of Arsi zone (Oromia Region Administrative Map, 2017)

### 1.1.1 Solar photovoltaic water pumping system

This section will explain the overall working concept of PV, its components, and the materials from which PV may be made, all of which are crucial to understand before using PV to pump water. A solar water pumping system consists of four main parts: the pump set, pump controller, the solar electric panels and a storage unit.

A typical PV pumping system consists of a photovoltaic cell array, a power conditioner and the load, Figure 1.2. Other accessories that form the PV system are the energy storage, cabling and protection. The power conditioning stage consists of a power converter associated with a suitable control unit. The load, for a pumping system, consists of a motor and a pump.

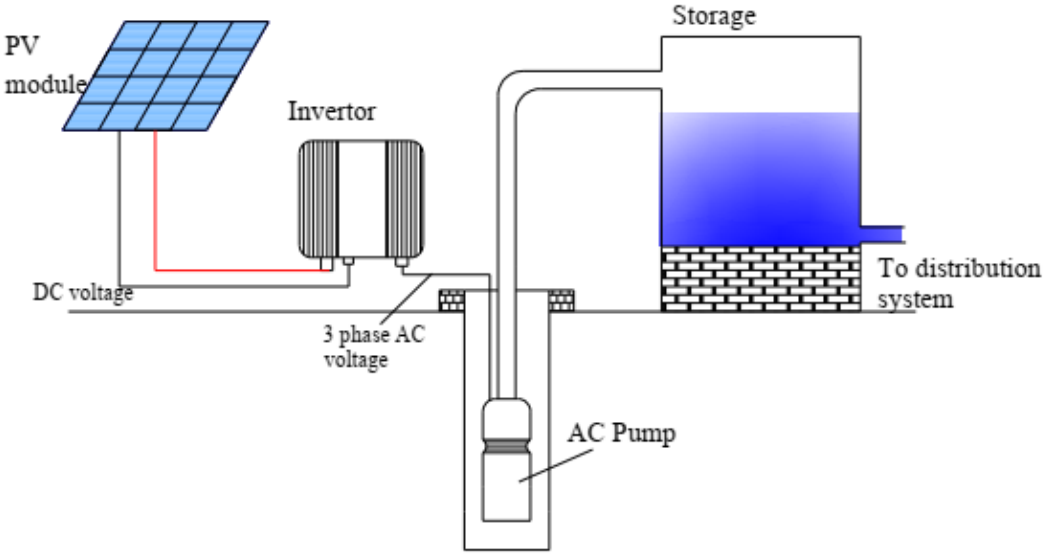


Figure 1. 2:block diagram of a stand-alone PV water pumping system (Bonsa, 2013)

**PV Module**

To make modules, PV manufacturers use crystalline silicon wafers or thin film technologies. In the former, single crystal silicon (single-Si), polycrystalline silicon (poly-Si) or ribbon silicon (ribbon-Si) wafers are made into solar cells. Solar cell manufacturers then assemble the cells into modules or sell them to module manufacturers for assembly. Because the first important applications of PV involved battery charging, most modules in the market are designed to deliver direct current (DC) at slightly over 12 Volts. A typical

crystalline silicon module consists of a series circuit of 36 cells, encapsulated in a glass and plastic package for protection from the environment. This package is framed and provided with an electrical connection enclosure, or junction box. Typical conversion (solar energy to electrical energy) efficiencies for common crystalline silicon modules are in the 11 to 15% range (Svarc, 2021).

Solar Array is the full collection of all solar photovoltaic generators for a larger pumping system several dozens of PV modules are interconnected. They are mounted on ground installations using a simple frame that holds the modules at a fixed tilt angle towards the sun.

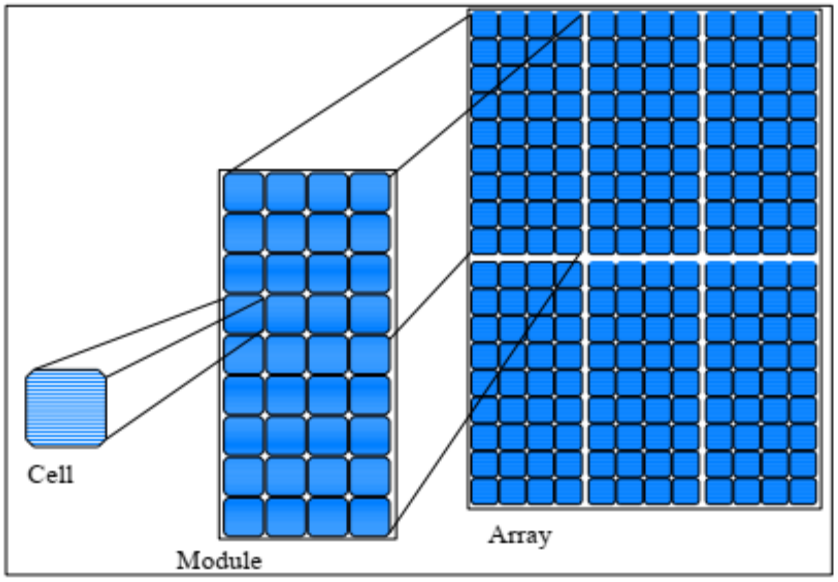


Figure 1. 3:photovoltaic cells, modules and Arrays (Svarc, 2021)

The direct conversion of solar irradiance into electrical current is done by the solar generator. It consists of mounting units called panels which again consist of solar modules. Modules are made of solar cells in which the conversion is performed as shown in Figure 1-4.

When sunlight impinges on a solar cell, the positive charge carriers (the holes) and the negative charge carriers (electrons) appear in pairs. If those pairs are able to reach the electric field before they recombine (meaning to reunite and, hence, to neutralize themselves). They are ultimately separated, with the electrons moving toward the front

wall (the n-type layer), where they collect on metallic contact fingers mounted above the surface and then return, by way of the external circuit, to the full-face, metal coated back wall of the cell, where they ultimately recombine with the holes.

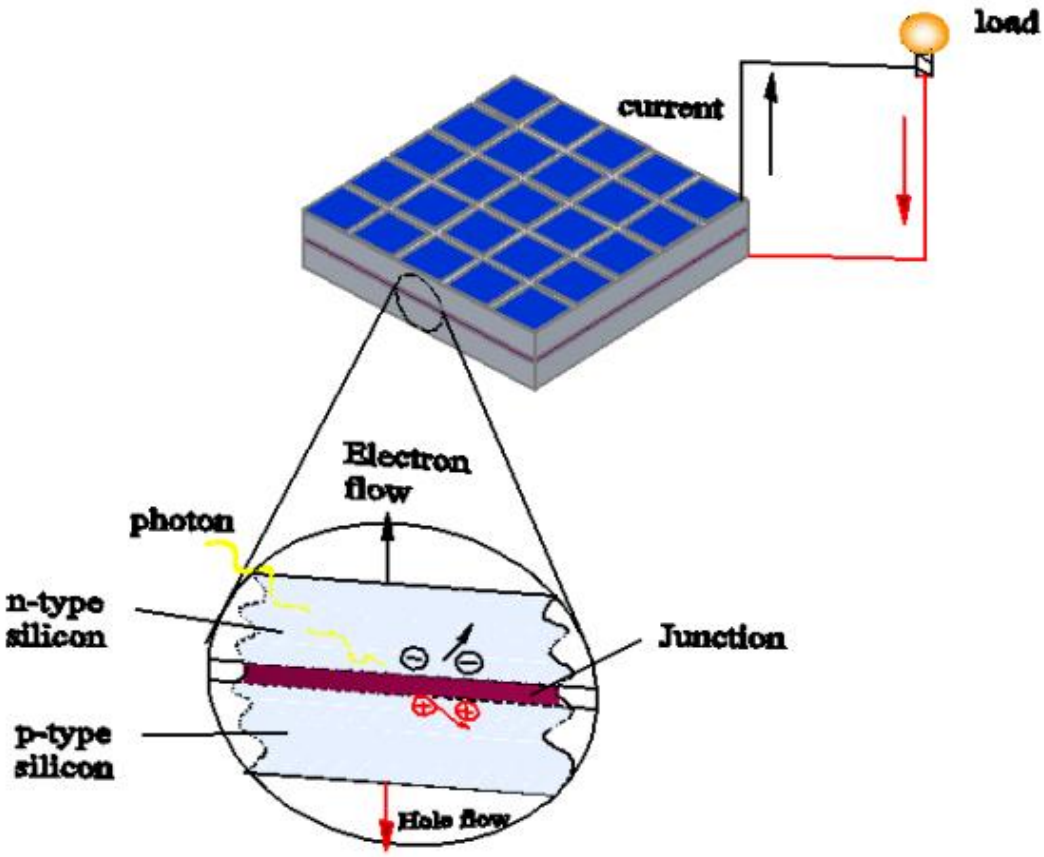


Figure 1. 4:basic operation of photovoltaic system (Photovoltaic Cell - Energy Education, 2018)

### 1.1.2 Wind powered water pumping system

The main aim of this section is to give the awareness on the wind system such as: types of wind turbine, component of wind turbine, mechanisms how wind can pump water, and knowing this is the base to select the type of wind we use for our design system and which mechanism is appropriate for our system. So this chapter is important for this purpose.

All the components and working of the wind pump are shown in figure 1-5. Windmill is a multi-bladed rotor which is mounted on a hub. There may be 8, 16, 18 and 24 blades depending upon the wind parameters and design. Multiple blades in the form of curved blades (sails) are rigidly mounted at some angle to the wind direction. Curved shape of blades helps to harness more energy when air passes over the sail of the blades. When all

the blades are mounted over the hub, they form the rotor. When wind passes through the rotor, it rotates to produce the mechanical energy. Rotor is connected to a shaft which tends to rotate the gears. Transmission system consists of gears, guide wheel, pitman arm and guide shaft. Pump rod passing through transfer the motion to the pump plunger. Tower is a high strong support holding windmill and gear mechanism. Tower must be high enough to surpass the top of nearby trees and buildings to avoid any obstruction in wind path approaching the windmill.

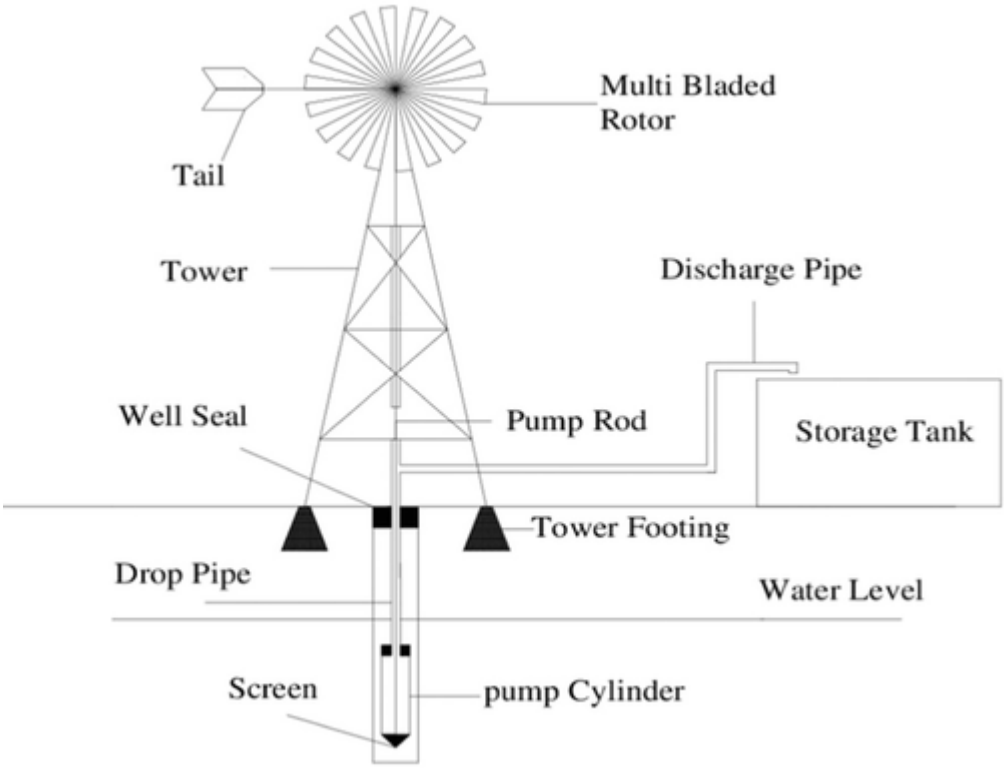


Figure 1. 5:components and working of a wind pump (Aized et al., 2019)

### 1.1.3 Hybridized solar photovoltaic and wind energy for water pumping

The word 'hybrid' refers to any energy sources with more than one form of energy, generating a conventional or diesel engine power generator and renewable energy sources such as photovoltaics, wind power generators, batteries etc. Now, paired with increased worries about global warming, depletion of oil and gas supplies have led to expectations of alternative/renewable energy sources. The integration of renewable energy sources such as solar and wind is more attractive and commonly used to replace oil-generated energy (Girma et al., 2015).

As technology in wind power and photovoltaic water pumps progress, hybrid systems are better and cheaper to utilize as stand-alone systems than wind or photovoltaic systems alone. Hybrid systems do not need to be developed for worse-case circumstances, as electricity from a single source is not available.

Hybrid systems allow for the use of reduced component sizes, which reduces the overall cost of the system. Though reliability improvements in hybrid systems and the total power system size are being reduced, their initial prices remain high. Highly skilled persons are also necessary to maintain hybrid systems. Thereby, hybrid systems are especially well-equipped and qualified workers for systems maintenance in economically strong areas. So, as stated in the introduction and above, the hybrid system is utilized for the site that have been chosen for this study, and in order to reduce the cost of maintenance, when the project is completed, we teach the expert who lives in the woreda from the related office, and they will maintain it.

## 1.2 Statement of the problem

The chosen area (Samira) is one of the biggest areas of land where agriculture is the major sector, and seasonal reliance on rainfall limits the sector's output. However, the presence of several river basins demonstrates the area's irrigation potential. It is critical to find a solution to the seasonal reliance on rainfall deficit to boost agricultural output. Because there is no power in the vicinity of Samira village which found 24Km from electric power source, the problem of water pumping will be handled by employing renewable energy as a viable alternative for meeting energy needs to pump water from the river basin without impacting the population's lifestyle or the environment. As a result, the goal of this research is to evaluate the performance of wind and solar energy hybridized water pumps to alleviate water shortages for potato irrigation in Samira district.

## 1.3 Objective of this thesis

### General objective

The ultimate objective of this research is the performance investigation of solar and wind energy hybridized water pumping system for potato irrigation in a climatic condition of Samira village.

### Specific objective

The following are the precise aims of these studies:

- Investigate Samira Village's solar and wind energy potential

- Determine water requirement of potatoes by CROPWATT software
- Build a water pumping system for irrigation that runs on a hybrid of solar and wind energy
- Simulate the hybrid wind and solar water pumping system using HOMER Pro software

### 1.4 Theoretical /conceptual framework

The main concept behind wind and solar energy hybridized water pumping application is being able to change the suns solar radiation and mechanical wind energy into a useful form of energy for pumping water used for irrigation system.

### 1.5 Scope

Based on Samira geographic and regional design data, the research will aim to construct an efficient and cost-effective hybrid wind turbine and photovoltaic energy water pumping system to irrigate potato farms in a designated location and highlight the benefits of using a wind turbine and solar PV energy hybridized water pumping system.

### 1.6 Significances of the study

The study is important in providing detailed information in the research on the potential of wind turbine and solar PV hybridized power to pump water for irrigation as a solution to food insecurity, the performance analysis of the hybrid PV and wind systems to resolve food problems in the village as water pumping solutions. The study's findings can be applied in the following ways:

- Minimized food insecurity problem
- Reduce irrigation's seasonal reliance.
- Agriculture output will be three times a year, resulting in a reduction in poverty for the society.
- To promote renewable water pumping systems for irrigation

# CHAPTER 2

# LITRATURE REVIEW

Many researchers utilized a variety of technology options and techniques to assess the various configurations of renewable energy resources for water pumping; such as solar energy, wind energy, and hybrid configurations. The findings of a number of researches have been published, and some of these are examined and assessed below.

## 2.1 Hybrid Energy water pumping systems

Any power with more than one type of resource, generally a conventional generator or power from a diesel or gas engine, and renewable energy sources such as a photovoltaic unit, wind generator, batteries, etc., is referred to as a hybrid system (Girma et al., 2015)

Today, the expectation is to explore alternative/renewable energy sources due to the depletion of oil and gas supplies, as well as rising worries about global warming. Renewable energy integration, such as solar and wind energy, is becoming increasingly appealing and is being widely employed to replace oil-produced energy (Ma et al., 2014).

Photovoltaic power generation has received a lot of attention in recent years as one of the most viable energy alternatives. The direct conversion of sunlight into energy is the source of this growing interest. However, due to cost constraints, PV power generation is not widely employed. Efforts are now being undertaken all around the world to lower the cost per watt through different technical breakthroughs. Wind energy is also employed efficiently in large-scale wind farms to supply power to rural communities and other remote sites. Wind energy is widely employed in countries such as Denmark, Germany, Spain, India, and some parts of the United States. It is one of the most widely used types of renewable energy in the world today. The performance of solar and wind energy systems is greatly influenced by the local meteorological conditions. The amount of energy generated by a PV system is greatly dependent on the weather. A PV system, for example, would not generate any power during overcast times or at night. Furthermore, storing the power generated by a PV system for future use is challenging. A PV system may be combined with various alternative power sources to solve this problem.

Irrigation systems, rural electricity, and wastewater treatment have all benefited from hybrid systems that combine wind and solar energy according to the work by M. Khattab et al. (2020).

As a result, a cost-effective, non-polluting and dependable hybrid power system was developed to alleviate the lack of energy for water pumping in the district. However, there was limited scientific evidence on the use of solar and wind hybrid systems to satisfy the district's irrigation energy needs. As a result, the primary goal of this research was to assess the feasibility of a wind and solar hybridized power drip irrigation system in the Samira district.

### 2.2 Basics of wind energy

The main goal of this chapter is to raise awareness about wind systems such as components of wind turbines, mechanisms by which wind can produce electricity, and knowing this is the foundation for selecting the type of wind we use for our design system and which mechanism is appropriate for our system. As a result, this portion is essential for this reason.

The movement of air produced by pressure differences in the atmosphere is referred to as wind. Pressure differences impose a force that causes air masses to migrate from a high-pressure zone to a low-pressure region. The term "wind" is used to refer to the movement of air. Such pressure variations are largely generated by the sun's uneven heating of the Earth's surface. Wind energy is thus an indirect type of solar energy. Wind power is the conversion of wind energy into more usable forms, generally electricity, through the use of wind turbines (Girma, 2016).

The wind turbine uses a rotor with two or more blades that are physically linked to an electrical generator to collect the wind's kinetic energy of air mass. To maximize energy extraction, the turbine is usually placed on a tall tower. Sites with consistent strong wind generate more energy throughout the course of the year (Aldjia et al., 2017).

#### 2.2.1 Energy extracted from the wind

The difference between the upstream and downstream wind powers is the actual power extracted by the rotor blades.

The mechanical power extracted by the rotor, which drives the generator, is as follows:

$$p_o = \frac{1}{2}\left[\rho \times A_r \times \frac{v+v_o}{2}\right] \times (v^2 - {v_o}^2) \quad \text{.....} \quad 2.1$$

The above expression can be algebraically rearranged:

$$p_o = \frac{1}{2}\rho A_r v^3 \frac{\left(1+\frac{v_o}{v}\right)\left[1-\left(\frac{v_o}{v}\right)^2\right]}{2} \quad \text{..... 2.2}$$

Where, Po= the mechanical power extracted by the rotor, also known as the turbine output power

$v$ =upstream wind velocity at the entrance of the rotor blades

$v_o$ = downstream wind velocity at exit of rotor blade

The power collected by the blades is often represented as a percentage of the upstream wind power, as can be seen here:

$$p_o = \frac{1}{2}\rho A_r v^3 c_p \quad \text{..... 2.3}$$

Where, $c_p = \frac{\left(1+\frac{v_o}{v}\right)\left[1-\left(\frac{v_o}{v}\right)^2\right]}{2}$ .....2.4

The proportion of upstream wind power collected by the rotor blades is denoted by $c_p$. The remains of the energy is released or wasted in the downstream wind. The power coefficient of the rotor, or rotor efficiency, is denoted by the factor $c_p$. Power changes linearly with the density of the air sweeping the blades as well as with the cube of wind speed. The blades cannot harvest all of the upstream wind power because some power is left in the downstream air, which continues to travel at a slow rate.

### 2.2.1.1 Rotor swept area

The wind turbine's output power varies linearly with the rotor swept area, as seen in the power equation. The rotor swept area for a horizontal axis turbine is determined by:

$$A_r = \frac{\pi}{4} D^2 \quad \text{..... 2.5}$$

Where, D is the rotor diameter

### 2.2.1.2 Air density

Wind power changes linearly with air density as it sweeps the blades.

According to the gas law, air density changes with pressure and temperature:

$$\rho = \frac{P}{R \times T} \quad \text{..... 2.6}$$

Where, p = air pressure

T = temperature on the absolute scale,

R = gas constant.

At sea level, one atmospheric pressure and 15.6°C, the density of the air is 1.225 kg/m$^3$. Using this as a guide is adjusted for the temperature and pressure at the location. Temperature and pressure are also affected by height. The following equation, which is applicable up to 6,000 meters (20,000 feet) of site elevation above sea level, expresses their combined impact on air density:

$$\rho = \rho_o \times e^{-\left\{\frac{0.297H_m}{3048}\right\}} \quad \text{..... 2.7}$$

### 2.2.2 Wind speed distribution

Wind speed, which has a cubic relationship with power, is the most essential metric required to assess the power potential of a particular location. The wind is never consistent at any location. The weather system, the local land terrain, and the height above the ground surface all have an impact on it. The wind speed changes according to the minute, hour, day, season, and year. As a result, the yearly mean speed must be averaged over a period of ten years or more. Such a long-term average boosts confidence in estimating a site's energy-capture potential. Long-term measures, on the other hand, are costly, and most enterprises cannot afford to wait that long. In such cases, the short-term data, say one year, is compared with long-term data from a neighboring location to estimate the long-term yearly wind speed at the site under consideration. This is referred to as the "measure, correlate, and forecast technique" according to (Girma, 2016).

Because wind is influenced by the sun and seasons, the wind pattern tends to repeat itself over the course of a year. The speed data averaged over months is generally used to define the wind location. For the sake of simplicity in describing the overall "windiness" of several places, the monthly data is sometimes averaged across the year. A probability distribution function can be used to explain the fluctuations in wind speed over time.

#### 2.2.2.1 Weibull probability distribution

The Weibull probability distribution function ‘h' with two parameters, the shape parameter ‘k' and the scale parameter ‘c', best describes the variance in wind speed. The following gives the likelihood of wind speed being v at any time interval (Girma, 2016).

$$h(v) = \left(\frac{k}{c}\right)\left(\frac{v}{c}\right)^{k-c} e^{-\left(\frac{v}{c}\right)^k} \text{ for } 0 < v < \infty \quad \text{..... 2.8}$$

### 2.3 Photovoltaic power system

Many solar energy systems need a thorough understanding of global and diffuse radiation availability. Although there are numerous global maps of solar radiation, they are insufficiently precise to be utilized for determining available solar energy in tiny regions. These situations led to the creation of analytical techniques to produce radiation estimates for locations where measurements are not performed and for stations where measurement records have gaps.

To compute global solar radiation using climatic factors, several empirical models have been used. Extraterrestrial radiation, sunlight hours, mean temperature, maximum temperature, soil temperature, relative humidity, number of wet days, altitude, latitude, total precipitation, cloudiness, and evaporation are among the characteristics considered. Sunshine duration, which is easily measurable and publicly available data, is the most often used metric for calculating global solar radiation (Olatomiwa et al., 2015).

It is generally known that most underdeveloped nations lack adequately collected radiation statistics. Typically, data on sunlight duration is available. Solar radiation data is the greatest source of information for evaluating the solar energy potential of a certain site, which is required for the appropriate design of a solar energy conversion system.

#### 2.3.1 Global Irradiation on Horizontal Surface

Extraterrestrial radiation is calculated from the solar constant, solar declination, and time of year for each day of the year and for different latitudes according to (Duffie et al., 1994):

$$R_a = \frac{24*60}{\pi} G_{sc} d_r [\omega_s \sin(\varphi) \sin(\delta) + \cos(\varphi) \cos(\delta) \sin(\omega_s)] \quad \text{.....2.9}$$

Where; Ra = extraterrestrial radiation [$MJm^{-2}day^{-1}$]

$G_{sc}$ = solar constant

$d_r$ = inverse relative distance sun-earth

$\omega_s$ = sunset hour angle (rad)

$\varphi$ = latitude (rad)

$\delta$ = solar declination (rad)

The inverse relative distance earth-sun, $d_r$, and the solar declination, $\delta$, are given by;

$$dr = 1 + 0.033\cos\left(\frac{2\pi}{365}n\right) \quad \text{.....2.10}$$

$$\delta = 0.409 \sin\frac{2\pi}{365}n - 1.39 \quad \text{.....2.11}$$

Where, n is the number of the day in the year and given as follow;

The sun set hour angle, $\omega_s$, is given by;

$$\omega s = \cos^{-1}[-\tan(\varphi)\tan(\delta)] \quad \text{..... 2.12}$$

Daylight hours are given by;

$$N = \frac{24}{\pi}\omega_s \quad \text{.....2.13}$$

For N is daylight hour and $\omega_s$ is calculated by above formula

Table 2. 1:the representative date of the month according to (Duffie et al., 1994)

| Months | n for $i^{th}$ day of the month | Date | Day of the year |
|---|---|---|---|
| Jan | I | 17 | 17 |
| Feb | 31+i | 16 | 47 |
| Mar | 59+i | 16 | 75 |
| Apr | 90+i | 15 | 105 |
| May | 120+i | 15 | 135 |
| Jun | 151+i | 17 | 162 |
| July | 18+i | 17 | 198 |
| Aug | 212+i | 16 | 228 |
| Sept | 243+i | 15 | 258 |
| Oct | 273+i | 15 | 288 |
| Nov | 304+i | 14 | 318 |
| Dec | 334+i | 10 | 334 |

## 2.4 Works linked to performance investigation of solar and wind energy hybridized water pumping system

Assefa (2010) investigated the viability of wind pumping for village water supply and irrigation in Ethiopia and compared it to diesel. Excel was used to create a cost analysis model, which included system sizing and cost estimation. Wind pumping cost 5.66, 6.71 and 7.01birr/$m^3$ at a normal delivery head of 20m for Mekele, Jijiga, and Assosa, respectively, whereas diesel pumping cost 25.10birr/$m^3$. Furthermore, the breakeven point for wind pumping at a normal delivery head of 20m is 1.9 years after the system is operational. As a consequence, wind pumping is shown to be more cost-effective for water delivery and irrigation than diesel pumping for stations with average wind speeds of 2.5m/s or higher during the key month.

Vick and Neal (2012) investigated solar photovoltaic and wind turbine operations as independent water pumping systems and a PV and wind turbine hybrid system. The aim was to determine whether there were any advantages or disadvantages of using a hybrid system instead of a wind turbine or a solar PV array alone; if one interfered with the output of the other; and which hybrid system was the most efficient for the site.

The alternating current rating of the wind turbine used in the study was 900 W (AC). Three different solar PV arrays with direct current ratings of 320, 480, and 640 W were investigated (DC). A rectifier converted the 3-phase variable voltage AC output from the wind turbine to DC before combining it with the DC output from the solar PV array. The combined renewable energy powered a single helical pump. The independent variable in the hybrid wind turbine and solar PV array research was measured in W/$m^2$. The 900W wind turbine combined with the 640W PV array had the highest pump efficiency of the hybrid systems in Bushland, TX. At a 75m pumping depth, the hybrid systems' greatest pump efficiencies were: 47 percent (wind turbine /320W PV array). The wind turbine and the different PV arrays interfered, although the wind turbine /320W PV array exhibited the least interference (due to a voltage difference between the wind turbine and the PV array. The hybrid system was shown to deliver 28% more energy than either solar or wind power alone. To enhance the hybrid PV and wind turbine water pumping system, an extra buck/boost converter was utilized as a controller.

Bonsa (2013) studied the economic viability of solar PV systems for water pumping projects in the Borana zone, where ground water is the population's major source of water,

to the traditional alternative of utilizing decentralized diesel-powered generators to produce energy to pump water from boreholes.

The findings show that the project would breakeven in the fourth year of operation, that the unit water cost for all PV system cases was lower than the unit water cost for diesel-powered generator systems, and that key financial parameters like equity pay-back and net present value show that the solar energy is a viable alternative source of energy for water pumping systems in the study area.

The latest advancements in research in the field of renewable energy-water pumping systems were discussed by (Gopal et al., 2013). They conducted a quick examination of hundreds of publications on water pumping systems and evaluated five alternative system configurations using various forms of energy, including solar, wind, biomass, thermal, and hybrid solar PV and wind turbine. They determined that adopting renewable energy (solar, wind, or hybrid) significantly decreases reliance on conventional energy while having a positive environmental impact. According to meteorological data collected in the city of Xanthi, Greece, and their systematic design method for three distinct water pumping systems, namely PV, wind turbine, and hybrid PV and wind turbine energy. The performance of a hybrid system outperformed that of a solar or wind system alone According to (Aldjia et al., 2017).

Laamari et al., (2015) described optimization technique for a hybrid (wind-solar) autonomous water pumping system. The findings show that using renewable hybrid solar and wind energy for water pumping is technically favorable.

Olatomiwa et al., (2015) created several hybrid energy system configurations in six geographical zones of Nigeria, and it can be determined economic feasibility solution using HOMER software with sensitivity scenarios based on NPC and COE. They offered a statistical study of the potentials of wind and solar energies for rural regions in Nigeria based on the availability of meteorological data. It makes use of HOMER software to build and size optimal technical and economic hybrid energy system components. Configuration two (hybrid) was the most economically viable option of the two, with a TNPC of $69,811 and a COE of 0.409 $/kWh.

Girma (2016) studied a feasibility of solar/wind and hybrid water pumping systems for off-grid rural areas in Ethiopia. His research goal was to investigate the viability of solar/wind

and hybrid water pumping systems in rural settlements in Ethiopia that were disconnected from the main grid line. Three Ethiopian areas were chosen for the study, and their solar and wind energy potential was assessed using data from the National Metrology Services Agency (NMSA) and NASA satellites. The solar PV system was planned to provide a daily average of 10.5, 7, and 6.5$m^3$/day for 700, 467, and 433 persons in the Siadberand Wayu, Wolmera, and Enderta locations, respectively.

The proposed system for Wind turbine findings reveal that a 5.7 m diameter windmill is required to pump water from a borehole via a total head of 75, 66, and 44 m for Siyadberand Wayu, Adami Tulu, and East Enderta respectively, to fulfill the daily water requirement of 10, 12 and 15 $m^3$. A hybrid (solar/wind) water pumping system was capable of supplying 20 $m^3$ of water per day for 1000 people with average daily water consumption of 20 liters per person at a total head of 50, 75 and 100 m has been designed. The finding shows that hybrid systems are eco-friendly and seek to preserve the environment by reducing pollution levels by a considerable amount when compared to diesel system.

Zegeye et al., (2017) studied the economics of a PV water pumping system for small-scale irrigation. The need for electric power to feed the irrigation pumps was analyzed and the optimal angle of inclination of the solar panel that can gather the most solar energy was found when the irrigation demand is higher based on seasonal change. Similarly, the irrigation water need was evaluated, and the maximum power was decreased in order to pick the power that can meet all irrigation times while keeping the PV system's cost low. The authors found that if irrigation water distribution regulations are good, it is possible to optimize a PV pumping system for irrigation.

Widyan et al., (2018) demonstrated a stand-alone Wind and PV hybrid power system capable of powering a three-phase induction motor for pumping applications. The authors found that the suggested hybrid stand-alone power system can tolerate step changes in the load connected to the motor as well as step variations in solar irradiation levels, demonstrating the resilience and dependability of the system's integration. According to the research, using PV cells in an all-electric or hybrid wind and PV solar system looks to be an almost perfect solar energy use for pumping irrigation water. However, it is critical that power conditioning be eliminated, as well as the cost of these systems is reduced.

Allouhi et al., (2019) investigate the sizing, modeling, and economic assessment of PV water pumping systems for household usage in distant regions. The goal of this work was to investigate an optimal PV system design capable of providing a solar submersible pump system to meet the household water demands of five isolated dwellings in a rural Moroccan location. Based on real-world water use data, a thorough strategy for designing an efficient PV water pumping system was provided. In addition, system design and performance evaluation were carried out using hourly climatic conditions. Overall, two techniques were examined in order to find the best design for the proposed system. Annual simulations revealed that, as a first choice, the direct connection looks to be unsuitable design for water pumping in this situation. According to the findings of a 30-month household water usage survey, the average water demand for the targeted project did not surpass $6m^3$ per day. Based on the basic features of the site and taking four days of autonomy into account, it was determined that two positive displacement pumps of 140W linked in parallel and a storage tank of $24m^3$ could meet the design requirements. When compared to direct-coupled control, using the MPPT DC method to the PV water pumping system results in a reduction in the needed capacity of PV modules (from 480W to 320W). This indicates an almost 30% reduction in PV module capacity to install, which significantly improves the economic viability of PV water pumping.

Kose et al., (2019) investigated a water pumping system powered by wind and solar energy for agricultural purposes. The scientists discovered that the system's daily average of generated power in July was sufficient to pump 44.1 $m^3$/day of water from a depth of 2.5 m and a total of 1368 $m^3$ of water for the month. With the drip irrigation method, it was also discovered that the amount of pumped water was sufficient to fulfill the water needs of the agricultural goods, which were 12.4 decares (da) of sugar beet, 13.0 da of potatoes, 13.4 da of maize, 13.6 da green bean and 10.8 da of sunflower. In relation to the hybrid system (PV/wind), a technique for the optimal design of a pumping system with water storage to deliver drinking water to homes in remote regions was also created. The finding shows that the proposed hybrid system sufficiently provides the demand.

Hussein (2019) investigated the analysis and performance of a solar-powered water pumping system. She intended to investigate the efficiency of solar water pumping under Jigjiga's climatic conditions. In this study, the precise electrical characteristics of 1800W non-tracking PV array on the current vs. voltage and power vs. voltage planes were calculated using the manufacturer's datasheet of the PV module as input. The electrical

parameters of the PV array and the performance equation for the solar PV water pumping system were used to forecast the hourly performance variation of the system (50, 60, 70, 80, and 90 meters of pumping heads). For sunny days with a total dynamic head of 80m and solar irradiation of 5000-7000 $Wh/m^2/day$, the modeled system yields a flow rate of 20-30 $m^3/day$.

M. Khattab et al., (2020) designed and tested a self-contained PV/ wind turbine and hybrid solar and wind energy system for pumping underground water for small farm irrigation. Different renewable energy systems were evaluated using annual simulations on an hourly basis using specialized commercial software simulation packages PVSYST and HOMER, to model system performance and arrive at the best configurations based on objective criteria. The net present cost and the cost of energy, along with the percentage of capacity shortage, are the parameters utilized in economic optimization. Solar PV only, PV with horizontal axis wind turbine, PV with vertical axis wind turbine, PV with horizontal axis wind turbine and diesel generator, and diesel generator only can be compared. For optimum functioning, simulations were also run for various load patterns. It was found that the system with hybrid solar PV and wind turbine energy was the most cost-effective and efficient.

In general, a cost-effective, non-polluting and dependable hybrid wind and solar power system was developed to alleviate the lack of energy for water pumping. However, there was limited scientific evidence on the use of solar and wind energy hybridized systems to satisfy the Samira district irrigation energy needs. As a result, the primary goal of this research was to assess the feasibility study of a wind and solar hybridized energy water pumping for potato drip irrigation system in Samira district.

# CHAPTER 3

# METHODOLOGY

This chapter provides a summary of the techniques used to accomplish the study's general and particular goals, as described in the preceding chapter. Data gathering, calculation of solar and wind energy potential, planning, and implementation are all part of the process. CropWAT Computer software is used to calculate the crop water requirements (CWR) of potatoes and HOMER Pro software is used to simulate the proposed system and do financial analysis.

## 3.1 Process model

The overall process of the research is described by flow diagram 3.1 below;

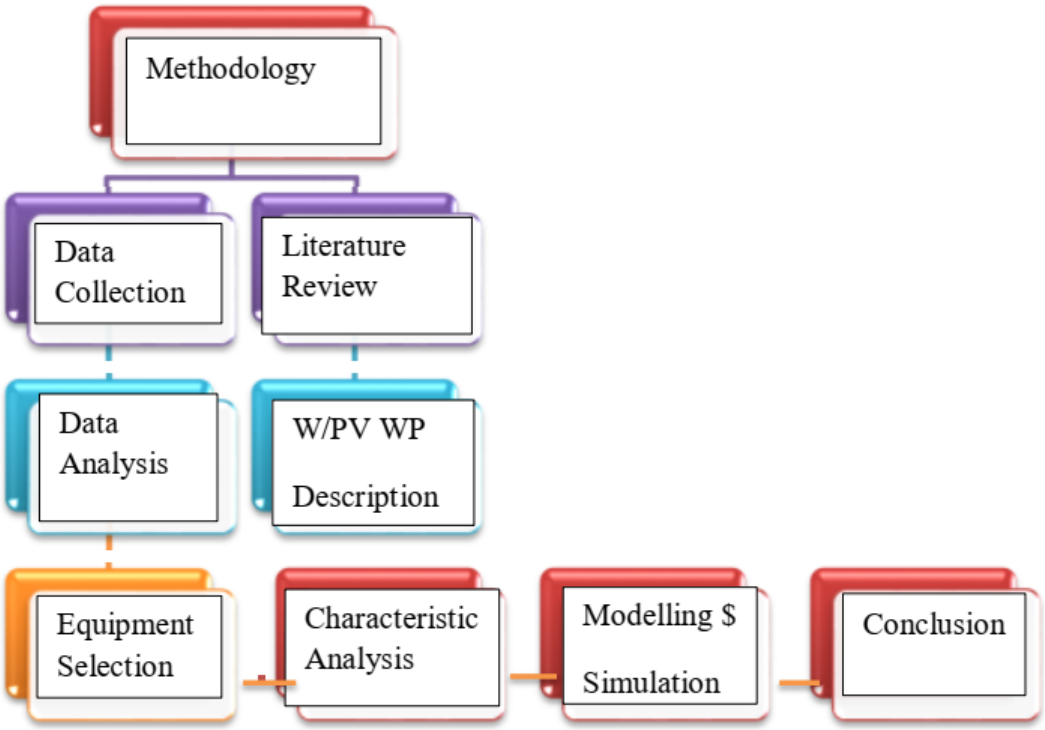


Figure 3. 1 Process podel

### 3.1.1 Data sources and collection method

The data was collected from National Metrology Services Agency (NMSA) and the NASA website. The following site data were gathered from the Ethiopian Meteorology Agency for ten years (2011-2020) and utilized as input for crop evapotranspiration calculations (ETo) for CROPWATT software.

- Temperature range (maximum and minimum)
- Rain fall
- sunshine Hours  and wind speed
- Relative humidity

Other key data such as the site's local geography, soil type, and agricultural output was obtained during the site visit and from local agricultural office.

The NASA satellite website was used to calculate the monthly average global solar radiation and monthly average wind speed based on the location's latitude, longitude, and elevation and compared with the calculated value that obtained from National Metrology Services Agency (NMSA). The majority of the country's rural locations lack metrological stations. As a result, the selected sites' sunlight hour and wind speed data were gathered from neighboring stations.

In general, the approaches to be used to fulfill the research objectives are as follows:

- Literature review;
- Data collection from the metrological agency for temperature range (maximum and minimum), rain fall, sunshine hours  and wind speed, and relative humidity as well as data collection from the literary and agricultural bureau for potato irrigation nearest to the location;
- Geographical data of the Area;
- Analysis of the collected data;
- Pumping systems and water storage system design;
- Design of the solar and wind hybridized energy system for powering the water pumping system;
- Financial analysis by using HOMER Pro software;

### 3.2 Water source

The water system's layout will be influenced by the type of water source utilized, as well as local geography and the position of the distribution point. Taji River is the intended system's water supply. With an average flow rate of 0.755$m^3$/sec as calculated below, (equation 3.2.1) and water quality adequate for irrigation, the river runs year-round with enough flow to serve the intended system. However, to protect the pump from failure, enough screening must be supplied for the pump intake.

#### 3.2.1 River flow rate

The river flow rate is calculated using the traditional float method. This approach requires two pieces of data: the cross-sectional area of the water flowing in the stream and the speed at which the water flows. Normally, this procedure involves filling a plastic container halfway with water and capping it to create a perfect float. The floating bottle will time its journey between two places separated by a specified distance. The stream's cross sectional area (CSA) is the first thing to examine (Baker, 2016).

Choose a stretch of the river that is generally straight and has a consistent cross-section. For the traveling floater, you must also define the distance between the release point and the time end. The measurement unit should be in meters. Measure the river's CSA by dividing it into four parts as shown in Figure 4-1. The CSA is calculated by utilizing (equation 4.1) (Baker, 2016).

$$A_n = l_n \times \left(\frac{d_{n-1}+d_n}{2}\right) \quad \text{..... 3.1}$$

Where, $A_n$ is the CSA

l is the segment length

n is the segment number

d is the point depth.

To avoid disrupting the water's surface, the measuring site should always be downstream. To determine the depth of a stream, start at the bottom and work your way up. After taking all of the necessary measurements, the area of each section must be calculated.

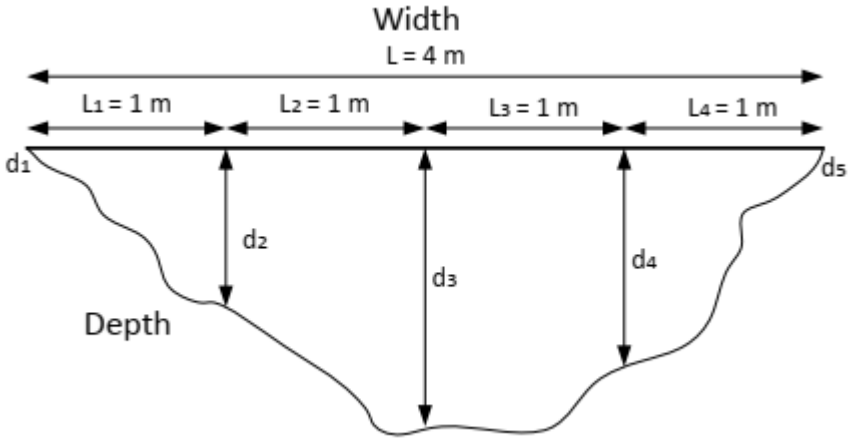


Figure 3. 2 Width and Length representation of river

Where measured depth are $d_1$=0.23, $d_2$=0.28, $d_3$=0.56, $d_4$=0.41 and $d_5$=0.24

By using (4.1) we can calculate the area of each segment:

- $A_1$ = 1m x (0.23m + 0.28m)/2 = 0.255$m^2$
- A2 = 1m x (0.28m + 0.56m)/2 = 0.42$m^2$
- A3 = 1m x (0.56m + 0.41m)/2 = 0.485$m^2$
- A4 = 1m x (0.41m + 0.24m)/2 = 0.325$m^2$

A = 0.255 + 0.42 + 0.485 + 0.325 = 1.485$m^2$

The floater (plastic bottle) can be dropped a few meters before the starting line after the cross sectional area (A) value has been calculated. The time it took the plastic bottle to travel the prescribed distance from the starting site to the measuring location was measured. We choose 10 meter spacing between the start and finish points for this thesis. Keep accurate notes and repeat at least 10 times to achieve better results. The travel time (T) is calculated from the job as shown in Table 4-1:

Table 3. 1 the time taken by floater to travel 10m

| No | Times | No | Times |
|---|---|---|---|
| $T_1$ | 14.98s | $T_6$ | 16.87s |
| $T_2$ | 18.58s | $T_7$ | 17.56s |
| $T_3$ | 17.21s | $T_8$ | 18.61s |
| $T_4$ | 17.56s | $T_9$ | 19.82s |
| $T_5$ | 18.23s | $T_{10}$ | 17.68s |

Count the average travel time:

$$T = \frac{(T_1+T_2+T_3+T_4+T_5+T_6+T_7+T_8+T_9+T_{10})}{10} \quad \text{.....3.2}$$

From the average calculation in (4.2), average travel time T = 17.71 second. The velocity (v) value is determined by this formula (4.3):

$$V_f = \frac{\text{distance}}{\text{time}} \quad \text{.....3.3}$$

$$V_f = \frac{10\text{m}}{17.71\text{s}} = 0.565\,{}^{m}/_{s}$$

Finally, determine a river flow by using equation (4.4):

$$Q = V_f \times A \times C \quad \text{.....3.4}$$

Where, C =is coefficient factor

C=0.8 for rocky bottom and 0.9 for muddy bottom;

$$Q = 0.565\,{}^{m}/_{s} \times 1.485\text{m}^2 \times 0.9 = 0.755\,{}^{m^3}/_{s}$$

### 3.3 Crop water requirement

The first step in designing hybrid wind and solar energy water pumping system is to determine the overall water requirement for irrigation. To design an effective irrigation

system, the suitable amount of water and correct timing of application has to be determined since only a certain amount of falling rain or water may be effective in raising the soil moisture that is actually useful for plant growth. Hence, for proper crop growth, the correct amount of water demand has to be supplemented to the farming field by irrigation.

The total amount of water needed by a crop from sowing to harvest is referred to as the crop's water requirement. Different crops may need different amounts of water in any given natural situation. Even for the same crop, the total water needed for its growth is not uniformly distributed over its entire life cycle, also known as crop duration, depending on the environment, cultivation process, successful rain, and type of soil (M. Heibloem, 2018).

Studying the complex relationship between crop prevalent climates is critical for minimizing water demand with minimal impacts on yields and yield quality to evaluate optimal and efficient water requirements.

Bean roots draw water from the soil, but the majority of it does not stay with the plant. Instead leaks to the atmosphere as vapor from the leaves and stems of the plants, a phenomenon known as transpiration that takes place mainly during the day.

During a rainstorm, evaporation loses the water on the soil surface as well as the water added to the leaves and stem flowers. As a result, the crop's water requirement is made up of not just transpiration but also additional evaporation, which is referred to as evapotranspiration. Evapotranspiration ranges from day to day depending on the weather cycle and is one of the most critical considerations to understand before making and executing any decisions for the design and management of water resources systems.

M. Heibloem (2018) investigated the primary climatic variables that impact crop water requirements are:

- Sunshine hour
- Temperature
- Wind speed
- Humidity

Evaporation and transpiration (ET) happen simultaneously, and it is difficult to tell the two apart. Evaporating demand from crops grown in vast fields under ideal soil water, outstanding management, and environmental conditions is referred to as crop evapotranspiration ETc under normal conditions. As Pereira et al. (2015) to prevent

ambiguity surrounding the word ET, the reference crop evapotranspiration ($ET_o$) was developed, which uses grass as a norm. It investigates the atmosphere's evaporative demand, which is unaffected by crop form, production, or management practices and is solely dependent on climatic variables. For deciding ETo, the FAO Penman-Monteith approach is suggested as the only method. The FAO's land and water production division developed the CROPWAT program to determine the irrigation water demand based on this recommendation.

### 3.3.1 Reference crop evapotranspiration

The first step to assess the irrigation water requirements is to compute the reference evapotranspiration ETo that measures the water loss owing to the evaporation and plant transpiration from a reference surface (Pereira et al., 2015). Grass has been used as the reference crop.

### 3.3.2 Determination of irrigation water requirement:-using CROPWAT software

Alternatively, the program CROPWAT may be used to assess irrigation water requirements. It is a decision support system designed by FAO's Land and Water Development Division for irrigation planning and management. CROPWAT is aimed as a practical tool to carry out conventional calculations for reference evapotranspiration, crop water requirements, and crop irrigation requirements, and more specifically the design and operation of irrigation schemes. It permits the generation of suggestions for enhanced irrigation techniques, the design of irrigation schedules under varied water supply circumstances, and the assessment of production in rain-fed circumstances or shortage for irrigation.

Crop water requirements and irrigation requirements are calculated using local climate, crop, soil, and geographical data.

Country Ethipia Station samira

Altitude 2565 m. Latitude 7.53 °N Longitude 38.93 °E

| Month | Min Temp | Max Temp | Humidity | Wind | Sun | Rad | ETo |
|---|---|---|---|---|---|---|---|
| | °C | °C | % | km/day | hours | MJ/m²/day | mm/day |
| January | 9.7 | 25.0 | 49 | 221 | 8.7 | 20.7 | 4.71 |
| February | 12.3 | 26.8 | 49 | 221 | 6.3 | 18.3 | 4.76 |
| March | 14.6 | 26.5 | 48 | 254 | 6.1 | 18.8 | 5.20 |
| April | 12.8 | 25.8 | 57 | 177 | 4.0 | 15.6 | 4.09 |
| May | 12.2 | 24.8 | 63 | 152 | 4.2 | 15.5 | 3.69 |
| June | 12.0 | 24.0 | 68 | 151 | 3.9 | 14.7 | 3.41 |
| July | 11.9 | 22.0 | 76 | 160 | 4.3 | 15.4 | 3.20 |
| August | 11.9 | 21.6 | 78 | 145 | 3.8 | 15.0 | 3.06 |
| September | 11.5 | 22.0 | 77 | 161 | 4.0 | 15.4 | 3.14 |
| October | 12.1 | 25.0 | 56 | 280 | 7.6 | 20.4 | 4.91 |
| November | 11.9 | 24.1 | 58 | 271 | 7.9 | 19.7 | 4.58 |
| December | 11.3 | 23.2 | 52 | 285 | 8.0 | 19.2 | 4.63 |
| **Average** | **12.0** | **24.2** | **61** | **207** | **5.7** | **17.4** | **4.12** |

Figure 3. 3 determination of reference evapotranspiration of the farm site (Samira)

According to the statistics, the amount of rainfall decreases dramatically beginning in October (Figure 4-3), and there is no rainfall for four months in a row, thus October month is chosen as the start date for potato irrigation.

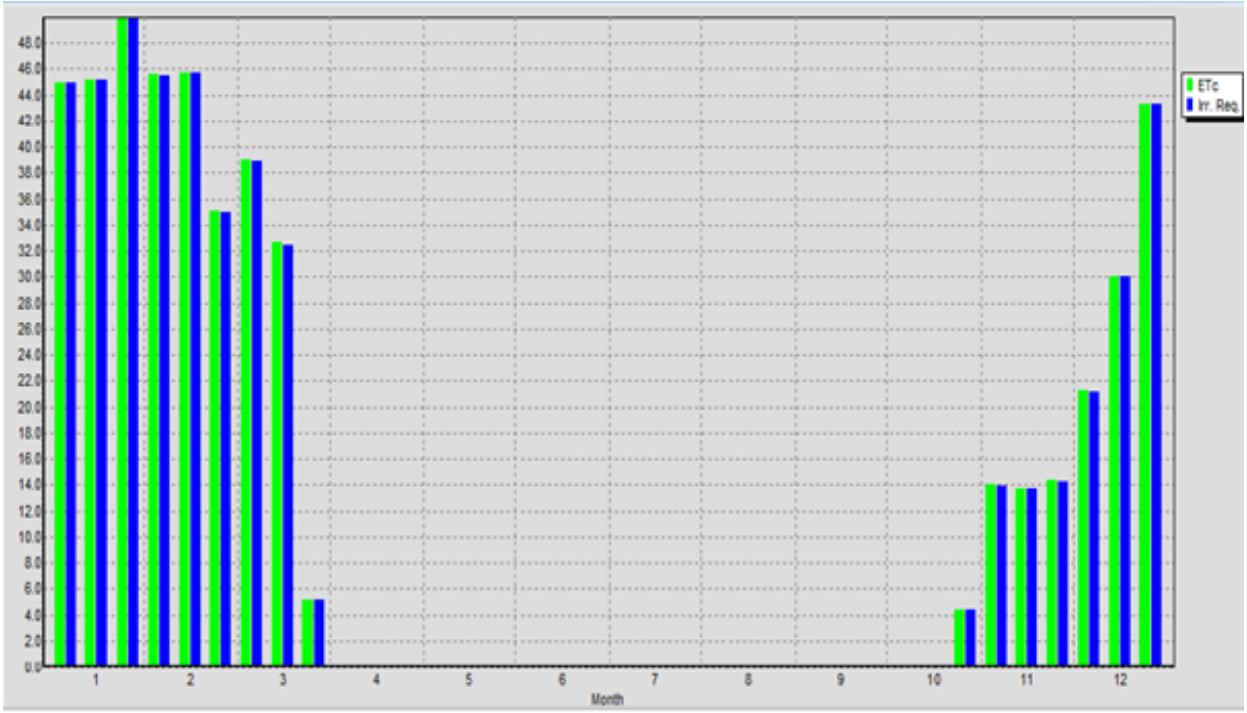


Figure 3. 4 Simulated irrigation water requirement (for one irrigation season)

$$IWR = ET_C - P_{eff} \quad \text{3.5}$$

Where, $P_{eff}$ = effective rain fall for the worst month

For Apple/cherry, apricot/almonds, onion, and potato, the covered area (canopy cover) was considered to be 70% (M. Heibloem, 2018).

Potato crop water requirement (CWR) is determined using the theoretical technique (Blaney Criddle), computer software (CROPWAT), and public papers from the Ministry of Agriculture. CROPWAT, on the other hand, is more accurate than the theoretical method, so its output should be used as system design data. The peak irrigation water requirement for the site was determined by CROPWAT and is calculated as in the next section.

### 3.4 Potatoes water requirement

Potatoes water demand is the quantity of water required to compensate for evapotranspiration (ETc) loss in the potato field. Crop evapotranspiration per decade is computed using CropWAT 8.0 software by multiplying the number of effective crop days by ten. Monthly rainfall data was converted to decade values using linear interpolation, and values for the first and third decades were determined using interpolation with the prior and succeeding months (Swennenhuis et al., 2009).

ETo station: samira | Crop: potatoes

Rain station: samira | Planting date: 29/10

| Month | Decade | Stage | Kc | ETc | ETc | Eff rain | Irr. Req. |
|---|---|---|---|---|---|---|---|
| | | | coeff | mm/day | mm/dec | mm/dec | mm/dec |
| Oct | 3 | Init | 0.30 | 1.48 | 4.4 | 0.0 | 4.4 |
| Nov | 1 | Init | 0.30 | 1.41 | 14.1 | 0.1 | 14.0 |
| Nov | 2 | Init | 0.30 | 1.37 | 13.7 | 0.0 | 13.7 |
| Nov | 3 | Deve | 0.31 | 1.43 | 14.3 | 0.0 | 14.3 |
| Dec | 1 | Deve | 0.46 | 2.12 | 21.2 | 0.0 | 21.2 |
| Dec | 2 | Deve | 0.65 | 3.00 | 30.0 | 0.0 | 30.0 |
| Dec | 3 | Deve | 0.85 | 3.94 | 43.4 | 0.0 | 43.3 |
| Jan | 1 | Mid | 0.96 | 4.49 | 44.9 | 0.0 | 44.9 |
| Jan | 2 | Mid | 0.96 | 4.52 | 45.2 | 0.0 | 45.2 |
| Jan | 3 | Mid | 0.96 | 4.54 | 49.9 | 0.0 | 49.9 |
| Feb | 1 | Mid | 0.96 | 4.55 | 45.5 | 0.1 | 45.5 |
| Feb | 2 | Mid | 0.96 | 4.57 | 45.7 | 0.1 | 45.7 |
| Feb | 3 | Late | 0.89 | 4.39 | 35.1 | 0.1 | 35.0 |
| Mar | 1 | Late | 0.76 | 3.90 | 39.0 | 0.2 | 38.8 |
| Mar | 2 | Late | 0.61 | 3.26 | 32.6 | 0.2 | 32.4 |
| Mar | 3 | Late | 0.53 | 2.58 | 5.2 | 0.0 | 5.2 |
| | | | | | **484.3** | **0.9** | **483.5** |

Figure 3. 5 crop water requirements for potato (for one irrigation season)

Crop water demand is the quantity of water required to irrigate the crop; it is computed as the difference between crop evapotranspiration and effective rainfall according to (Pereira et al., 2015).

Table 3. 2 total available water (Pereira et al., 2015)

| Soil | Crop | Max root depth, Zr | Field capacity, $\Theta_{Fc}$ | Wilting point, $\Theta_{WP}$ | Depletion fraction, p |
|---|---|---|---|---|---|
| Loamy sand | Potatoes | 0.45m | 0.17 | 0.06 | 0.35 |

The quantity of water a crop can collect from its root zone is referred to as total available water (TAW). It is computed as follow:

$$TAW = (\Theta_{Fc} - \Theta_{WP}) \times Z_R \quad \text{..... 3.6}$$

$$TAW = (0.17 - 0.06) * 450mm$$

$$TAW = 49.5mm\ per\ irrigation$$

Crops can only draw water from soil to a particular depth, which is known as effective rooting depth (Zr), and soil water availability is the soil's ability to maintain water available to the plant.

The quantity of water that a well-drained soil can hold against gravitational force is known as field capacity (FC).

Wilting point (WP): As water intake increases, the remaining water becomes more firmly linked to soil particles, decreasing its potential energy and complicating plant extraction. Because water availability till wilting point is just theoretical, actual readily available water (RAW) is the proportion of TAW that can be drawn from the root zone without experiencing water stress.

The average percentage of total accessible soil water that may be withdrawn from the root zone is represented by (P) and it is provided on the table for various crops and soil types (Pereira et al., 2015).

$$\text{RAW} = \text{(TAW) P} \quad \text{..... 3.7}$$

$$RAW = 49.5mm \times 0.35 = 17.32mm$$

### 3.4.1 Net depth application of water

Net depth application ($d_{net}$) is the quantity of water that should be applied during irrigation to replenish the water which is lost due to evapotranspiration which is equal to readily available water.

$$d_{net} = \text{RAW} = 17.32\text{mm}$$

### 3.4.2 Irrigation frequency at peak water requirement

Irrigation frequency (I) is the time it takes a crop to deplete the soil moisture at a given soil depletion level. The maximum irrigation interval for potato farm is calculated as equation below:

$$\text{I} = \frac{\text{H}_\text{w} \times \text{D}_\text{w} \times \text{D}_\text{A}}{\text{ET}_\text{c}} + 1\text{day} \quad \text{..... 3.8}$$

Where, $H_w$ =soil water holding capacity in mm/m (table 4.3)

Dr=root zone depth (m)

DA=allowable depletion, Potato can be irrigated at 35% depletion of available soil moisture without losing any significant yield (Rossi Pisa & Bigaran, 1990).

$ET_C$=peak daily evapotranspiration (mm/day)

$$I = \frac{80mm/m \times 0.45m \times 0.35}{4.99\ mm/day} + 1day = 3.39days$$

Therefore, the system should deliver 17.32mm of water every 3.39 days. To avoid the fraction of days, the irrigation frequency has to be 3 days.

Soil Water Holding Capacity: Soil serves as the reservoir for plant nutrient and water needs. Soil has a finite capacity to hold water against gravity.

Table 3. 3 water holding capacity of agricultural soils (Olorunfemi et al., 2016)

| | Water holding capacity (mm/m) | |
|---|---|---|
| Soil type | Average | Range |
| Sand | 80 | 50-110 |
| Loamy sand | 80 | 60-120 |
| Sandy loam | 130 | 110-150 |
| Loam | 150 | 110-180 |
| Silt loam | 150 | 110-190 |
| Silt | 170 | 120-200 |
| Silty clay loam | 150 | 120-180 |
| Silty clay | 150 | 110-190 |
| Clay | 150 | 100-200 |

### 3.4.3 Irrigation scheduling

To determine how much water is required to be applied the soil moisture condition should be known. At ideal conditions, the irrigation schedule is set to manage optimal agricultural production at the expense of minimal water use and cost. Though crop growth stage, climatic condition, and soil moisture are the factors that determine the depth of irrigation schedule by using fixed and center pivot irrigation systems it is possible to attain a nearly perfect irrigation schedule.

#### 3.4.3.1 Gross depth of water application

The gross depth of water ($d_{gross}$) application is calculated by dividing the net depth application by the irrigation efficiency (E).

$$d_{gross} = \frac{d_{net}}{E} \quad \text{..... 3.9}$$

Irrigation efficiency of the farm depends on the average temperature of the site including the losses through the pipes (Pereira et al., 2015).

Table 3. 4 farm irrigation efficiency for different climate

| Climate | Irrigation efficiency |
|---|---|
| Cool | 80% |
| Moderate | 75% |
| Hot | 70% |
| Desert | 65% |

Since the average temperature of the Samira village is 18$^{o}$C, according to FAO the climatic condition is classified as moderate with corresponding irrigation efficiency of 75%.

$$d_{gross} = \frac{d_{net}}{E} = \frac{17.32mm}{0.75} = 23.1mm$$

### 3.5 Preliminary system capacity

The amount of flow rate or discharge of the irrigation system at which the water is supplied from the source to farmland is defined as preliminary system capacity (Qs).

$$Q_s = \frac{A * d_{gross}}{I} \quad \text{..... 3.10}$$

Where, A is total area to be irrigated

$d_{gross}$ gross depth of water according to the irrigation frequency (I)

$$Q_s = \frac{1 \text{ hectare } \times 10 \times 23.1 \text{ mm}}{3.39 \text{days}} = 68 \text{ m}^3/\text{day}$$

The system has to be capable of providing $68m^3$ of water per day which is the irrigation water requirement for the vegetation.

#### 3.5.1 Design flow rate of the system

The pump's design flow rate is based on the operation's estimated daily potato irrigation water requirement divided by the number of peak sun hours per day, as shown below.

Average sun hour per day = 5.7(table 4.1)

$$\text{design flow rate} = \frac{68\text{m}^3/\text{day}}{5.7 \text{ peak sun hour} * 60 \text{ min/hour}} = 0.20\text{m}^3/\text{min}$$

#### 3.5.2 Water storage sizing

A water storage tank is usually a necessary component of a cost-effective for hybrid wind and solar powered water pumping system. In the case of overcast weather or power system maintenance difficulties, a tank can be utilized to store enough water during peak energy output to satisfy water requirements. The tank should be large enough to hold at least three days' worth of water from solar or wind alone.

Most publications advocate storing solar or wind-water pumps separately for 4-6 days on overcast days. However, because this is a solar and wind energy hybrid system, the wind and solar will not change at the same time. As a result, conserving water for 4-6 days is not necessary. The water storage for this study must only hold enough water for three additional days to meet the needs of the irrigation requirement.

The minimum storage capacity for a three-day supply is obtained using the water need indicated in Section 4.4 with an additional $2m^3$ of water for evaporative and other loss.

$$\text{water storage volume} = 68\,{}^{m^3}/_{\text{day}} \times 3\text{day} + 2m^3 = 206m^3$$

As a result, the reservoir volume should be $206m^3$

Water tank cost ranges between 4 cents per gallon to over $1.20 per gallon (Vertical Water Storage Tanks | U.S. Plastic Corp., 2019), however, for our country since the labor is cheap, 3 cents per gallon is enough. Therefore a cost for our storage tank is:

$$54419.4 gallon \times \$0.03/gallon = \$1632$$

### 3.5.3 Selection and sizing of piping material

Pipe materials are devices through which the fluid can passes. There are many types of pipes are there among these Concrete pipe, PVC pipe, HD pipe are some of them, but the best pipe designed for irrigation water supply must be free from any chemical composition, corrosion and also be cost-effective, and also its selection based on the fluid property of the materials.

There are three key issues to consider when choosing pipe materials. The pipe used must fulfill the system's mechanical requirements, be corrosion resistant enough to avoid corrosion build-up, and be cost-effective. The most desirable piping material for water pumping applications, according to the McGraw-Hill Piping Handbook, is Polyvinyl Chloride (PVC) piping. PVC schedule 40 piping material has a yield strength of $\sigma_{ys}$=57,571,223.3N/$m^2$. Schedule 40 PVC is less expensive than schedule 80 and has a larger inner diameter. It will be applied to all pipelines. All the piping for the system will be 11/2inch diameter with a conversion factor of 25.4mm, with a nominal wall thickness of t= 3.68mm, an outer diameter of do= 48.26mm, and an inner diameter of di = 40.894mm [appendix A]. It is locally fabricated by the Oromia Pipe factory with a joint venture between Oromia Water Works Construction Enterprise (Government-owned enterprise) and Golden Trade Company.

In order to ensure that the pipes in the system will not burst it is necessary to compute the maximum allowable pressure for the pipe. The maximum allowable pressure rating for the piping material is determined from the hoop stress experienced when the material is

stressed at its yield strength. For thin-walled pressure vessels where the ratio of the wall thickness to the outer diameter is less than or equal to 10%, Barlow's formula provides an accurate representation of the maximum allowable pressure in the pipe. Barlow's formula, which is given by:

$$\sigma_{ys} = \frac{pd_o}{t} \Rightarrow p_{max} = \frac{2t\sigma_{ys}}{d_o} \quad \text{..... 3.11}$$

For Schedule 40 pipe the ratio t/do=0.10, and by applying Equation 4.11 it is determined that $p_{max}$=12341615.5N/$m^2$.

The price of selected pipe for 6m length (with effective length of 5.8m) is 900birr with a 15% tax (Oromia Pipe Factory PLC, 2019).

The total length is 284m and the effective length can be calculated as:

$$\frac{284}{5.8} = 49 pieces$$

Therefore, 49 pieces of pipes are required. The total price is:

$$49 pieces \times 900 birr = 44{,}100 birr$$

Changing to dollar:

$$\frac{44{,}100}{44.30} = \$995.4$$

**3.6 Hydraulics of drip irrigation system**

The mainline, sub-mains, and laterals of a drip irrigation system are all constructed of plastic pipes. The design of a drip irrigation system must guarantee almost equal dripper discharge in each segment regulated by a valve and watered as a unit of the system. A maximum pressure difference of 23% is permitted in a system, and the maximum pressure differential between the head and tail ends of a lateral should not exceed 9%. Manufacturers' catalogs can provide information on the connection between pressure and discharge for various types of emission devices. The pressure loss can be calculated using tables from monographs or formulae expressing relationships. The friction between the pipe walls and the water as it travels through the system causes head loss. Turns, curves, pipe expansions and contractions, and other obstacles in the path of flow enhance head losses.

To compute the pressure head, the following assumptions were made:

- Size of the land: one hectare ($100m \times 100m$) potato to be irrigated
- Dripper spacing:1.5m
- Emitter spacing:1.3m
- Land slope: $7^o$
- Depth of water source: 2m

Water required for the whole field per day was then obtained above to be $68m^3$/day and the pump design flow rate is $12m^3$/hr. As a result, the irrigation time (h) was calculated as follows;

$$\text{irrigation time (h)} = \frac{\text{water requirement } (m^3/day)}{design\ flow\ rate(m^3/hr)} \quad \text{.....3.12}$$

$$\text{irrigation time (h)} = \frac{68\,m^3/day}{12\,m^3/hr} = 5.7\,hr/day$$

Number of emitter per potato plant is taken to be $2Lh^{-1}$

Number of emitter per lateral is calculated:

$$\text{Number of emitter per lateral} = \frac{\text{Lateral length}}{\text{emitter spacing on lateral}} \quad \text{.....3.13}$$

$$\text{Number of emitter per lateral } = \frac{100\text{m}}{1.3\text{m}} = 77$$

$$\text{Discharge through one lateral}(Q_{lateral}) \ = 77 \times 2\text{L}h^{-1} = 154Lh^{-1}$$

### 3.6.1 Determining lateral total length

The total Length (LL) required by laterals as shown in (4.14) is obtained by dividing the total area ($m^2$) to be irrigated by minimum row spacing length in meters (Roberts & O'Hern, 1990).

$$\text{LL} = \frac{\text{total area to be irrigated}}{\text{row length}} \quad \text{.....3.14}$$

Where, row length is 1.5 for potato (Rossi Pisa & Bigaran, 1990)

$$LL = \frac{100m \times 100m}{1.5m} = 6{,}666.67m$$

### 3.6.2 Total discharge required ($T_{ds}$)

The total lateral discharge is obtained from (4.15) by dividing the product of lateral total length and Emitter flow rate (LPH) of the selected lateral by emitter spacing in meters.

$$T_{ds} = \frac{LL \times \text{emitter flow rate}(Lh^{-1})}{\text{emitter spacing}(m)} \quad \ldots\ldots 4.15$$

Table 3. 5 typical spacing of emitters of 2 & 4 L h-1 discharge for different soil texture (Kifle & Gebretsadikan, 2016)

| Emitter capacity($Lh^{-1}$) | Type of soil | Emitter spacing(cm) |
|---|---|---|
| $4Lh^{-1}$ | Sandy soil | 60 |
| | Medium soil | 100 |
| | Fine soil | 130 |
| $2Lh^{1}$ | Sandy soil | 30 |
| | Medium soil | 130 |
| | Fine soil | 100 |

Since the irrigation rate considered is $2Lh^{-1}$ and soil type is medium soil emitter spacing 1.3m.

$$T_{ds} = \frac{6{,}666.67m \times 2Lh^{-1}}{1.3m} = 10{,}256.42Lh^{-1}$$

$$\text{Number of emitter per one manifold} = \frac{T_{ds}}{Q_{lateral}} \quad \ldots\ldots 3.16$$

$$\text{Number of emitter per one manifold} = \frac{10{,}256.42lh^{-1}}{154lh^{-1}} = 66.6$$

So the number of emitter per one manifold is 67 and breadth of the field is 100m with distance between two laterals is 1.5m

$$\text{total number of lateral} = \frac{\text{breadth of feild}}{\text{raw spacing}} + 1 \quad \text{.....3.17}$$

$$\text{total number of lateral} = \frac{100\text{m}}{1.5\text{m}} + 1 = 68$$

$$\text{Q}_{\text{manifold}} = \text{Qmain} = \frac{\text{Q}_{\text{latera}} \times \text{total number of lateral}}{\text{no of emitter per one manifold}} \quad \text{..... 3.18}$$

$$\text{Q}_{\text{manifold}} = \frac{154\text{lh}^{-1} \times 68}{67} = 156.3\text{lh}^{-1}$$

(Jamil, 2019) studied the total energy drop by friction for lateral can be expressed as in equation (4.18)

$$\text{H}_L = 5.35 \times \frac{\text{Q}^{1.852}}{\text{D}^{0.871}} \times \text{L} \quad \text{..... 3.19}$$

Where, H = total energy drop by friction at the end of lateral (m)

Q = total discharge at the inlet of lateral (l/sec)

D = inside diameter of lateral (0.40894cm)

L = length of lateral in (100m)

$$\text{H}_L = 5.35 \times \frac{0.043^{1.852}}{0.40894^{0.871}} \times 100 = 3.43\text{m}$$

### 3.6.3 Head loss in the mainline

The Darcy-Weisbach, Hazen Williams or Scobey equation can be used to compute head loss due to friction, $H_f$. The general form of these equations can be written as

$$\text{H}_\text{f} = \frac{\text{KcLQ}^\text{m}}{\text{D}^{2\text{m+n}}} \quad \text{..... 3.20}$$

Where, K = friction factor that depends on pipe material

L = length of pipe, m

Q = flow rate (4.1lmin$^{-1}$)

D = diameter of pipe, mm

c, m, n = constants can be obtained from Table 4-6

Table 3. 6 constants of friction loss equations (Source: G. Allen, 1996)

| Equation for computing $H_f$ | C | M | N |
|---|---|---|---|
| Darcy-Weisbach | 277778 | 2.00 | 1.00 |
| Hazen-Williams | 591722 | 1.85 | 1.17 |
| Scobey | 610042 | 1.90 | 1.10 |

For the Darcy-Weisbach equation, K is given by the equation

$$K = 0.811\left(\frac{f}{g}\right) \quad \text{3.21}$$

$$V = \frac{Q}{A} \quad \text{3.22}$$

$$V = \frac{156.3 l/s}{\frac{\pi(40.894 mm)^2}{4}} = 0.12\ m/s$$

$$R_e = \frac{Vd}{\nu} \quad \text{3.23}$$

$$R_e = \frac{0.12 m/\sec * 0.040894 m}{0.5 * 10^{-5}\ m^2/_s} = 9815$$

For Re between 2000 and 10,000 (turbulent flow)

$$f = 0.32 R_e^{-0.25} = 0.32 \times 9815^{-0.25} = 0.032$$

$$K = 0.811\left(\frac{0.042}{9.81}\right) = 2.7 \times 10^{-3}$$

Where, Re= Reynolds number (dimensionless); D = diameter of pipe;

ρ = density of water; V = average velocity;

μ = viscosity of the fluid; K = unit constant,

f = friction factor can be obtained from Reynold number equation

g = acceleration due to gravity (9.81 m $s^{-2}$)

$$H_m = \frac{2.7 \times 10^{-3} \times 6{,}666.67\text{m} \times 277778 \times (4.1\text{lmin}^{-1})^2}{40.894\text{mm}^{2\times2+1}} = 0.74\text{m}$$

The total mainline loss is calculated as:

$$\text{total mainline presure loss} = H_m \times \text{total number of laterals} \quad \text{.....3.24}$$

$$\text{total presure loss} = 0.74\text{m} \times 68 = 50.32\text{m}$$

As a result, the length of mainline (the reservoir's head) is calculated as total mainline pressure loss multiplied by a correction factor of 1.3.

$$L = 50.32\text{m} \times 1.3 = 65\text{m}$$

Determination of Operating Pressure (Ho):
The operating pressure is the sum of the lateral and mainline head. This is given by the relationship:

$$Ho = Hm + HL \quad \text{..... 3.25}$$

$$Ho = 65m + 3.43m = 67.1m$$

### 3.6.4 System layout design for drip irrigation system

The next step is to design the layout of the irrigation system. As illustrated in Figure (4-6), we will need to figure out all of the essential distances and altitudes for the intake point, pump, and water tank. Based on the site-specific data, the site has good south-facing exposure and is well suited for solar and wind power. Flow from the tank to the field will be by gravity. The natural arrangement of the site, based on the available elevations, offers an appropriate height difference between the tank and the field. In addition, the pump, controller and PV panels, and a wind turbine can all be located in close proximity to one other in order to minimize electric power losses. Figure (4-6), is a profile of the proposed layout showing all the related information needed to pump water into the irrigation field.

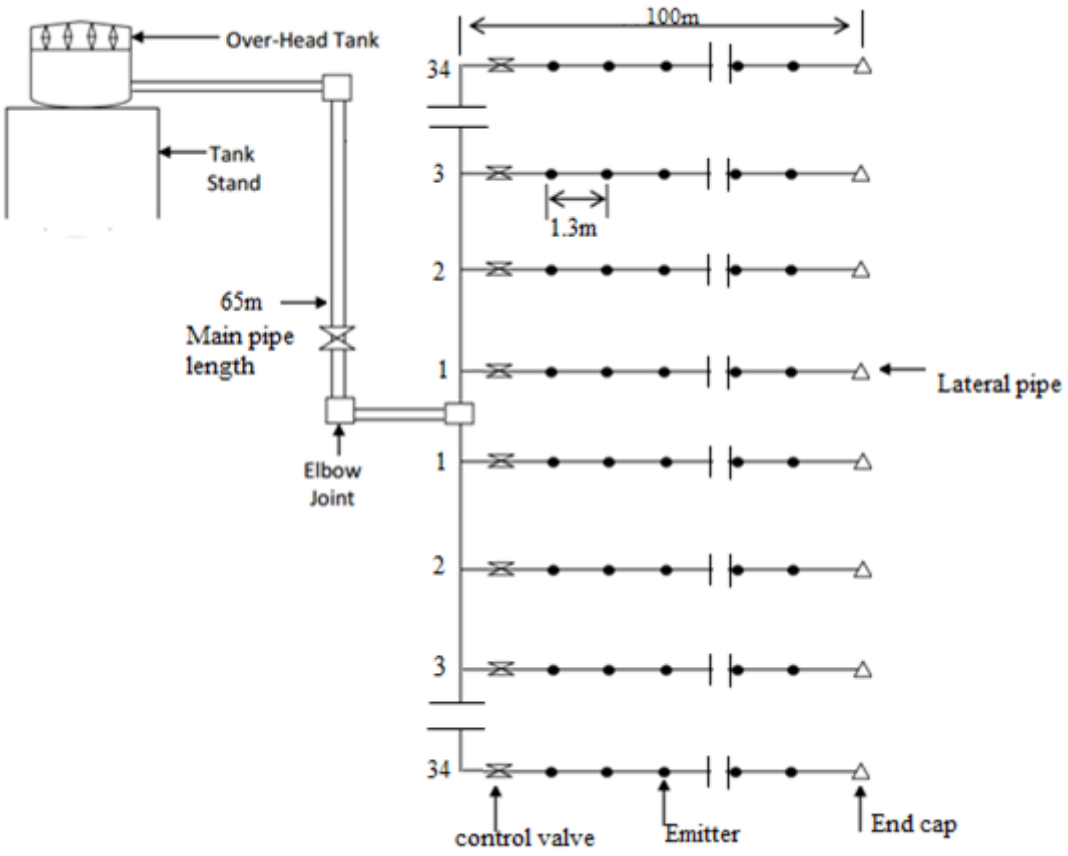


Figure 3. 6 schematic layout of the Gravity Drip Irrigation System

### 3.7 Performance characteristic of piping system

A system-head curve is a graphical illustration of the flow-hydraulic-loss relationship in a specific piping system. Each system has its own distinctive curve and unique values since hydraulic losses are factors of rate flow, pipe size and length, number, and type of fittings. The system curve is frequently unaffected by pump characteristics.

#### 3.7.1 Static head of the system

Static head is the vertical distance between the water surface at the intake point (the river's water surface) and the water surface at the delivery point (the reservoir).

As calculated in section (4.5.3) the water surface at the delivery point is 65m and the water depth is 2m.

Therefore, static head (H) = 65m +2m = 67m

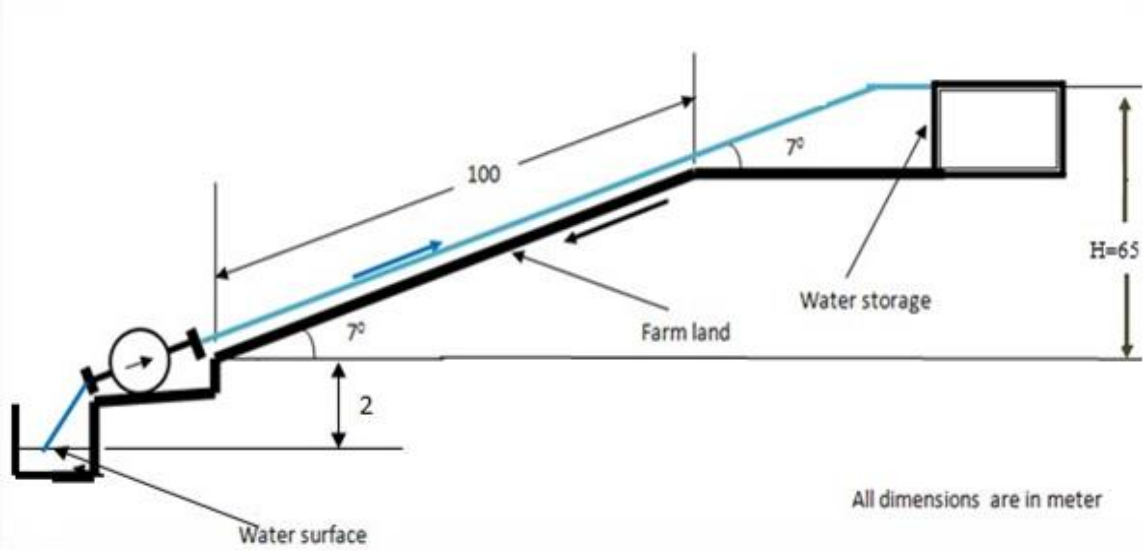


Figure 3. 7 static head of the system

### 3.7.2 Head loss due to friction

Friction loss in fluid flow is the loss of pressure or "head" that happens in a pipe owing to the viscosity of the fluid near the pipe's surface. All liquids have momentum because they have weight. This implies the liquid will strive to keep flowing in the same direction at all times. When a liquid changes direction (such as an elbow), the momentum of the liquid drives the flow to the fitting's outer edge, reducing the effective area of the fitting. The velocity of the liquid increase and the head loss due to friction increases.

Since the system has three elbows and two valves (foot valve and check valve), other valves (gate valves) that are found between water storage and field are not considered because the flow is fed by gravity. The following is a general formula for calculating system head loss due to friction:

$$h_f = h_{pipe} + 3 * h_{elbow} + h_{fv} + h_{cv} + h_{screen} + \text{velocity loses} \quad \ldots\ldots 3.26$$

Consider design flow rate of the system, Q = 0.20$m^3$/min = 0.0033$m^3$/sec

Average velocity,

$$V = \frac{Q}{A} \quad \ldots\ldots 3.27$$

Where, $A = \pi\frac{d}{4} = \pi * (0.040894m)^2/4 = 0.0013m^2$

$$V = \frac{0.0033\text{m}^2/\text{sec}}{0.0013m^2} = 2.5\text{m/sec}$$

Table 3. 7 common pipe materials

| Material | Roughness (m) |
|---|---|
| Steel | 0.0003 |
| PVC | 0.0000015 |
| Copper | 0.0000015 |

For PVC, roughness (ε) is, ε = 1.5*10$^{-6}$m and relative roughness

$$\text{r} = \frac{\varepsilon}{\text{d}} = \frac{1.5 * 10^{-6}\text{m}}{0.040894\text{m}} = 3.7 * 10^{-5}$$

Reynold number

$$R_e = \frac{Vd}{\nu} = \frac{2.5m/\text{sec} * 0.040894m}{0.5 * 10^{-5}} = 20447$$

**Darcy friction factor**

The Darcy friction factor in turbulent flow is determined from the Moody diagram (Appendix-D) or by solving it from the Blasius, Swamee-Jain, or Haaland equations (4.26).

For calculating the Darcy friction factor, the Blasius equation is the simplest. The Blasius equation is only applicable for smooth pipes since it lacks a term for pipe roughness. However, due to its simplicity, the Blasius equation is sometimes employed in rough pipes.

The Blasius equation is valid up to the Reynolds number $10^5$. The Blasius equation is:

$$\text{f} = \frac{0.316}{\text{R}_\text{e}^{0.25}} \quad \text{..... 3.28}$$

Where, f = Darcy friction factor

$R_e$ = Reynolds number

$$f = \frac{0.316}{20447^{0.25}} = 0.043$$

Swamee and jain have developed the following equation to the darcy friction factor

$$f = 0.25\left[\log\left(\frac{r}{3.7} + \frac{5.74}{R_e^{0.9}}\right)\right]^{-2} \quad \text{3.29}$$

For, r is relative roughness

$$f = 0.25\left[\log\left(\frac{3.7 * 10^{-5}}{3.7} + \frac{5.74}{20447^{0..9}}\right]^{-2} = 0.042\right.$$

The accuracy of the Darcy friction factor solved from this equation is claimed to be within about 2 %, if the Reynolds number is greater than 3000.

From the moody diagram, f = 0.043

From the Blasius equation, f = 0.043

From swamee-jain equation, f = 0.042

Now, calculating all possible losses, taking the approximate Darcy friction factor f = 0.043

Loss coefficient for pipe components,

$$h_{pipe} = f\frac{L}{D}\frac{V^2}{2g} \quad \text{3.30}$$

$$h_{pipe} = 0.043 * \frac{115m}{0.040894m}\frac{\left(2.5\frac{m}{sec}\right)^2}{\left(2 * 9.81\frac{m}{sec^2}\right)} = 15.4$$

From Appendix-C for long radius 45$^o$ flanged elbow, the Kr value is 0.2

Loss coefficient for elbow components,

$$h_{elbow} = K_r * \frac{V^2}{2g} \quad \text{3.31}$$

There are three elbows in the system layout

$$h_{elbow} = 0.2 * \frac{(2.5\,{}^{m}/_{s})^2}{2 * 9.81\,{}^{m}/_{sec^2}} * 3 = 0.076m$$

**Foot valve,** a check valve positioned at the water intake is the foot valve. It is necessary for any scenario when the pump is higher than the source's water level. To avoid losing prime, choose a high-quality spring-loaded kind. Water can only flow in one way through a check valve. Make sure you install it correctly.

$$h_{fv} = K_r \frac{V^2}{2g} \quad \text{..... 3.32}$$

For a piston foot valve $K_r$ value is 15

$$h_{fv} = 15 * \frac{(2.5\,\mathrm{m/sec})^2}{2 * 9.81\,\mathrm{m/sec^2}} = 4.78\mathrm{m}$$

**Check Valve at the pump outlet,** a check valve at the pump outlet is required if there is more than a 10 m/30ft lift above the pump, or in any pressurizing system. This makes it easier for the pump to start. When replacing filter cartridges, it also prevents backflow.

$$h_{cv} = K_r \frac{V^2}{2g} \quad \text{..... 3.33}$$

For disk type check valve $K_r$ value is 10

$$h_{cv} = 10 * \frac{(2.5\,\mathrm{m/sec})^2}{2 * 9.81\,\mathrm{m/sec^2}} = 3.18\mathrm{m}$$

Velocity loss;

$$\text{velocity loss} = \frac{V^2}{2g} \quad \text{.....3.34}$$

$$\text{Velocity loss} = \frac{(2.5\,\mathrm{m/sec})^2}{2 * 9.81\,\mathrm{m/sec^2}} = 0.32\mathrm{m}$$

Assuming a 0.15m loss for the screen, the overall friction loss is:

$$h_f = 15.4 + 0.076 + 4.78 + 3.18 + 0.32 + 0.15 = 24\mathrm{m}$$

Total dynamic head (TDH) of the piping system

To determine total dynamic head of the system; use the following equation:

$$\mathrm{TDH} = \text{static head} + \text{friction losses} \quad \text{.....3.35}$$

$$\mathrm{TDH} = 67\mathrm{m} + 24\mathrm{m} = 91\mathrm{m}$$

### 3.8 Water pumping technology

A pump is a mechanical device that uses suction pressure to lift, move, convey, and compress fluids. Sizing of a pump for the water pump involves matching the fluid flow rate and pressure rating of a pump required for a specific process. A pump that can create a

high enough pressure to overcome the hydraulic resistance of the systems, such as pipes and valves, is required for mass flow rate. The system head refers to the hydraulic resistance. It is defined as the amount of pressure necessary in the system downstream of the pump to produce a particular flow rate.

### 3.8.1 Types of water pump

For hybridized wind and PV power water pumping applications, there are two types of pumps that are typically utilized. Positive displacement and centrifugal pumps are the two types of pumps. Low-volume pumps utilize a positive displacement pump. Centrifugal pumps have relatively high efficiency and can pump a large amount of water. The most fundamental distinction between a reciprocating and a centrifugal pump is that centrifugal pumps employ the kinetic energy of their impeller to constantly provide fluid. Fluid is discharged continuously using centrifugal pumps. A centrifugal pump was chosen for this system because of its capacity to pump fluids with high viscosity.

Using irrigation pump selector software, the centrifugal pump was selected appropriately at a head of 91m and a flow rate of $12m^3$/hr.

Specification of selected pump:

| | |
|---|---|
| Type | franklin electric |
| Model | 75FH3S6-PE |
| Application | water pumping for irrigation |
| Max. Head | Up to 104m |
| Motor type | 3 phase |
| Normal speed | 360RPM |
| Rated power | 7.5Kw |
| Efficiency | 61% |

Depending on the power required and head of selected pump, the price of pump and motor differs (FRANKLIN ELECTRIC Submersible Pump, 2021). Therefore, for the selected

system the estimated price of pump and motor is $8,000 including the tax, transportation and others.

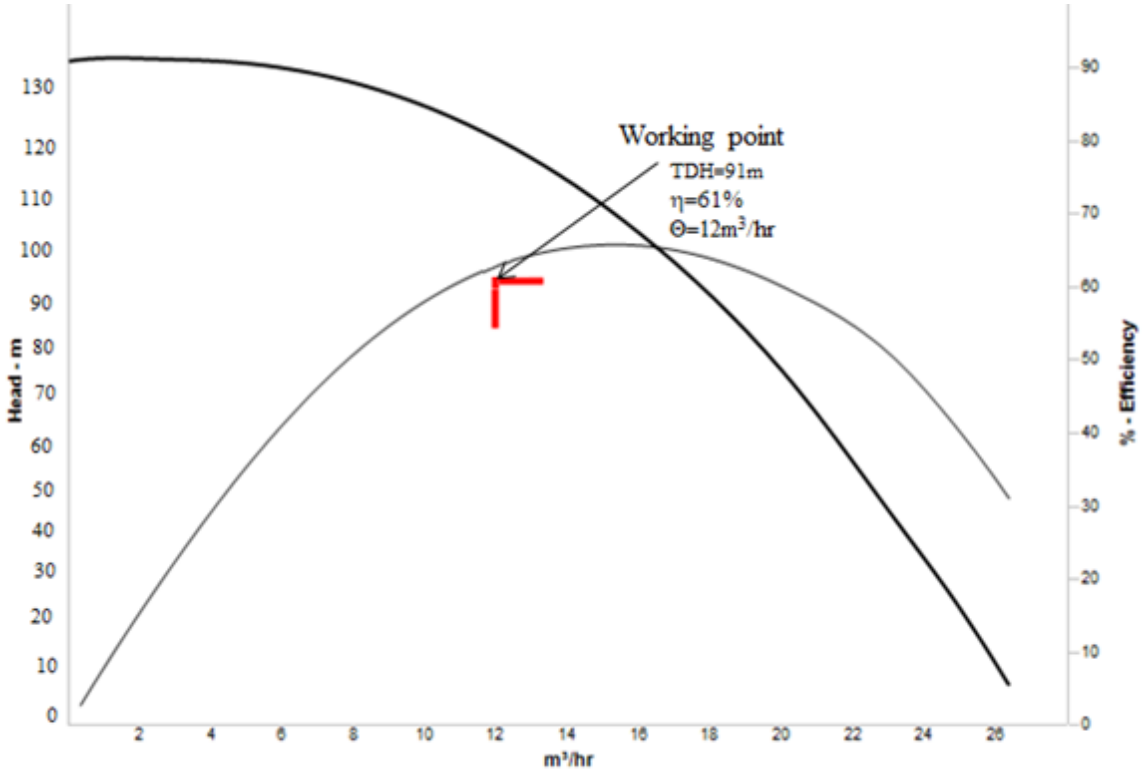


Figure 3. 8 selected pump curve

### 3.8.2 Working point

The TDH-flow pair corresponding to the pump function is the working point, taking into consideration the pipe system's head-losses. When the pump is turned on, it reaches a certain operating point, which corresponds to the balance of flow and TDH.

A graph showing the pipe system's characteristic curve is constructed in advance to establish this functioning point. Calculating the head-losses for various theoretical flows in the system yielded this graph (figure 4.8). The point where this curve intersects with the pump's characteristic curve is the pump's working point in the pipe system (Figure 4-9). As a result, the pump flow rate at the working point (Qw) is 200 l/min, the pump head at the working point (Hw) is 91m, and the pump efficiency at the working point ($\eta_w$) is 61%.

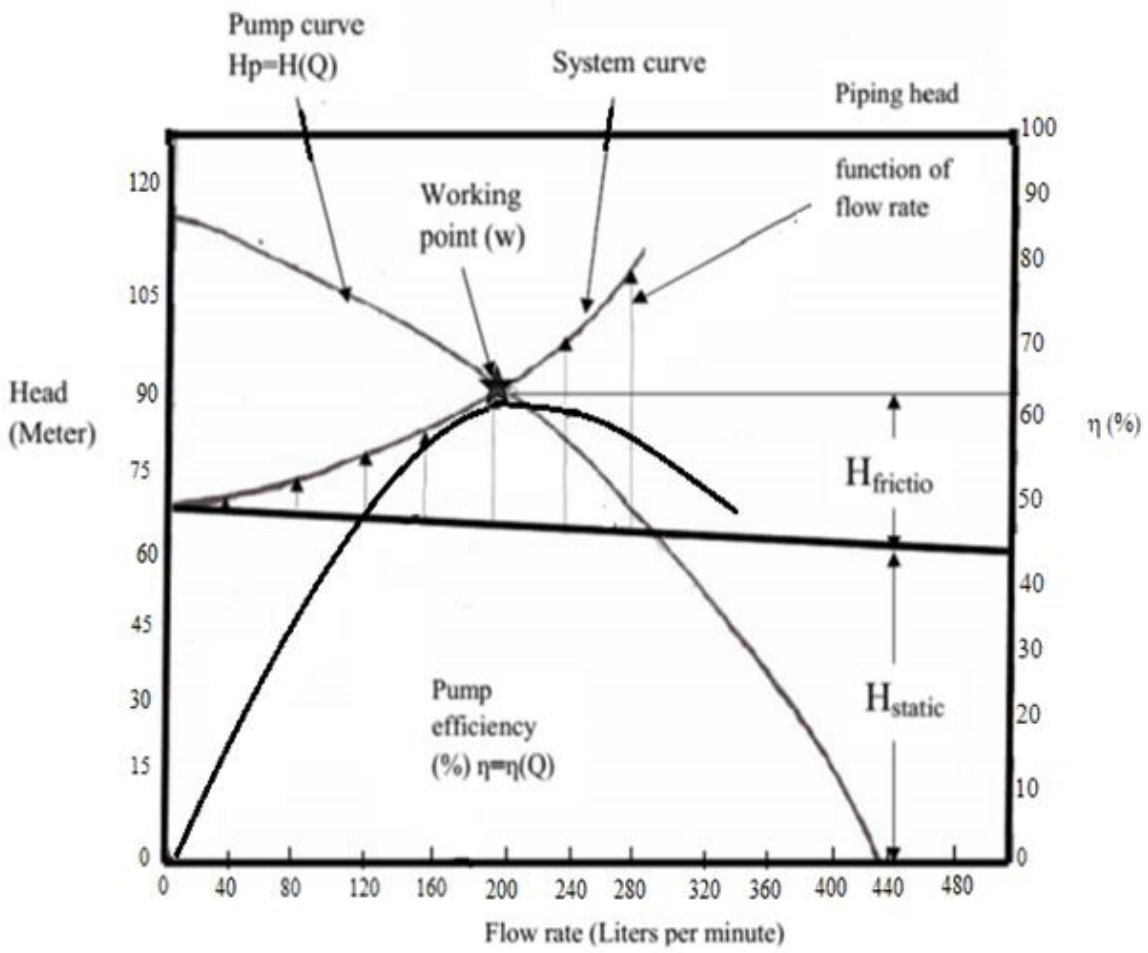


Figure 3. 9 system working point

### 3.8.3 Power of pump

The pump that selected must handle the flow rate required and the power associated with it is hydraulic power, $P_h$

$$P_h = \rho g Q_w H_w \ldots\ldots\ldots\ldots\ldots\ldots\ldots\ldots\ldots\ldots\ldots\ldots\ldots\ldots\ldots\ldots\ldots\ldots 3.36$$

Where; $P_h$ = hydraulic power in W

$\boldsymbol{\rho}$ = density of water (1000kg/$m^3$)

g = gravity of earth (9.81m/$sec^2$)

$Q_w$ =volume flow rate of water ($m^3$/sec)

H = Total Dynamic Head (m)

$$p_h = 1000 \times 9.81 \times 0.0033 \times 91 = 2946w = 2.95kW$$

$$\eta_{syst} = \frac{p_h}{p_{ew}} = \frac{2.95kW}{7.5kW} = 39.3\%$$

Where, $\eta_{syst}$ is System efficiency at working point and pump input power at working point is 7.5kW.

$$\mathrm{p_{mech}} = \frac{p_h}{\eta_{pw}} = \frac{2.95kW}{0.61} = 4.76kW$$

Where, $\eta_{pw}$ = pump efficiency at working point and pump efficiency at working point is 61%

$$\text{System efficiency} = \text{pump efficiency} \times \text{motor efficiency} = 0.39$$

From this relationship motor efficiency at working point is: $\eta_{mw} = \frac{0.39}{0.62} = 0.63$

But, $\eta_{mw} = \frac{p_m}{p_e}$

Where, $\eta_{mw}$ is motor efficiency at working point

$$p_e = \frac{p_m}{\eta_{mw}} = \frac{4.76kW}{0.63} = 7.56kW$$

### 3.8.4 Cavitation

When pump pressure drops below vapor pressure vapor bubbles will form. If the pressure increases above the vapor pressure downstream, the bubbles will collapse. Such a phenomenon is called “cavitation.” They often occur in pumps, hydroelectric turbines, pipe valves, and ship propellers.

Problems caused by cavitation are;

- ✓ Degrades the performance
- ✓ Fluctuates the flow rate and head
- ✓ Pitting causes physical damage to impellers
- ✓ Noise and vibration

#### 3.8.4.1 Net positive suction head (NPSH)

Net Positive Suction Head (NPSH) is a number that is used to assess whether the pumping pressure is vulnerable to cavitation or not. Available NPSH (NPSHa) and required NPSH

(NPSHr) are determined to prevent the condition of cavitation. The required net positive suction head at the pump's entry is 2m in this scenario.

The ambient pressure head minus all losses in suction piping (upstream side of the pump), vapor pressure, and velocity head in the suction pipe, and static lift equals available NPSH (NSPHa). According to the equation in

$$NSPH_a = 8.185m - 2m - 0.25m - 0.32m - 0.978m = 4.637m$$

Where; Atmospheric pressure, at 1930m above mean sea-level, $h_{atm} = 8.185m$ (appendix E)

Vapor pressure, for water at $20^0$, $h_{vap} = 0.25m$

Friction loss in suction piping, $h_f = 0.978m$

Velocity loss, $h_v = 0.32m$

The center of the surface pump is 2 meters above the water surface in a static suction lift.

**Requirement to avoid cavitation**

- Cavitation is expected if NPSHr = NPSHa.
- If $NPSH_r \leq NPSH_a$, there would be no cavitation
- As the available NPSH drops below the required value, cavitation will become stronger, efficiency will drop, and the flow rate will decrease, at the same point, the pump would “break suction” and the flow rate will go to zero

The available net positive suction head is larger than the required net positive suction head, based on the results. As a result, cavitation is not an issue in the proposed system.

### 3.8.5 Solar insolation and PV panel location and wind velocity data

The following table shows the average wind velocity of Samira for the last 10 years.

Table 3. 8 average wind speed of the site

| Years | Jan | Feb | Mar | Apr | May | Jun | Jul | Aug | Sep | Oct | Nov | Dec |
|---|---|---|---|---|---|---|---|---|---|---|---|---|
| 2011 | 4.36 | 4.85 | 2.39 | 2.01 | 2.05 | 4.10 | 5.12 | 2.05 | 1.64 | 3.63 | 3.40 | 3.56 |
| 2012 | 5.01 | 2.95 | 2.40 | 2.86 | 3.20 | 2.86 | 2.33 | 2.14 | 2.35 | 3.02 | 3.28 | 3.96 |
| 2013 | 4.90 | 4.20 | 2.08 | 3.50 | 2.22 | 3.10 | 2.07 | 3.21 | 3.23 | 2.85 | 3.01 | 2.79 |
| 2014 | 4.60 | 3.90 | 2.98 | 2.80 | 2.75 | 3.65 | 2.15 | 2.31 | 2.15 | 2.49 | 2.14 | 2.98 |
| 2015 | 4.20 | 4.30 | 3.80 | - | 3.24 | 5.10 | 1.98 | 2.96 | 1.99 | 3.09 | 5.10 | 3.15 |
| 2016 | 4.00 | 4.70 | - | - | - | - | 1.89 | - | 1.89 | 2.32 | 2.94 | 4.10 |
| 2017 | 4.34 | 4.50 | 2.14 | 2.73 | 3.12 | 2.96 | 1.78 | 3.52 | 2.84 | 3.97 | 2.95 | 3.55 |
| 2018 | 2.50 | 3.60 | 2.84 | 2.38 | 2.15 | 2.83 | 2.98 | 2.88 | 1.98 | 3.03 | 2.89 | 2.57 |
| 2019 | 4.85 | 4.36 | 2.40 | 3.10 | 4.23 | 3.20 | 2.16 | - | 2.98 | 2.21 | 2.62 | 2.70 |
| 2020 | 3.60 | 4.12 | 3.85 | 2.27 | 2.30 | 2.26 | - | - | - | 1.97 | 4.21 | 3.35 |
| AWV (m/s) | 4.35 | 4.18 | 2.76 | 2.71 | 2.81 | 3.34 | 2.49 | 2.72 | 2.34 | 2.86 | 3.25 | 3.27 |

Note that in table 4.8 the line (-) indicates the months in which its wind velocity is not measured due to different reasons.

The data taken from the Ethiopian meteorological office is in m/s, therefore there is no need to convert it to SI units before using it in the program that will be used in the following chapter. The wind data collected is approximately identical to that gathered at the same location, although it is not accurate and there is some variation from the location.

The figure we chose for both sunlight hour and wind velocity is the minimum result because the sunshine hour increases as we go from Goljota town to Samira village.

As we give the input for the software, it will give the viability of the wind turbine, and the type of the wind turbine that is selected is specified by the person depending on the situation of the site such as the availability of the road, the price of the turbine, and other. More of it will be explained in the next chapter.

### 3.8.6 Calculation of solar radiation based on the data given in a monthly average solar sunshine hour

The extraterrestrial radiation for each day of the year and different latitudes is estimated from the solar constant, the solar declination, and the time of the year is calculated as discussed in chapter 2:

$$Ra = \frac{24*60}{\pi} G_{sc} d_r [\omega_s \sin(\varphi) \sin(\delta) + \cos(\varphi) \cos(\delta) \sin(\omega_s)]$$

Where;

Ra = extraterrestrial radiation [$MJm^{-2}day^{-1}$]

$G_{sc}$ = solar constant

$d_r$ = inverse relative distance sun-earth

$\omega_s$ = sunset hour angle (rad)

$\varphi$ = latitude (rad)

$\delta$ = solar declination (rad)

The inverse relative distance earth-sun, $d_r$, and the solar declination ($\delta$), are given by;

$$d_r = 1 + 0.033\cos(\frac{2\pi}{365} n)$$

$$\delta = 0.409 \sin \frac{2\pi}{365} n - 1.39$$

Where n is the number of the day in the year and given in the following table;

Daylight hours are given by;

$$N = \frac{24}{\pi} \omega_s$$

For N is daylight hour and $\omega_s$ is calculated by above formula

Table 3. 9 the representative date of the month (Duffie et al., 1994)

| Months | n for $i^{th}$ day of the month | Date | Day of the year |
|---|---|---|---|
| Jan | I | 17 | 17 |
| Feb | 31+i | 16 | 47 |
| Mar | 59+i | 16 | 75 |
| Apr | 90+i | 15 | 105 |
| May | 120+i | 15 | 135 |
| Jun | 151+i | 17 | 162 |
| July | 18+i | 17 | 198 |
| Aug | 212+i | 16 | 228 |
| Sept | 243+i | 15 | 258 |
| Oct | 273+i | 15 | 288 |
| Nov | 304+i | 14 | 318 |
| Dec | 334+i | 10 | 334 |

The sun set hour angle, $\omega_s$, is given by;

$\omega_s = \cos^{-1}[-\tan(\varphi)\tan(\delta)]$

Table 3. 10 monthly average solar sun shine hour and calculated solar radiation in kwh/m2day for the Semira village

| Years | Jan | Feb | Mar | Apr | May | Jun | Jul | Aug | Sept | Oct | Nov | Dec |
|---|---|---|---|---|---|---|---|---|---|---|---|---|
| 2011 | 9.05 | 7.22 | 6.9 | 4.98 | 3.34 | 1.59 | 1.34 | 2.19 | 2.69 | 6.70 | 7.85 | 7.31 |
| 2012 | 8.37 | 5.42 | 5.15 | 3.65 | 3.12 | 1.73 | 2.30 | - | 3.28 | 7.44 | 7.12 | 7.40 |
| 2013 | 8.04 | 4.33 | 4.82 | 3.63 | 1.55 | 1.53 | - | - | 3.04 | 7.63 | 7.81 | 7.20 |
| 2014 | - | 5.86 | - | - | - | 3.91 | - | - | - | 7.71 | 7.89 | - |
| 2015 | - | 5.43 | 4.71 | 3.82 | 4.58 | 1.59 | 1.85 | 2.62 | 3.46 | 7.80 | 7.01 | 6.89 |
| 2016 | 8.23 | 4.90 | 7.97 | 3.19 | 1.52 | 1.71 | 4.42 | 3.30 | 4.39 | 8.14 | 8.13 | 8.39 |
| 2017 | 8.54 | 6.35 | 5.17 | 2.17 | 6.63 | 7.61 | 5.07 | - | 4.02 | 7.89 | 8.63 | 9.60 |
| 2018 | 8.85 | 7.51 | 7.04 | 4.89 | 7.02 | 6.08 | 7.91 | 4.97 | 6.35 | 7.30 | 9.23 | 8.64 |
| 2019 | 9.65 | 8.32 | 7.92 | 6.41 | 7.21 | 6.24 | 4.34 | 6.60 | 3.86 | 7.40 | 6.94 | 8.58 |
| 2020 | 7.81 | 7.79 | 6.14 | - | - | 7.12 | 7.58 | - | 4.71 | 8.13 | 8.65 | - |
| Aver. sum sunshine hour | 8.70 | 6.31 | 6.08 | 4.01 | 4.29 | 3.91 | 4.34 | 3.83 | 4.00 | 7.61 | 7.97 | 8.00 |
| Rad($MJm^{-2}day^{-1}$) | 18.6 | 14.2 | 14.2 | 9.3 | 9.6 | 8.5 | 9.6 | 8.7 | 9.3 | 17.3 | 17.2 | 16.9 |
| Rad($kWh/m^2day$) | 5.2 | 4.0 | 4.0 | 2.6 | 2.7 | 2.4 | 2.7 | 2.4 | 2.6 | 4.8 | 4.8 | 4.7 |

The final result of solar radiation in $kWh/m^2day$ is used as input data for the average daily radiation of the site, which is used by the program to analyze the system.

To get maximum sun exposure and optimize the solar-powered system's energy output, the panels should be oriented south with no substantial shade in their proximity. The tilt of the PV panel in our country should be towards the southern half, which is the equator.

# CHAPTER 4

# HYBRID ENERGY SYSTEM MODELLING WITH HOMER

HOMER (Hybrid Optimization Model for Electric Renewables) is a computer model for hybrid-power optimization created by the United States. To aid in the design of micro-power systems and to simplify the comparison of power production technologies across a wide variety of applications, the National Renewable Energy Laboratory (NREL) was established (Shiroudi et al., 2012).

HOMER can model grid-connected and off-grid micro-power systems for electric and thermal loads that include photovoltaic (PV) modules, wind turbines, small hydro, biomass power, reciprocating engine generators, fuel cells, batteries, and hydrogen storage.

Because of the enormous number of design possibilities and the uncertainty in critical characteristics such as load size and future fuel price, analyzing and designing hybrid-power systems may be difficult. Renewable energy sources add to the complexity by varying, seasonal, and non-dispatchable power generation, as well as the uncertainty of renewable resource supply. HOMER was created to address these issues.

Simulation, optimization, and sensitivity analysis are the three main activities that HOMER does. HOMER evaluates the technical feasibility and life-cycle cost of a hybrid-power system configuration by simulating its performance for each hour of the year. HOMER simulates several possible system configurations throughout the optimization process to find the one that fulfills the technical criteria at the lowest life-cycle cost. HOMER uses several optimizations under a variety of input assumptions to evaluate the impacts of uncertainty or changes in model inputs throughout the sensitivity analysis phase. The ideal value of variables over which the system designer has control, such as the assembly of system components and the size or amount of each, is determined via optimization. The impact of uncertainty or changes in factors over which the designer has no control, such as average wind speed or future fuel price, can be assessed using sensitivity analysis.

The image below depicts the link between simulation, optimization, and sensitivity analysis. To reflect the fact that a single optimization comprises numerous simulations, the optimization oval encloses the simulation oval. Similarly, because a single sensitivity

analysis consists of numerous optimizations, the sensitivity analysis oval spans the optimization oval.

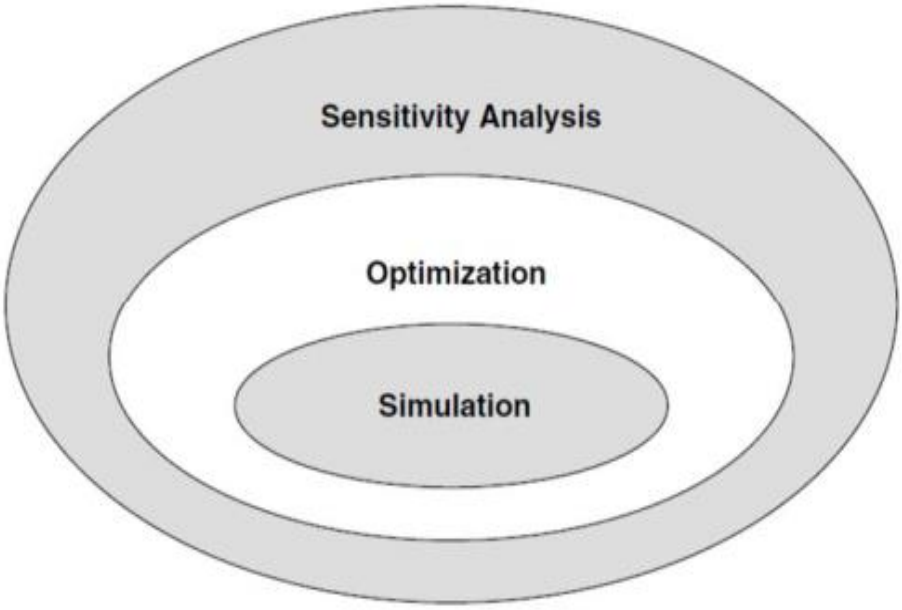


Figure 4. 1:relationship between simulation, optimization and sensitivity analysis ("Optimization of Hybrid Renewable Energy System Using Homer," 2019)

Limiting input complexity and allowing for quick enough processing to enable optimization and sensitivity analysis feasible;

- The simulation logic of HOMER is less detailed than that of several other time-series simulation models for hybrid-power systems, including;
  - PV-Design pro,
  - Hybrid2, and
  - PV-SOL.
- HOMER, on the other hand, is more comprehensive than statistical models like RET Screen, which does not undertake time-series simulations.
- HOMER is the most adaptable Hybrid-power modeling system in terms of the variety of systems it can mimic ("Optimization of Hybrid Renewable Energy System Using Homer," 2019)

**4.1 Simulation**

Simulating the long-term operation of a hybrid-power system is one of HOMER's primary skills. This simulation capacity is essential for optimization and sensitivity analysis. The

simulation method establishes how a certain system arrangement, a hybrid of system components of different sizes, and an operating strategy that describes how those components interact, will behave in a given context over time.

The simulation approach accomplishes two goals.

1. Determines the system's practicality. If the system can efficiently fulfill the electric, deferrable or thermal loads, as well as fulfill any additional limits given by the user, HOMER deems it practical.
2. It calculates the system's life-cycle cost, which is the overall cost of installing and operating the system over its entire lifespan. A useful statistic for evaluating the economics of various system configurations is the life-cycle cost.

The total net present cost is the number HOMER uses to represent the system's life-cycle cost (NPC). All expenses and revenues that occur over the project's lifetime are included in one single value, with future cash flows discounted to the present.

The following items are included in the total net present cost:

- the system components' initial capital cost
- Component maintenance and operation costs that occur during the project lifetime

HOMER models how the system operates for a year, assuming that the primary simulation findings for that year (surplus power production) are indicative of all subsequent years in the project's lifetime. It does not take into account changes over time, such as load growth or battery performance decline as batteries age. Many of these impacts, however, may be examined via sensitivity analysis by the modeler.

The simulation input data for our thesis analysis are as follows:

1. Deferrable load
2. The detailed components
    - The PV
    - The Wind Turbine
    - The Converter
3. Resource detail
    - Wind resource

- Solar resource

### 4.2 Optimization

The optimization process identifies the optimum potential system configuration, despite the fact that the simulation process simulates a specific system configuration. The best conceivable, or optimum, system design in HOMER is the one that meets the user's restrictions at the lowest total net present cost. Finding the best system design may entail determining the components that should be included in the system, the size or amount of each component, and the system's dispatch technique. HOMER simulates several various system configurations, discards the infeasible ones (those that do not match the user supplied criteria), ranks the feasible ones according to total net present cost, and offers the viable one with the lowest total net present cost as the ideal system configuration throughout the optimization process.

The optimization method seeks to determine the ideal value of each decision variable of interest to the modeler. A decision variable is a variable that is within the control of the system designer and for which HOMER can examine numerous alternative values throughout the optimization process. The following are some of the decision factors that might be used in HOMER to analyze the hybrid water pumping system:

- The number of wind turbines
- The size of the PV array
- The size of the converter

As a result, during system optimization, different types of solar PV arrays, different numbers of wind turbines, and different types of converters are sent to the program, and the software subsequently optimizes based on net present cost of the system.

### 4.3 Sensitivity analysis

During the optimization process, HOMER seeks the system configuration that is best under a given set of user input assumptions. During the sensitivity analysis, HOMER executes numerous optimizations, each with a unique set of user input assumptions. A sensitivity analysis demonstrates how responsive the outputs are to changes in the inputs.

The HOMER user inputs a range of values for a single input variable in a sensitivity analysis. A sensitivity variable is one for which the user has supplied several values

(numerical input). We employed the following fundamental sensitivity factors in our thesis for software analysis:

- Wind resource
- Deferrable load
- Solar resource

The primary use of sensitivity analysis is to cope with uncertainty. If a system designer is unsure about the value of a variable, they can input many values that span the anticipated range and examine how the results change over time. Sensitivity analysis has another application aside from uncertainty. Sensitivity analysis may be used by a system designer to examine trade-offs and answer problems like;

- How much extra capital expenditure is required to achieve renewable energy generation of 50% or 100%?
- Under varied situations, an energy planner can determine which technologies, or combinations of technologies, are best.
- A policy analyst can determine how much of an incentive is required to boost the market for a particular technology, or how much of an emissions penalty is required to shift the economics toward cleaner technologies.
- A market analyst can figure out how much a product costs or under what conditions it competes with replacements.

### 4.4 Physical modelling

A hybrid-energy that must be included in HOMER;

- The electrical or thermal energy source (in our case, wind turbine and solar PV)
- Conversion device (converter)
- That energy's final destination (in our case, water pumping for potato irrigation)
- Energy storage device (in our case, water tank)

### 4.5 Loads

The term “load” in HOMER refers to a demand for electric or thermal column energy. Serving a large number of people is the reason for the existence of micro-power systems, thus the modeling of the micro divinity system intersects with the modeling of the load or loads that the system must assist (Lambert et al., 2006).

HOMER models three different kinds of loads.

1. Electrical Load: the amount of electrical demand that the power system must fulfill at a given moment. Primary load is often characterized as the electrical demand associated with computers, lighting, TV, household appliances, radio,stove, and industrial activities.
2. Deferrable Load: an electrical demand that can be satisfied at any moment during a specified time period. Deferrable loads include water pumps, battery charging stations, and ice machines. This is since the storage inherent in each of those loads provides some flexibility in terms of when the system can serve them. The flexibility to postpone supplying a demand is frequently helpful for systems comprised of intermittent renewable energy sources since it minimizes the requirement for exact control of power output schedule. This sort of load was chosen for our software study since the electric output is used for pumping water for potato irrigation rather than immediately for primary load.
3. Thermal Load: HOMER models thermal load in the same way as it models main electric load, with the exception that the thermal load does not have an operational reserve. The boiler, waste heat recovered from a generator, or resistive heating utilizing extra energy power is the system's thermal load.

**4.6 Economic modelling**

Economic modeling is crucial in both the reduction of total net present cost and the optimization process. It looks for the system configuration that has the cheapest total net present value. The cost characteristics of renewable and nonrenewable energy sources are often very different. Renewable energy sources have high initial capital costs but low running costs, whereas nonrenewable energy sources have cheap capital but high running costs. HOMER must often assess the economics of a wide range of system configurations containing various quantities of renewable and nonrenewable energy sources as part of its optimization process. Such comparisons must take into account both capital and operational expenditures to be fair. In a life-cycle cost study, all expenses that occur over the system's lifetime are included.

The total net present cost (NPC) is used by HOMER to represent a system's life-cycle cost. The total NPC condenses all project expenses and revenues into a single lump amount in today's dollars, with future cash flow discounted back to the present using the discount rate. The discount rate and project duration are specified by the modeler. The NPC covers

the expenses of original construction, component replacements, maintenance, fuel, as well as the cost of purchasing electricity from the grid and other costs like pollution fines. Revenues include money earned from selling electricity to the grid, as well as any salvage value realized at the end of the project's lifespan. The NPC has a positive cost structure but a negative income structure. The net present value is the polar opposite of this. As a result, the net present cost differs only in sign from the net present value.

Over the project's lifetime, HOMER assumes that all prices will rise at the same rate. With that assumption, inflation may be factored out of the analysis by discounting future cash flows energy to the present using the real (inflation-adjusted) interest rate rather than the nominal interest rate. The real interest rate, which is generally equal to the nominal interest rate minus the inflation rate, is consequently entered by the HOMER user. In HOMER, all expenses are real expenses, meaning they are expressed in constant dollars.

The modeler defines the initial capital cost, which occurs in year zero, the replacement cost, which occurs each time the component has to be replaced at the end of its lifetime, and the operation and maintenance cost, which occurs each year of the project's lifespan. Most components' lifetimes are specified in years by the user, although HOMER estimates the battery and generator lifetimes.

For a variety of reasons, a component's replacement cost may differ from its initial capital cost. A modeler could presume that a wind turbine nacelle will need to be replaced after 15 years, but that the tower and base will endure the whole project's life. The replacement cost would be significantly lower than the initial capital cost in that situation. Some or all of the original capital cost of a PV array may be covered by donor agencies or buy-down schemes, but not the replacement cost. The replacement cost may be more than the initial capital cost in this situation. The original capital cost of the diesel engine would be $0 when considering a refit of an existing diesel system, but the replacement cost would not (Lambert et al., 2006).

The following equation is used by HOMER to determine the salvage value of each component at the end of the project's life cycle:

$$S = c_{rep} \frac{R_{rem}}{R_{comp}} \quad \text{..... 4.1}$$

Where, S = Salvage value

$C_{rep}$ = replacement cost of the component

$R_{rem}$ = remaining life of the component

$R_{comp}$ = life time of the component

HOMER calculates the component's yearly cost by combining the capital, replacement, maintenance, and fuel expenses, as well as the salvage value and any other expenditures or income. This is the estimated yearly cost that, if incurred every year of the project's existence, would result in a net present cost equal to the sum of all the component's individual costs and revenues over the project's lifespan. The overall annualized cost of the system is calculated by combining the yearly costs of each component, as well as any other expenditure, such as fines for pollution emissions. This number is significant because HOMER utilizes it to determine the system's total net present cost and levelized cost of energy, which are both important economic figures of merit.

HOMER utilizes the following equation to determine net present cost (Lambert et al., 2006):

$$C_{NPC} = \frac{C_{ann;total}}{CRF_{(iR_{proj})}} \quad \text{..... 4.2}$$

Where; $C_{NPC}$ is total net present cost,

$C_{ann;total}$ is total annualized cost

CRF is the capital recovery factor

i is the annual real interest rate (the discount rate)

Rproj is the project lifetime

The following equation gives the capital recovery factor:

$$CRF\ (i, N) = \frac{i(1+i)^N}{i(1+i)^N - 1} \quad \text{..... 4.3}$$

Where, N is the number of the years

## 4.7 HOMER software steps for wind and solar PV hybridized energy water pumping system for irrigation

The HOMER processes are detailed in the eleven stages below. We begin by supplying HOMER with information, or inputs, about power system ideas that you are interested in. HOMER will simulate system configurations; provide a list of viable system designs, and order the list according to cost-effectiveness. In the third stage, you will do a sensitivity analysis using HOMER. The following are the general steps:

### 4.7.1 Create a question that HOMER can help you to answer

HOMER can provide answers to a wide range of issues concerning tiny power system design. Before you start working with HOMER, it is a good idea to have a clear notion of a question you would like HOMER to assist you with the answer. This thesis was prepared for a potato irrigation system in the Samira area during periods of low rainfall, especially two times a year production when the land is dry. As a result, the program is asked to answer the following question: "Is it possible to create a design capable of providing energy to pump water used for potato irrigation at the lowest possible cost to fulfill the deferrable load?"

### 4.7.2 Create HOMER file

A HOMER file holds all of the information needed to study power system designs, including technology possibilities, component pricing and resource availability.

### 4.7.3 Build schematic

In order to construct a power system, HOMER examines several technological possibilities. The schematic depicts all of the technological alternatives that you want HOMER to take into account; it is not a schematic of a specific system's setup. We design the schematic to provide information to HOMER about the components to consider, thereby addressing your inquiry. It is possible that the schematic may have components that are not in the best design. To develop the schematic for this thesis, the deferrable load, selected wind turbine, selected solar PV, and converter are graphically represented on the program. The wind resource, solar resource and other diagrams are also displayed. With this schematic, HOMER simulates the issue, "Is it possible to create a design capable of providing energy to pump water used for potato irrigation at the lowest possible cost to fulfill the deferrable load?"

HOMER shows buttons on the schematic that reflect the load and components (wind turbine, PV and converter). In the Resources section, HOMER displays buttons for the resources that each component will use (immediately below the schematic). In this scenario, the resources part of the design has buttons for wind and PV resources. There is a section under additional resources in front of the resource section (Economics, system control, Emissions, constraints).

### 4.7.4 Enter load detail

The load information is fed into the HOMER simulations. The load inputs specify the amount of electricity that the system must provide to meet the required water. The deferrable load is the sort of load that we utilize, and the average load that we manually populate the table with is determined as follows: The average daily water required is $68\text{m}^3/\text{day}$ and the pump can deliver $12\text{m}^3/\text{h}$.

The hours required to fulfill $68\text{m}^3/\text{day}$ with the pump that can deliver $12\text{m}^3/\text{h}$ is:

$$\frac{68\text{m}^3/\text{day}}{12\text{m}^3/\text{h}} = 5.7\,\frac{\text{hrs}}{day}$$

It would take the pump 5.7hrs at full power to meet the daily water requirement for irrigation, so the average deferrable load is 5.7hours per day times 7.56kW, which is:

$$7.56\text{kW} \times 5.7\,\text{hrs/day} = 43.1\,\text{kWh/day}$$

Pumping water requires 4.76kW of mechanical power. As a result, based on the above estimated number, we fill in the table below to show which months require more load and which months require less.

Table 4. 1:average monthly deferrable loads of the Samira village

| Month | Jan | Feb | Mar | Apr | May | Jun | Jul | Aug | Sep | Oct | Nov | Dec | Avr |
|---|---|---|---|---|---|---|---|---|---|---|---|---|---|
| Avr. load (Kwh/day) | 55 | 51 | 47.5 | 34 | 35 | 30 | 32 | 30.5 | 45 | 50 | 53.5 | 54 | 43.1 |

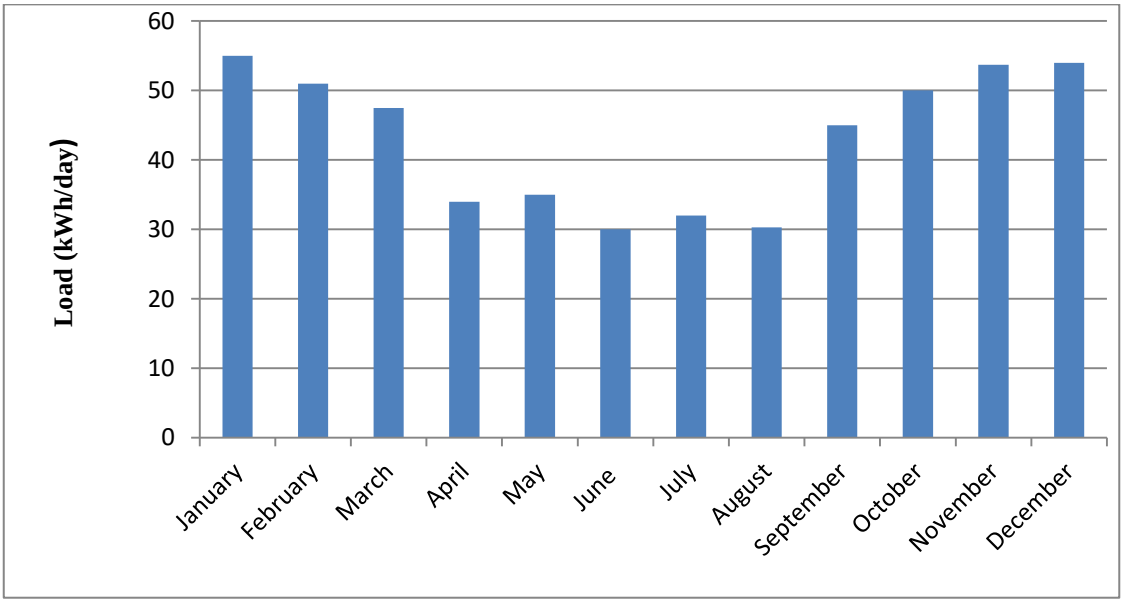


Figure 4. 2:average monthly deferrable loads

I. Base line data

The baseline data is a collection of 12 numbers for each month of the year that indicate the average deferrable load in kWh. The pace at which energy exits the deferrable load storage tank is known as the average deferrable load. As a result, it is the amount of energy necessary to maintain a constant level in the reservoir.

In the table on the left (table 5.1), enter the average deferrable load for each month of the year. The deferrable load is assumed to be constant during each month by HOMER. The yearly average deferrable load calculated by HOMER is displayed below the table. As you input the monthly average numbers, they are presented in the deferrable load graph.

II. Scaled data for simulation

For its computations, HOMER scales the baseline deferrable load data. HOMER divides each of the 12 baseline values by a common factor to produce an annual average value equal to the number you provide in Scaled annual average to scale the baseline data. HOMER divides the scaled yearly average by the baseline annual average to get the value

of this factor. The seasonal shape of scaled data is preserved, but the magnitude may be altered. The baseline annual average is the default value for the scaled yearly average. The scaled data and baseline are equivalent when the two values are equal. A scaled yearly average of zero is interpreted by HOMER to signify that there is no deferrable load.

III. Peak load

The greatest amount of power, in kW, that can supply the deferrable load is called the peak load. It is equal to the rated electricity consumption of the pump in a water pumping application. The peak load in our instance is 7.56kW, as computed in the previous chapter.

IV. Storage capacity

The storage capacity of a storage tank is represented as kWh of energy required to fill the tank. The time needed to fill the reservoir and the tank on an hourly basis is:

$$\frac{206m^3}{12\,{}^{m^3}/_{h}} = 17h$$

From this it take 17h to fill the tank. So the storage capacity is:

$$17h \times 4.76kW = 81kWh$$

So for the software analysis scaled annual average is 43.1kWh/d, storage capacity is 81kWh and peak load of 7.56kW is given as an input.

### 4.7.5 Cost data and size specifications of each component

The HOMER program is used to calculate the best optimum system size and feasibility research. The initial size of the component is determined by the site load profile. Some of the software's input values are stated in terms of size and quantity. Wind turbines, solar PV and converters are of different sizes. The primary goal of the effort is to identify the best power system design for meeting load demand while minimizing net present cost and cost of energy.

#### 4.7.5.1 Solar PV size and cost

A basic flat plate PV with a rated capacity of 1kW is used as the solar panel. The selected panel has 14 to 15% efficiency and costs $0.7 per watt and all cost is according to (China PV Solar Panel, Pv Solar Panel Manufacturers, Suppliers, Price | Made-in-China, 2020). The initial installation costs for solar PV is $910 considering transportation and taxes to

30% of costs obtained on internet and annual replacement, operating and maintenance costs of unit price to be 50($/yr.). This study used a solar PV array with a 25-year lifetime, a derating factor of 0.9, a reflectance of 20%, and no tracking system. The utilized solar PV panels have simulation values of 0, 4, 8, 10, 16, 20, 24, 28, and 32 in kW.

The capital cost is the original purchase price, the replacement cost is the cost of replacing the PV panels when they reach the end of their useful life (important only if the project life exceeds the PV array life), and the operating and maintenance cost is the yearly cost of operating and maintaining the PV array (often assumed to be zero). The following table (4.2) shows the cost of PV per kilowatt-hour.

Table 4. 2:the cost of the PV per kW

| Size(kW) | Capital($) | O&M ($/yr.) |
|---|---|---|
| 1.00 | 910 | 50 |

We specify the PV array sizes that HOMER should take into account while determining the best system. If the systems wish to examine systems without PV, we need to add a zero size. HOMER will compute the expenses of each PV array size based on the data we put in the cost table, interpolating and extrapolating as needed. The size indicated in the table below is dependent on the power demand.

Table 4. 3:the size of PV array to be considered during the simulation of the systems

| Size(kW) | 0 | 4 | 8 | 10 | 16 | 20 | 24 | 28 | 32 |
|---|---|---|---|---|---|---|---|---|---|

#### 4.7.5.2 Wind turbine size and cost

In this part, we provide input, choose the type of wind turbine to model, set its price, and tell HOMER how many to consider while it searches for the best solution.

The type of wind turbine selected critical attributes should be stated based on the turbines available in the HOMER program or on the internet. The power curve, which determines the turbine's power production over a range of wind speed, is the most important feature.

This graph is used to confirm that the wind turbine we choose is the correct size for our system.

We enter the wind turbine cost curve in as much information as we like in the cost table. In the most basic situation, when each wind turbine costs the same no matter how many are purchased, we only need to put one row of data into the cost table. We would input a quantity of one, as well as the capital, replacement, and operating and maintenance expenditures per turbine. HOMER extrapolates these costs as needed, so if we modeled a system with three wind turbines, the corresponding construction, operation and maintenance costs would be three times what is shown in the cost table (4-4).

It is important to note that the capital cost is the original purchase price, the replacement cost is the cost of replacing the wind turbine at the end of its lifespan (only significant if the project lifespan exceeds the wind turbine lifetime), and the operating and maintenance cost is the yearly cost of operating and maintaining the turbine (in this thesis typically about 20 percent of the capital cost is taken).

The number of wind turbines inputted should be determined by us as the number of factors that HOMER should take into account when searching for the best solution. We should include a zero since the program should take into account systems that do not have wind turbines. HOMER will determine the associated expenses using the information we supplied in the cost table, interpolating and extrapolating as needed. The cost curve graph below shows the results.

Bergey Wind power Co. (BWC) Excel

The BWC EXCEL is a contemporary 7 meter diameter, 10 kilowatt wind turbine that is intended for high dependability, minimum maintenance, and autonomous operation in inclement weather. It comes in three different versions: battery charging, water pumping, and grid-connected. The BWC Excel is a toughly constructed turbine with the industry's best guarantee (5 years).

BWC EXCEL battery chargers are available with outputs of 24, 48, 120, or 240V DC. For large rural residences, distant communities and amenities, eco-tourism destinations, and big telecommunication installations are also good candidates.

The BWC EXCEL, as a water pumper, may be placed up to 60 meters from the well to take advantage of better wind conditions.

At modest wind settings, the BWC EXCEL may provide the majority of the power for an average complete electric household when connected to the grid. The GridTek 10 power processor (inverter) is the industry's most sophisticated, with complete certification to the most recent utility requirements.

The BWC EXCEL is typically erected on a guyed lattice tower, which is available in heights ranging from 18 to 37 meters. The prices range between $5,000 and $7,500. For sites lacking crane access, tilt-up variants of these towers are available. The initial installation costs considered for our system is $11,200 considering transportation and taxes to 60% of costs obtained on internet and annual operating and maintenance costs to be 100($/yr.). There is a list of criteria for customer-supplied towers and costs are according to (Rue Henripré, 2020).

Excel-S 10.0 kW with GridTek Specifications:

| | |
|---|---|
| Start-up wind speed | 3.4m/s |
| Cut-in Wind Speed | 3.1m/s |
| Rated Wind Speed | 13.8ms |
| Rated Power | 10 kW (grid & pumping), 7.5 kW for battery-charging |
| Cut-Out Wind Speed | None |
| Furling Wind Speed | 15.6 m/s |
| Max. Design Wind Speed | 54 m/s |
| Type | 3 blades upwind |
| Rotor Diameter | 7 m |
| Blade Pitch Control | POWERFLEX® |
| Over speeds Protection | AUTOFURL |
| Gearbox | None, Direct Drive |
| Temperature Range | -40$^{o}$C to +60 $^{o}$C |
| Generator | Permanent Magnet Alternator |
| Output Form | 3 Phases AC, Variable Frequency |

Based on the following reasons, we chose this type of turbine for our system.

- Because the availability of electricity from a wind turbine is highly dependent on wind fluctuations, the Bergey Wind Power Co. (BWC) Excel wind turbine type was chosen for this system.
- For many years, the Bergey Wind Power Co. (BWC) Excel has been utilized for water pumping.
- Because the site's infrastructure is unsuitable for transportation, big wind turbines, which would reduce the system's cost, are not an option.
- The Bergey Wind Power Co. (BWC) Excel is inexpensive when compared to other wind turbines of same size.

Table 4. 4:the cost of the wind turbine per 10kW

| Quantity | Capital($) | O&M($/year) |
|---|---|---|
| 1 | 11,200 | 100 |

The size of the wind turbine is determined by the amount of electricity necessary for our system.

Table 4. 5:the size of wind turbine to be considered during the simulation of the systems

| Size(kW) | 0 | 7 | 8 | 9 | 10 | 11 | 12 | 13 | 14 | 15 | 16 | 17 |
|---|---|---|---|---|---|---|---|---|---|---|---|---|

The power output of the specified wind turbine at the available wind speed is displayed in the table and graph below. It depicts the property of the wind turbine that we have chosen.

Table 4. 6:the power extracted from selected wind turbine

| | Wind speed(m/s | Power output(kW) |
|---|---|---|
| 1 | 0.00 | 0.000 |
| 2 | 1.00 | 0.000 |
| 3 | 2.00 | 0.000 |
| 4 | 3.00 | 0.046 |
| 5 | 4.00 | 0.247 |
| 6 | 5.00 | 0.587 |
| 7 | 6.00 | 1.028 |
| 8 | 7.00 | 1.678 |
| 9 | 8.00 | 2.620 |
| 10 | 9.00 | 3.690 |
| 11 | 10.00 | 4.750 |
| 12 | 11.00 | 6.150 |
| 13 | 12.00 | 7.330 |
| 14 | 13.00 | 8.680 |
| 15 | 14.00 | 10.130 |
| 16 | 15.00 | 11.300 |
| 17 | 16.00 | 12.000 |
| 18 | 17.00 | 11.940 |
| 19 | 18.00 | 11.600 |
| 20 | 19.00 | 11.040 |
| 21 | 20.00 | 10.480 |
| 22 | 21.00 | 9.800 |
| 23 | 22.00 | 9.120 |
| 24 | 23.00 | 8.440 |
| 25 | 24.00 | 7.760 |
| 26 | 25.00 | 7.080 |

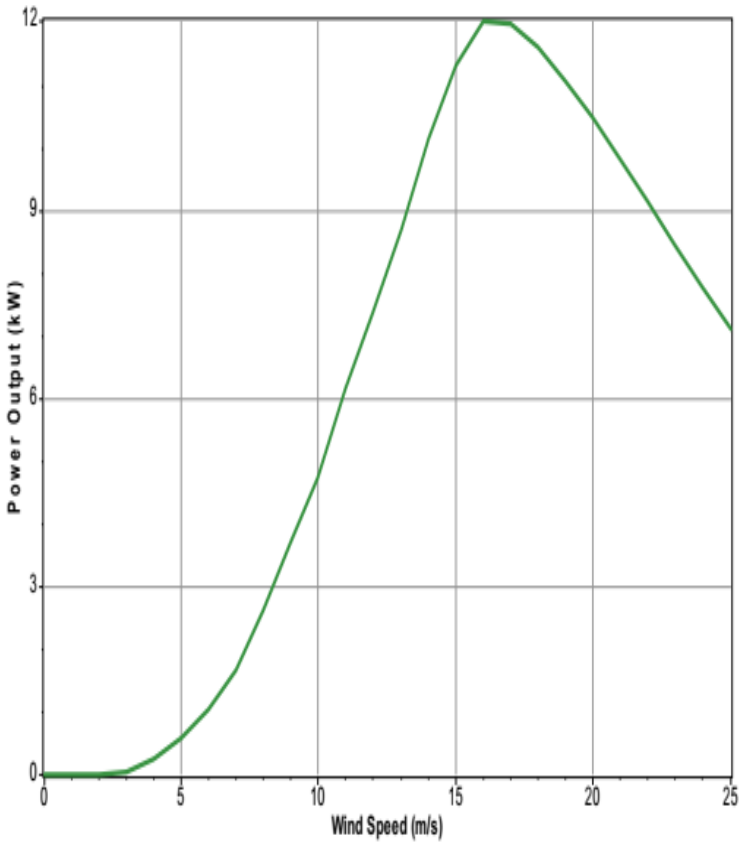


Figure 4. 3:the power curve of the selected wind turbine

#### 4.7.5.3 Converter size and cost

Any system that incorporates both AC and DC components necessitates the use of a converter. As a result, we must specify the converter's cost curve and select the sizes that we want HOMER to take into account as it searches for the best solution.

Enter the converter's cost curve in the cost table, which describes how its cost changes with size. Remember to include all expenses related to the converter, including installation, when calculating the capital and replacement expenses.

The capital cost is the initial purchase price of the converter, the replacement cost is the cost of replacing the converter at the end of its lifespan (important only if the project lifespan exceeds the converter lifespan, which it does not in our case), and the operating and maintenance cost is the annual cost of operating and maintaining the converter.

We must specify the converter sizes that we want HOMER to consider while determining the best solution. We provided zero sizes since we want to evaluate systems that do not use converters. HOMER will compute the expenses of each converter size based on the information we put in the cost table, interpolating and extrapolating as needed.

Table 4. 7:the cost of the converter with 25% tax and transportation addition from (AIMS POWER, 2020)

| Quantity | Capital($) | O&M($/year) |
|---|---|---|
| 3kW | 600 | 20 |

The size of the converter is supplied to the program as follows to optimize by utilizing it, depending on the need of the system that is converted to ac.

Table 4. 8:the size of the converter should take into account while optimizing systems

| Size(kW) | 0 | 10 | 20 | 30 | 40 | 50 | 60 | 70 | 80 |
|---|---|---|---|---|---|---|---|---|---|

### 4.7.6 Renewable energy resources assessment

The term "resource" refers to everything that comes from outside the system and is used by the system to create electricity. These are the resources of solar and wind. The placement of renewable resource is highly important. The solar resource is highly influenced by latitude and climate, whereas the wind resource is influenced by large-scale air circulation

patterns and geographic factors. Furthermore, a renewable resource at any one site may display significant seasonal and hour-to-hour fluctuation. Because the resource controls the quantity and time of renewable power generation, the type of the available renewable resources influence the behavior and economics of renewable power systems. As a result, proper modeling of renewable resource is a crucial component of system modeling. This section describes how to simulate the renewable resources used in this thesis.

#### 4.7.6.1 Solar energy resource

The latitude and amount of solar radiation accessible to the photovoltaic (PV) array throughout the year are specified here. This data is used by HOMER to compute the output of the PV array every hour of the year.

The latitude indicates your position on the Earth's surface. It is an essential variable in solar computations. It is used to calculate radiation levels from clearness indices and vice versa. It is also used to compute the radiation incidence on a slanted surface.

The baseline data consists of 8,760 values representing global average solar radiation on the horizontal surface, given in $kWh/m^2$, for each hour of the year. The solar resource table and graph by HOMER show the monthly average radiation and clearness index of the baseline data.

To produce baseline data, we have two options: we can use HOMER to synthesize data or we may import hourly radiation data from a file. HOMER is used to synthesize data in our situation.

In order to synthesize data, we enter twelve average monthly values of either solar radiation or clearness index, in our case average monthly solar radiation. We do not need to input both; HOMER will compute one from the other based on the latitude. Fill in the relevant row and column of the solar resource table with each monthly figure. As we add data into the table, HOMER generates a set of 8,760 solar radiation values, one for each hour of the year. The Graham algorithm is used by HOMER to generate the synthesized values, resulting in a data sequence with realistic day-to-day and hour-to-hour fluctuation and autocorrelation.

For computations, HOMER uses scaled data. HOMER scales data by multiplying each of the 8,760 baseline values by a common factor, yielding an annual average value equal to the scaled annual average value you provide. HOMER divides the scaled yearly average by

the baseline yearly average solar radiation to get the value of this component. The scaled data keeps the form and statistical properties of the baseline data, but the magnitude may change. The baseline yearly average solar radiation serves as the default value for the scaled annual average. The scaled data and baseline are the same when the two values are equal. A scaled yearly average of zero is interpreted as no solar radiation by HOMER.

Unit conversion and sensitivity analysis are two reasons to use a scaled yearly average instead of the baseline annual average.

Place: Samira
Latitude: 7 degrees 33 minutes North
Longitude: 38 degrees 54 minutes East
Time zone: GMT +3:00
Data source: Synthetic

Table 4. 9:the average daily radiation for each of the 12 months

| Month | Jan | Feb | Mar | Apr | May | Jun | Jul | Aug | Sep | Oct | Nov | Dec |
|---|---|---|---|---|---|---|---|---|---|---|---|---|
| Clearness index | 0.57 | 0.41 | 0.39 | 0.25 | 0.26 | 0.24 | 0.27 | 0.23 | 0.25 | 0.49 | 0.52 | 0.53 |
| Daily radiation ($kWh/m^2/day$) | 5.20 | 4.00 | 4.00 | 2.60 | 2.70 | 2.40 | 2.70 | 2.40 | 2.60 | 4.80 | 4.80 | 4.70 |

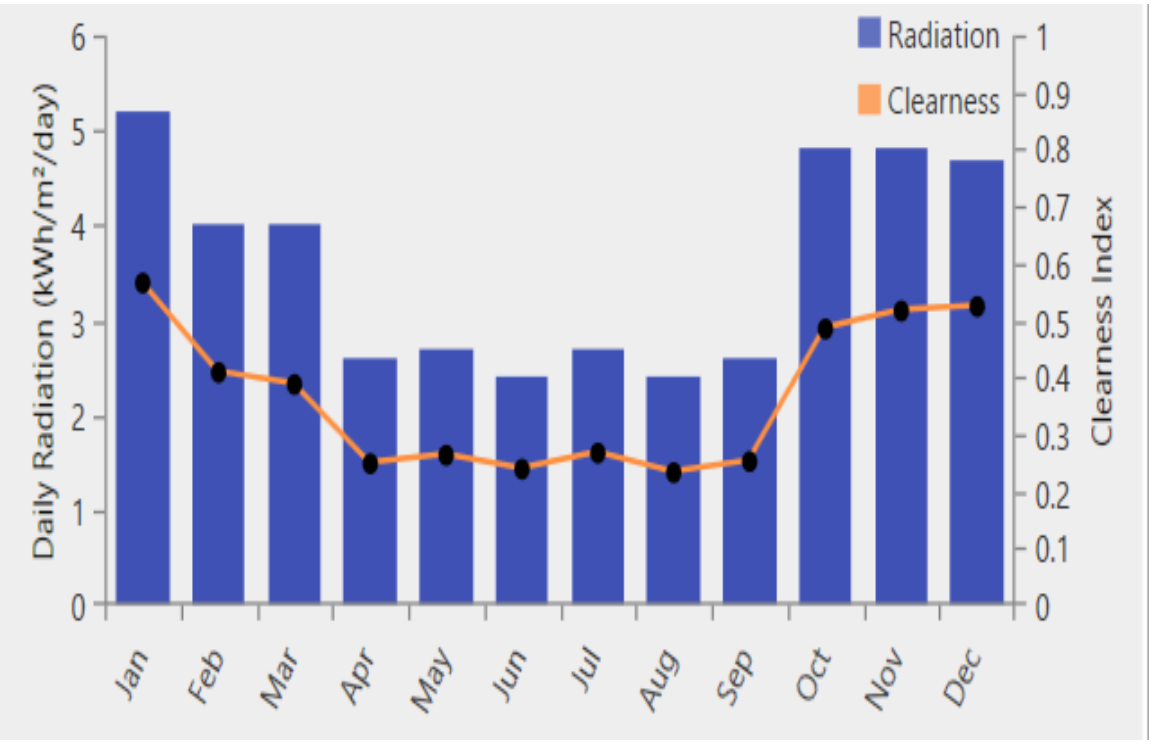


Figure 4. 4:the graph of the average daily radiation with respect to clearness index of the site

#### 4.7.6.2 Wind energy resource

The available wind resource for the site that we are working on is described here. This information is used by HOMER to determine the output of the wind turbine every hour of the year.

The baseline data consists of a collection of 8,760 values that indicate the average wind speed in meters per second for each hour of the year. In the wind resource table and graph, HOMER provides monthly averages generated from baseline data.

Using HOMER to synthesize data or importing hourly data from a file are the two methods for creating baseline data. Because the only data we have is the site's monthly average wind velocity, we employed the HOMER to synthesize data in our scenario.

We must enter twelve average wind speed figures to synthesize data: one for each month of the year. HOMER creates a collection of 8,760 values, or one wind speed value for each hour of the year when we put values in the table. Seasonal and daily trends, as well as the desired Weibull distribution and autocorrelation, are all present in the synthesized data series.

For computations, HOMER uses scaled data. HOMER scales data by multiplying each of the 8,760 baseline values by a common factor, yielding an annual average value equal to the value specified in the Scaled annual average. HOMER divides the scaled yearly average by the baseline annual average to get the value of this factor. The scaled data keeps the same structure and statistical features as the baseline data, but the magnitude may alter. The scaled yearly average's default value is the baseline annual average. The scaled data and baseline are equivalent when the two values are equal. A scaled yearly average of zero, according to HOMER, indicates that there is no wind resource.

Unit conversion and sensitivity analysis are two reasons to employ a scaled yearly average that differs from the baseline annual average.

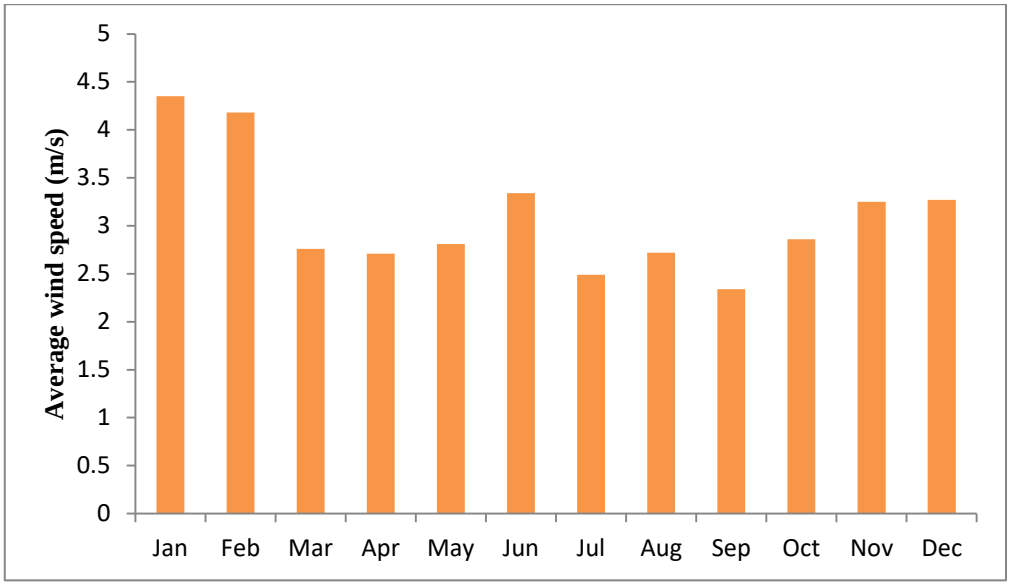


Figure 4. 5: the graph of average monthly wind speed for Samira

**4.8 Add sensitivity analysis**

HOMER simulates using scaled resource data based on the methods outlined above. This section explains how to enter sensitivity values for both the wind speed scaled yearly average and the solar radiation scaled yearly average in order to do sensitivity analysis on these variables. The sensitivity analysis will allow you to investigate how changes in average yearly wind speed and average yearly solar radiation impact the system's best design. Another way to put it is that the study will show you the range of average annual wind speeds and average yearly solar radiation for which we must consider the solar and wind hybridized energy, solar PV, or wind turbine alone when designing the system.

1. To open the Wind Resource Inputs panel, click Wind resource.
2. Fill in the Average Wind Speed sensitivity table with the values 2m/s, 2.5m/s, 3.5m/s, 4m/s, and 4.5m/s. Row 1 already has the basic value of 3.1m/s hard-coded in it.
3. Click a solar resource to open the solar Resource Inputs window.
4. Add the values 2kwh/$m^2$/d, 3kWh/$m^2$/d, 4kWh/$m^2$/d, and 6kWh/$m^2$/d to the Average solar radiation sensitivities table. Notice that the base value of 5.36kWh/$m^2$/d is already hard-coded into row 1.
5. To open the Sensitivity Input box, click the Scaled yearly average Sensitivities button.
6. Add the values 30kWh/d, 40kWh/d, 50kWh/d, 60kWh/d, and 70kWh/d to the average deferrable load table. Note that the base value of 43.1kWh/d is already hard-coded into row 1.

# CHAPTER 5

# RESULTS AND DISCUSSION

## 5.1 Optimization results

HOMER simulates system configurations using all of the component combinations given in the component inputs. HOMER eliminates any infeasible system configurations from the results, which are those that do not sufficiently satisfy the deferrable load given the available resource or the limitations you have set.

HOMER provides a list of the solar and wind hybridized energy system configurations that it determined were viable in the Overall Optimization Results table. They are sorted from most cost-effective to least cost-effective. A system configuration's cost-effectiveness is determined by its net present cost, which is reported in the result tables under the heading "Total NPC" That is, in this arrangement, a solar PV system is more practical than a PV and wind turbine hybridized energy system; however wind turbines alone are not practical.

### 5.1.1 PV system

When the HOMER Pro software evaluates PV alone, wind turbine alone and PV and wind hybridized energy systems, the PV system wins with 25kW PV, 30kW converter, Total NPC $47,494.90, and levelized cost of energy (COE) $0.363/kWh, based on net present cost. When we double-click a row in the optimization result to open the simulation results window for that system, the top of the window displays the system's components as well as three outputs: total net present cost, levelized cost of energy, and operational cost. The following tabs are available in this window:

#### 5.1.1.1 Cost of PV system

The cost summary tab provides the overall cash flow, which may be classified by component or cost category.

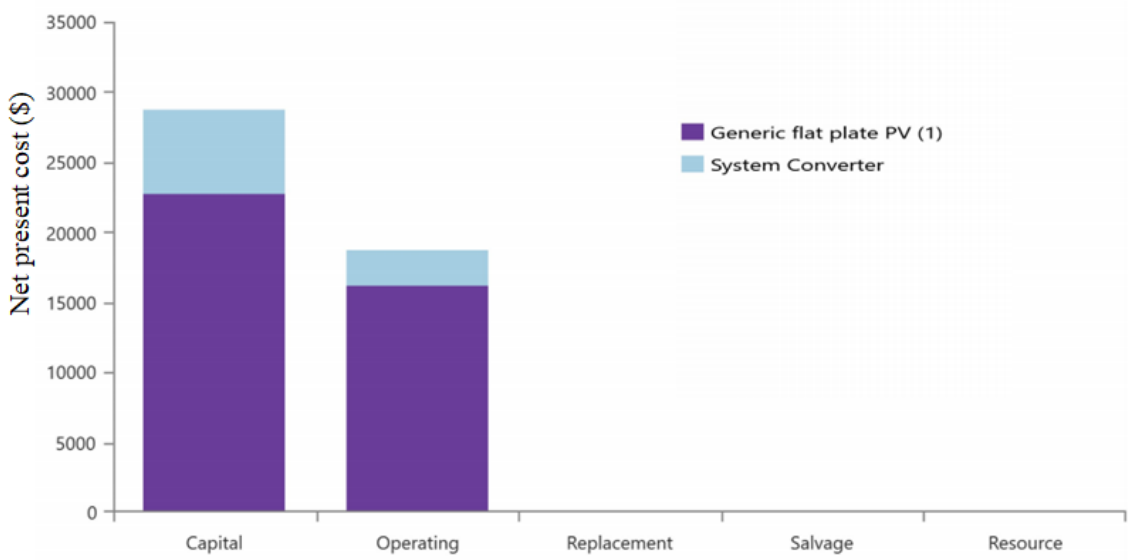


Figure 5. 1:cost summary of PV system alone

Table 5. 1:net present Cost analysis for PV system alone

| Component | Capital ($) | Operating ($) | Fuel ($) | Total ($) |
|---|---|---|---|---|
| PV | 22,750 | 16,159 | 0 | 38,909 |
| Converter | 6,000 | 2,586 | 0 | 8,586 |
| System | 28,750 | 18,745 | 0 | 47,495 |

### 5.1.1.2 Electrical production of PV alone

The Electrical tab offers information regarding the system's electricity output and usage. The total electrical production is the total quantity of electrical energy generated by the power system over the course of a year. It is the total amount of electrical energy produced by all of the system's components. The renewable fraction is the percentage of total energy generation in the system that comes from renewable sources. The renewable percent is calculated by dividing the total yearly renewable power output (the energy produced by the PV array and wind turbines) by overall energy output. Excess electricity is surplus electrical energy that cannot be used to serve a load and must be disposed of. The term "unmet load" refers to an electrical load that the power system is unable to fulfill. It occurs when the demand for electricity surpasses the supply. A capacity deficit happens when there is a gap between the desired operating capacity and the amount of operating capacity

that the system can supply. HOMER maintains track of such shortages and determines the overall quantity that happens over the course of the year.

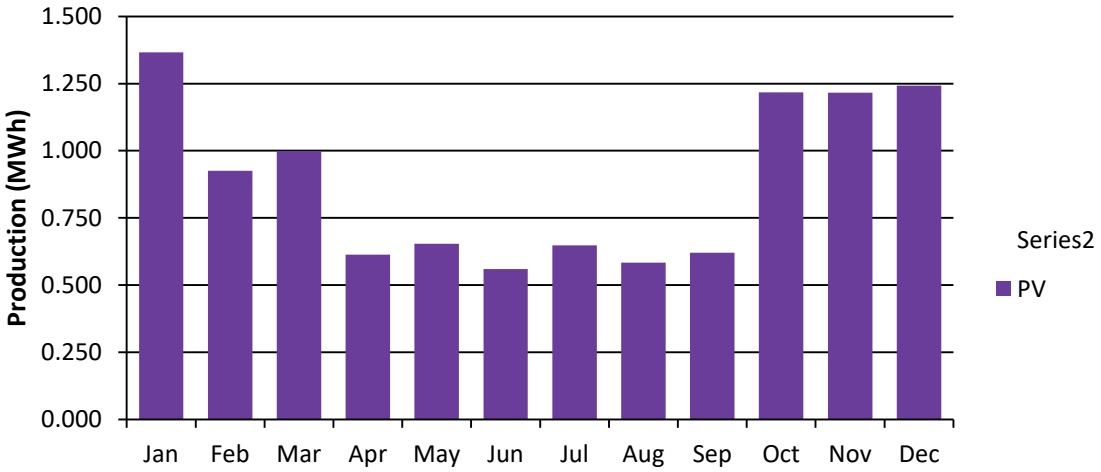


Figure 5. 2:the monthly average electric production of the PV

### 5.1.2 Hybrid wind and solar energy system

The summary of the PV alone and the PV and wind hybridized energy system is given in the following table.

Table 5. 2:the summary of the PV system alone and PV-wind hybrid system

| | PV | xls | Convete r | Tot. NPC capital cost | Total NPC | Tot.ann. cap. Cost | Tot. O.&M. cost | COE | Total fuel cost |
|---|---|---|---|---|---|---|---|---|---|
| No | kW | | kW | $ | $ | $/yr | $ | $/kWh | $/yr |
| 1 | 25 | 0 | 30 | 34,000, | 47,495 | 2,224 | 18,745 | 0.363 | 0 |
| 2 | 10 | 7 | 20 | 93,500 | 111,599 | 7,233 | 18,099 | 0.00978 | 0 |

| PV | xls | Convete r | Tot. ann. cost | Tot.ann Operati ng cost | PV produc tion | Wind produc tion | Tot.electrica production | Deferrabl load served |
|---|---|---|---|---|---|---|---|---|
| kW | | kW | $/yr | $/yr | kWh/yr | kWh/yr | kWh/yr | kWh/yr |
| 25 | 0 | 30 | 3,674 | 1,450 | 21,290 | 0 | 21,290 | 14,603 |
| 10 | 7 | 20 | 8,633 | 1,400 | 26,613 | 24,310 | 50,9232 | 15,731 |

| PV | Xls | Conveter | Cap. Shorta ge | Unmet load | Excess electrici ty | Co2 emiss ions | Co, Nox, Pm and So2 Emissions | UHC emissions |
|---|---|---|---|---|---|---|---|---|
| kW | | kW | kWh/yr | kWh/yr | kWh/yr | Kg/yr | Kg/yr | Kg/yr |
| 25 | 0 | 30 | 1,112 | 1,112 | 5,919 | 0 | 0 | 0 |
| 10 | 7 | 20 | 0 | 0 | 34,863 | 0 | 0 | 0 |

The third alternative, wind turbine power generation alone, is not possible for this system and was ignored by the program. Because wind turbines are more cost-effective when they are huge, and because the site is inconvenient, we cannot choose a large one.

### 5.2 Examine sensitivity analysis

In graphs and tables, HOMER presents sensitivity results. This section explains how to see and understand the sensitive data to determine if a solar and wind system is more cost-effective than a solar system alone or a wind turbine system alone under specific conditions.

1. To begin the simulation, click Calculate. The progress indicator displays how much time is left until the simulation and optimization procedure is finished.
2. To view the table of sorted system designs, navigate to the Optimization Results page and choose Categorized.
3. To view the table of sorted system designs, go to the Sensitivity Results page and click Graphic. Make or confirm the following choices of Sensitivity variable:
    I. Deferrable load (kWh/d)=x-axis, global solar (kWh/$m^2$/d) = y-axis, and wind speed (m/s) = 2.6,3.1, 3.5, 4, 4.6
    II. Under Variables to plot, select Optimal System Type in the Primary list. Select <none> in the superimposed list.

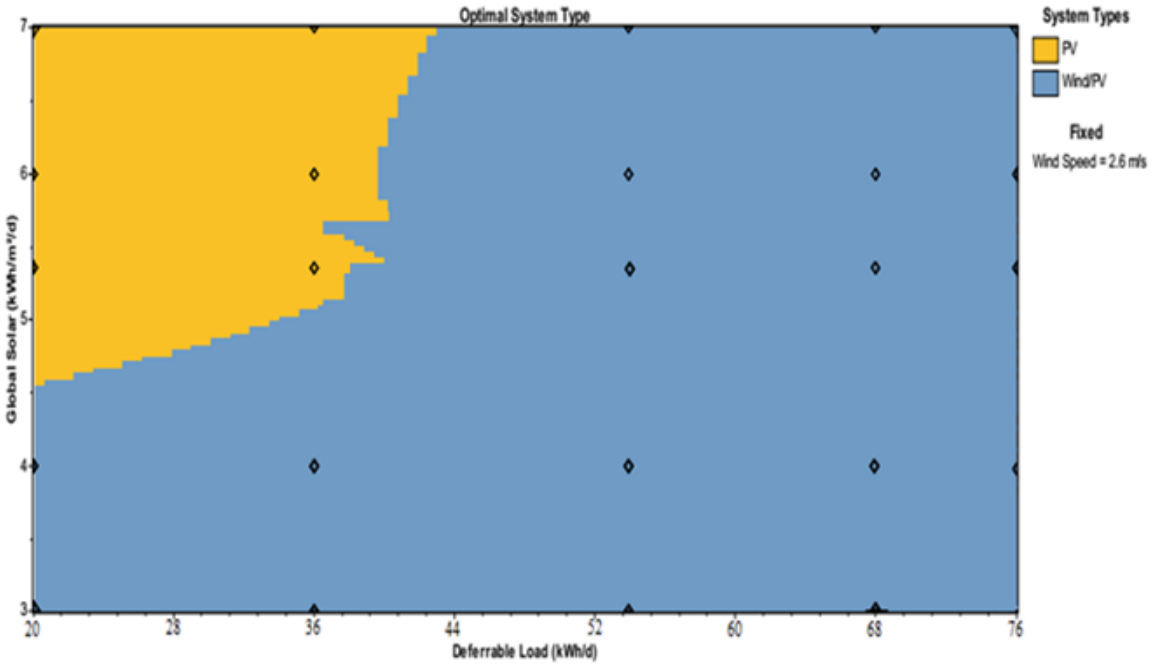


Figure 5. 3:shows the optimal system type as the demand and global solar radiation increase

According to this graph, when the deferrable load increases, employing PV or wind turbine alone is not suggested; rather, a hybrid of solar and wind turbine system is preferred.

The leading one is the hybridized solar and wind energy system, when we click on the optimization results and examine the details:

### 5.2.1 Cost summary

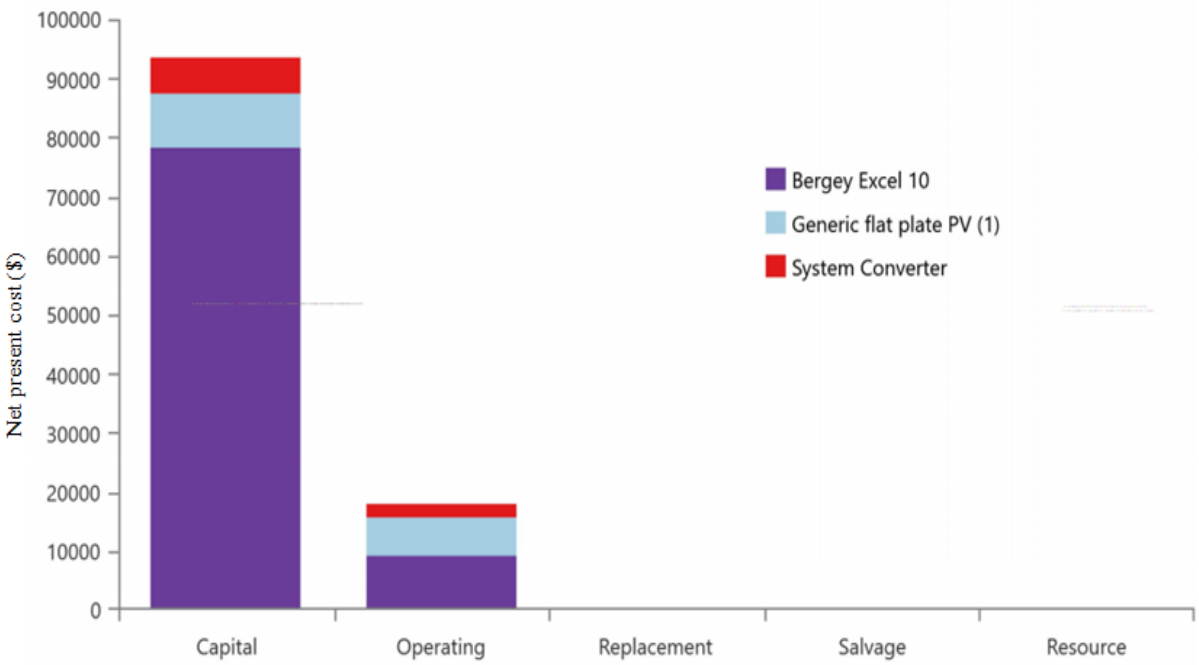


Figure 5. 4:cost summary of hybrid solar and wind energy system alone

Table 5. 3:shows the summary of the NPC of hybridized solar and wind energy

| Component | Capital ($) | Operating ($) | Fuel ($) | Total ($) |
|---|---|---|---|---|
| PV | 9,100 | 6,464 | 0 | 87,449 |
| BWC Excel-S | 78,400 | 9,049 | 0 | 15,564 |
| Converter | 6,000 | 2,586 | 0 | 8,8586 |
| System | 93,500 | 18,099 | 0 | 111,599 |

Table 5. 4:annualized Costs of hybrid solar and wind energy system

| Component | Capital ($) | Operating ($) | Fuel ($) | Total ($) |
|---|---|---|---|---|
| PV | 703.92 | 700 | 0 | 1,204 |
| BWC Excel-S | 6,065 | 500 | 0 | 6,765 |
| Converter | 464.13 | 200 | 0 | 664.13 |
| System | 7,233 | 1,400 | 0 | 8,633 |

### 5.2.2 Electrical production summary

Table 5. 5:shows the % of the PV and wind turbine for the productions and consumptions of the deferrable load

| Production | kWh/yr | % |
|---|---|---|
| PV array | 26,613 | 52.3 |
| Wind turbine | 24,310 | 47.7 |
| Total | 50,923 | 100 |

| Consumption | Consumption kWh/yr | % |
|---|---|---|
| Deferrable load | 15,731 | 100 |
| Total | 15,731 | 100 |

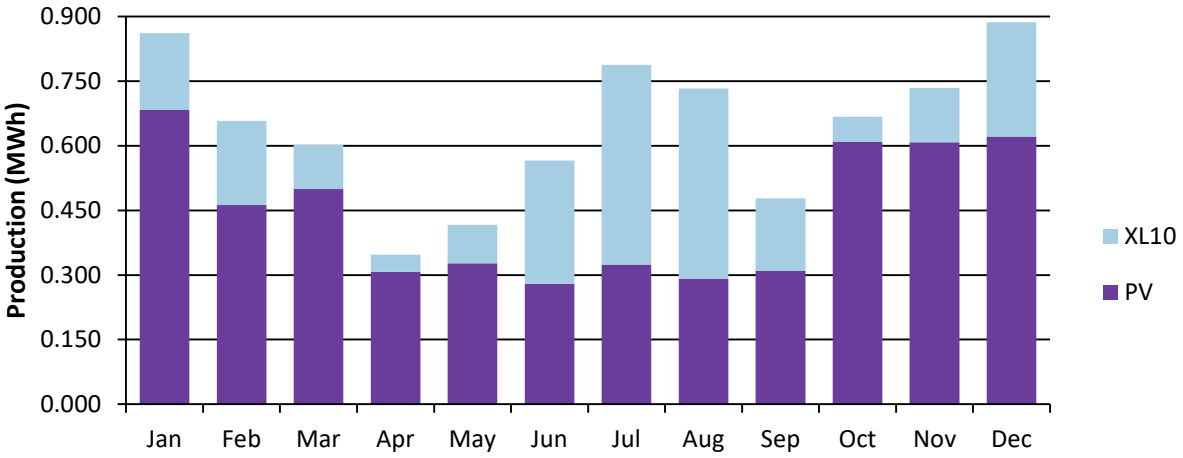


Figure 5. 5:shows the monthly average electric production of the system

### 5.2.2.1 PV system electrical production

Table 5. 6:shows the property of the selected PV

| Quantity | Value | Units |
|---|---|---|
| Rated capacity | 10 | kW |
| Mean output | 3.04 | kW |
| Mean output | 72.9 | kWh/d |
| Capacity factor | 12.2 | % |
| Total production | 26,613 | kWh/yr |
| Minimum output | 0 | kW |
| Maximum output | 24.3 | kW |
| PV penetration | 0 | % |
| Hours of operation | 4,452 | hrs/yr |
| Levelized cost | 0.00982 | $/kWh |

#### 5.2.2.2 Wind turbine: BWC Excel-s electrical production

Table 5. 7:shows the property of the selected wind turbine

| Quantity | Value | Units |
|---|---|---|
| Minimum output | 0 | kW |
| Maximum output | 64.2 | kW |
| Wind penetration | 0 | % |
| Hours of operation | 6,393 | hrs/yr |
| Levelized cost | 0.0197 | $/kWh |
| Total rated capacity | 70 | kW |
| Mean output | 2.78 | kW |
| Capacity factor | 3.96 | % |
| Total production | 24,310 | kWh/yr |

#### 5.2.2.3 Converter

Table 5. 8:shows the property of the Converter selected

| Quantity | Value | Units |
|---|---|---|
| Capacity | 20 | kW |
| Mean output | 0.714 | kW |
| Minimum output | 0 | kW |
| Maximum output | 7.56 | kW |
| Capacity factor | 2.38 | % |
| Hours of operation | 2,758 | hrs/yr |
| Energy in | 6,581 | kWh/yr |
| Energy out | 6,252 | kWh/yr |
| Losses | 329 | kWh/yr |

#### 5.2.2.4 Emission

Table 5. 9:shows the Emission from the systems

| Pollutant | Emission (kg/yr) |
|---|---|
| Carbon monoxide | 0 |
| Unburned hydrocarbons | 0 |
| Particulate matter | 0 |
| Sulfur dioxide | 0 |
| Nitrogen oxides | 0 |

# CHAPTER 6

# CONCLUSION AND RECCOMENDATION

## 6.1 Conclusions

This thesis suggests that the seasonal problem of potato irrigation water in Samira village, which is located in the East Arsi Zone, may be easily solved by pumping water from the Teji River utilizing wind and solar energy hybridized systems. The suggested system's economic assessment is explored using economic optimization. It has also been demonstrated that the proposed system can produce an average daily water demand of 68$m^3$ of water per day for potatoes at an energy cost of $0.00978/kWh over a 20-year period and a total cost for the installation, operation and maintenance of the system is $10,627.4 + $111,598.50= $122,225.90.

In general, the hybrid energy system simulation is as follows:

- 10kW PV
- 7 BWC Excel-s
- 20 kW converter
- Total NPC is: $111,598.50
- Levelized COE: $0.00978/kWh

From the sensitivity analysis in figure (6.3) as the deferrable load increases, the practicality of the system shifts to the wind and solar energy hybridized system rather than the PV system or wind turbine alone. As the need for power grows, a hybrid system is preferred. Because power from solar or wind turbines is seasonal, we may not acquire enough electricity and will incur additional costs for the power storage system. As a result, the wind and solar energy hybridized water pumping system will reduce this extra cost while providing nearly constant power production.

## 6.2 Recommendation and Future work

This study offers a technical, economic, and environmental analysis of the performance of solar and wind energy hybridized water pumping system for irrigation of a potato field in Munessa woreda, especially at Samira village. The research gives a solid knowledge and motivation for using solar and wind energy hybridized technologies for potato irrigation

for the station. More work must be completed in order to get a better operating state for the system. The following works will be specifically set:

- To reduce water consumption and system costs, suitable drip irrigation should be designed;
- Investigate the impacts of a wind and solar energy hybridized system for irrigation on the local water balance in order to resolve the contentious issue of over-exploitation of water resources.
- Take into account the implications of various potato species on system design, economy, and water resources.
- Because wind and solar combined energy output are in excess, future works will utilize this energy for a variety of purposes, notably during non-irrigation seasons.

# REFERENCES


| *FAO | food and agriculture organization of the united nations*. (2012, December 31). Google. http://www.fao.org/news/archive/news-by-date/2012/en/

AIMS POWER. (2020). *Converters*. Aimscorp. https://www.aimscorp.net/AC-to-DC-Converters/

Aized, T., Sohail Rehman, S. M., Kamran, S., Kazim, A. H., & Ubaid Ur Rehman, S. (2019). Design and analysis of wind pump for wind conditions in Pakistan. *Advances in Mechanical Engineering*, *11*(9), 168781401988040. https://doi.org/10.1177/1687814019880405

Aldjia, L., Mohamed, K., Djalloul, A., & Chaib, A. (2017). Energy management and control of a hybrid water pumping system with storage. *Applied Solar Energy*, *53*(2), 190–198. https://doi.org/10.3103/s0003701x17020025

Allouhi, A., Buker, M., El-houari, H., Boharb, A., Benzakour Amine, M., Kousksou, T., & Jamil, A. (2019). PV water pumping systems for domestic uses in remote areas: Sizing process, simulation and economic evaluation. *Renewable Energy*, *132*, 798–812. https://doi.org/10.1016/j.renene.2018.08.019

Assefa, D. (2010, November). *Assessment of feasibility of wind pumping for village water supply and irrigation in ethiopia*. Addis Ababa University.

Baker, R. C. (2016). *Flow measurement handbook: Industrial designs, operating principles, performance, and applications* (2nd ed.). Cambridge University Press.

Benghanem, M., Daffallah, K., Alamri, S., & Joraid, A. (2014). Effect of pumping head on solar water pumping system. *Energy Conversion and Management*, *77*, 334–339. https://doi.org/10.1016/j.enconman.2013.09.043

Bond, E. A. (2013). *Report on the measurement of the volume of streams and the flow of water in the state of new york*. Book on Demand Ltd.

Bonsa, M. (2013, June). *Feasibility study for replacement of diesel water pumping system with PV water pumping system (a case of borana zone water supply, ethiopia)*. Addis Ababa university Institute of Technology.

C.B., & M. Heibloem, A. G. (2018, August 22). *CHAPTER 2: CROP WATER NEEDS* [Slides]. FAO Land and Water Development Division. http://www.fao.org/3/s2022e/s2022e02.htm

Chandel, S., Naik, M. N., & Chandel, R. (2017). Review of performance studies of direct coupled photovoltaic water pumping systems and case study. *Renewable and Sustainable Energy Reviews*, *76*, 163–175. https://doi.org/10.1016/j.rser.2017.03.019

*China pv solar panel, pv solar panel manufacturers, suppliers, price | Made-in-China*. (2020). Metallurgy_Mineral_Energy. https://www.made-in-china.com/products-search/hot-china-products/Pv_Solar_Panel.html

Duffie, J. A., Beckman, W. A., & Worek, W. M. (1994). Solar Engineering of Thermal Processes, 2nd ed. *Journal of Solar Energy Engineering*, *116*(1), 67–68. https://doi.org/10.1115/1.2930068

*Franklin electric  Submersible Pump*. (2021). EBay. https://www.ebay.com/itm/313611797322?_trkparms

Girma, M. (2016, June). *Viability of Solar/Wind and hybrid water pumping system for Off-Grid rural areas in ethiopia*. Addis Ababa Institute of Technology (AAIT).

Girma, M., Molina, M., & Assefa, A. (2015). Feasibility study of a wind powered water pumping system for rural Ethiopia. *AIMS Energy*, *3*(4), 851–868. https://doi.org/10.3934/energy.2015.4.851

Gopal, C., Mohanraj, M., Chandramohan, P., & Chandrasekar, P. (2013). Renewable energy source water pumping systems—A literature review. *Renewable and*

*Sustainable Energy Reviews*, *25*, 351–370. https://doi.org/10.1016/j.rser.2013.04.012

G.research: 29Th annual pump, valve & water systems symposium. (2019). *Pump Industry Analyst*, *2019*(1), 2–32. https://doi.org/10.1016/s1359-6128(19)30003-5

Hussein, S. (2019, June). *Analysis and Performance Simulation of Solar Powered Water Pumping System: A Case Study in Jigjiga*. ADDIS ABABA INSTITUTE OF TECHNOLOGY (AAiT).

Jamil, R. (2019). Frictional head loss relation between Hazen-Williams and Darcy-Weisbach equations for various water supply pipe materials. *International Journal of Water*, *13*(4), 333–354. https://doi.org/10.1504/ijw.2019.106047

Kamel, S. (2005). The economics of hybrid power systems for sustainable desert agriculture in Egypt. *Energy*, *30*(8), 1271–1281. https://doi.org/10.1016/j.energy.2004.02.004

Kassaye, K. T., Yilma, W. A., Fisha, M. H., & Haile, D. H. (2020). Yield and Water Use Efficiency of Potato under Alternate Furrows and Deficit Irrigation. *International Journal of Agronomy*, *2020*, 1–11. https://doi.org/10.1155/2020/8869098

Kelley, L. C., Gilbertson, E., Sheikh, A., Eppinger, S. D., & Dubowsky, S. (2010). On the feasibility of solar-powered irrigation. *Renewable and Sustainable Energy Reviews*, *14*(9), 2669–2682. https://doi.org/10.1016/j.rser.2010.07.061

Kifle, M., & Gebretsadikan, T. (2016). Yield and water use efficiency of furrow irrigated potato under regulated deficit irrigation, Atsibi-Wemberta, North Ethiopia. *Agricultural Water Management*, *170*, 133–139. https://doi.org/10.1016/j.agwat.2016.01.003

Kose, F., Aksoy, M., & Ozgoren, M. (2019). Experimental investigation of solar/wind hybrid system for irrigation in Konya, Turkey. *Thermal Science*, *23*(6 Part B), 4129–4139. https://doi.org/10.2298/tsci180515293k

Kumar, A., & Kandpal, T. (2007). Renewable energy technologies for irrigation water pumping in India: A preliminary attempt towards potential estimation. *Energy*, *32*(5), 861–870. https://doi.org/10.1016/j.energy.2006.05.004

Laamari, S., Zghal, W., & Kchaou, H. (1970). Optimization of hybrid system (wind-solar energy) for pumping water. *International Journal of Engineering, Science and Technology*, *7*(2), 11–26. https://doi.org/10.4314/ijest.v7i2.2

Lambert, T., Gilman, P., & Lilienthal, P. (2006). Micropower System Modeling with Homer. *Integration of Alternative Sources of Energy*, 379–418. https://doi.org/10.1002/0471755621.ch15

Locascio, S. J. (2005). Management of Irrigation for Vegetables: Past, Present, and Future. *HortTechnology*, *15*(3), 482–485. https://doi.org/10.21273/horttech.15.3.0482

M. Khattab, N., A. Badr, M., Tawfik El Shenawy, E., Sharawy, H., & S. Shalaby, M. (2020). Economic Analysis of Stand-Alone Hybrid Wind/PV/Diesel Water Pumping System: A Case Study in Egypt. *Modeling, Simulation and Optimization of Wind Farms and Hybrid Systems*. Published. https://doi.org/10.5772/intechopen.89161

Ma, T., Yang, H., Lu, L., & Peng, J. (2014). Technical feasibility study on a standalone hybrid solar-wind system with pumped hydro storage for a remote island in Hong Kong. *Renewable Energy*, *69*, 7–15. https://doi.org/10.1016/j.renene.2014.03.028

Odeh, I., Yohanis, Y., & Norton, B. (2006). Influence of pumping head, insolation and PV array size on PV water pumping system performance. *Solar Energy*, *80*(1), 51–64. https://doi.org/10.1016/j.solener.2005.07.009

Olatomiwa, L., Mekhilef, S., Huda, A., & Ohunakin, O. S. (2015). Economic evaluation of hybrid energy systems for rural electrification in six geo-political zones of Nigeria. *Renewable Energy*, *83*, 435–446. https://doi.org/10.1016/j.renene.2015.04.057

Olorunfemi, I., Fasinmirin, J., & Ojo, A. (2016). Modeling cation exchange capacity and soil water holding capacity from basic soil properties. *EURASIAN JOURNAL OF SOIL SCIENCE (EJSS)*, *5*(4), 266. https://doi.org/10.18393/ejss.2016.4.266-274

Optimization of Hybrid Renewable Energy System Using Homer. (2019). *International Journal of Recent Technology and Engineering*, *8*(2S11), 2542–2550. https://doi.org/10.35940/ijrte.b1301.0982s1119

*Oromia Pipe Factory PLC*. (2019, May 13). Ethiopia Construction. https://ethiopiaconstruction.com/directory/company/oromia-pipe-factory-plc/

*Oromia region administrative map*. (2017, August 15). [Map].

Pereira, L. S., Allen, R. G., Smith, M., & Raes, D. (2015). Crop evapotranspiration estimation with FAO56: Past and future. *Agricultural Water Management*, *147*, 4–20. https://doi.org/10.1016/j.agwat.2014.07.031

*Photovoltaic cell - Energy Education*. (2018, June 25). Energy Education. https://energyeducation.ca/encyclopedia/Photovoltaic_cell

R. G. Allen. (1996). Relating the Hazen-Williams and Darcy-Weisbach Friction Loss Equations for Pressurized Irrigation. *Applied Engineering in Agriculture*, *12*(6), 685–693. https://doi.org/10.13031/2013.25699

Rathod, S. A., & Shah, S. D. (2012). Design Principales And Consideration For Pressurized Irrigation System ---- A Case Study. *Paripex - Indian Journal Of Research*, *2*(3), 137–139. https://doi.org/10.15373/22501991/mar2013/49

Roberts, B. W., & O'Hern, C. W. (1990). Small-scale, low-cost filters for drip irrigation systems. *HortScience*, *25*(9), 1103d–11103. https://doi.org/10.21273/hortsci.25.9.1103d

Rossi Pisa, P., & Bigaran, F. (1990). Irrigation timing by climate: plot and district application for potato. *Acta Horticulturae*, *278*, 789–796. https://doi.org/10.17660/actahortic.1990.278.78

Rue Henripré, W. (2020). *Bergey Excel 10kW Wind turbine*. Wattuneed. https://www.wattuneed.com/en/wind-turbine/1595-10kw-bergey-excel-wind-turbine-230-vac-or-48-vdc-0712971129559.html#/bergey_excel_model-excel_10_48_v_dc

Sba, K. M., Bakelli, Y., Kaabeche, A., & Khenfous, S. (2018). Sizing Of A Hybrid (Photovoltaic/Wind) Pumping Systembased On Metaheuristic Optimization Methods. *2018 International Conference on Wind Energy and Applications in Algeria (ICWEAA)*. Published. https://doi.org/10.1109/icweaa.2018.8605053

Shiroudi, A., Rashidi, R., Gharehpetian, G. B., Mousavifar, S. A., & Akbari Foroud, A. (2012). Case study: Simulation and optimization of photovoltaic-wind-battery hybrid energy system in Taleghan-Iran using homer software. *Journal of Renewable and Sustainable Energy*, *4*(5), 053111. https://doi.org/10.1063/1.4754440

Svarc, J. (2021, July 18). *Most efficient solar panels 2021 — Clean Energy Reviews*. https://www.cleanenergyreviews.info/blog/most-efficient-solar-panels

Swennenhuis, J. S., Smith, M., van Halsema, G. V. H., Maraux, F., Izzi, G., Wahaj, R., & Munoz, G. (2009). *CROPWAT 8.0* [Computer software]. microsoft. http://www.fao.org/land-water/databases-and-software/en/

Tolulope, J. O., Afolabi, A., & I., R. (2020). Impact of small scale irrigation development on farmers' livelihood improvement in ethiopia: A review. *Journal of Resources Development and Management*, 61–72. https://doi.org/10.7176/jrdm/62-02

*Vertical Water Storage Tanks | U.S. Plastic Corp.* (2019). Usplastic. https://www.usplastic.com/catalog/item.aspx?itemid

Vick, B. D., & Neal, B. A. (2012). Analysis of off-grid hybrid wind turbine/solar PV water pumping systems. *Solar Energy*, *86*(5), 1197–1207. https://doi.org/10.1016/j.solener.2012.01.012

Widyan, M. S., Sweidan, T. O., Abuashour, M. I., & Momani, M. A. (2018). Modelling, simulations and operational performance of a stand-alone hybrid wind/PV energy system supplying induction motor for pumping applications. *International Journal of Engineering Systems Modelling and Simulation*, *10*(1), 12. https://doi.org/10.1504/ijesms.2018.10011280

*world bank annual report*. (2015, June). World Bank: https://www.worldbank.org/en/about/annual-report-2015

Zegeye, M., Aman, A., & Tadiwos, T. (2014, September). *Optimal sizing of solar water pumping system for small scale irrigation: Case study of Dangila* (No. 3). International Journal of Renewable and Sustainable Energ. https://doi.org/10.11648/j.ijrse.20140305.13

# APPENDIX

**Appendix A: Schedule 40 PVC Pipe Dimensions and Pressure Rating**

| Nom. Pipe size (In) | O.D. (In) | Average I.D. (In) | Min. wall (in) | Nominal Wt./Ft. | Maximum w.p.psi |
|---|---|---|---|---|---|
| 1/8 | 0.405 | 0.249 | 0.068 | 0.051 | 810 |
| ¼ | 0.540 | 0.344 | 0.088 | 0.086 | 780 |
| 3/8 | 0.675 | 0.473 | 0.091 | 0.115 | 620 |
| ½ | 0.840 | 0.602 | 0.109 | 0.170 | 600 |
| ¾ | 1.050 | 0.804 | 0.113 | 0.226 | 480 |
| 1 | 1.315 | 1.029 | 0.133 | 0.333 | 450 |
| 1-1/4 | 1.660 | 1.360 | 0.140 | 0.450 | 370 |
| 1-1/2 | 1.900 | 1.590 | 0.145 | 0.537 | 330 |
| 2 | 2.375 | 2.047 | 0.154 | 0.720 | 280 |
| 2-1/2 | 2.875 | 2.445 | 0.203 | 1.136 | 300 |
| 3 | 3.500 | 3.042 | 0.216 | 1.488 | 260 |
| 3-1/2 | 4.000 | 3.521 | 0.226 | 1.789 | 240 |
| 4 | 4.500 | 3.998 | 0.237 | 2.118 | 220 |
| 5 | 5.563 | 5.016 | 0.258 | 2.874 | 190 |
| 6 | 6.625 | 6.031 | 0.280 | 3.733 | 180 |
| 8 | 8.625 | 7.942 | 0.322 | 5.619 | 160 |
| 10 | 10.750 | 9.976 | 0.365 | 7.966 | 140 |
| 12 | 12.750 | 11.889 | 0.406 | 10.534 | 130 |

**Appendix B: Friction Factor as a Function of Reynolds Number and Relative Roughness for Round Pipes the Moody Chart**

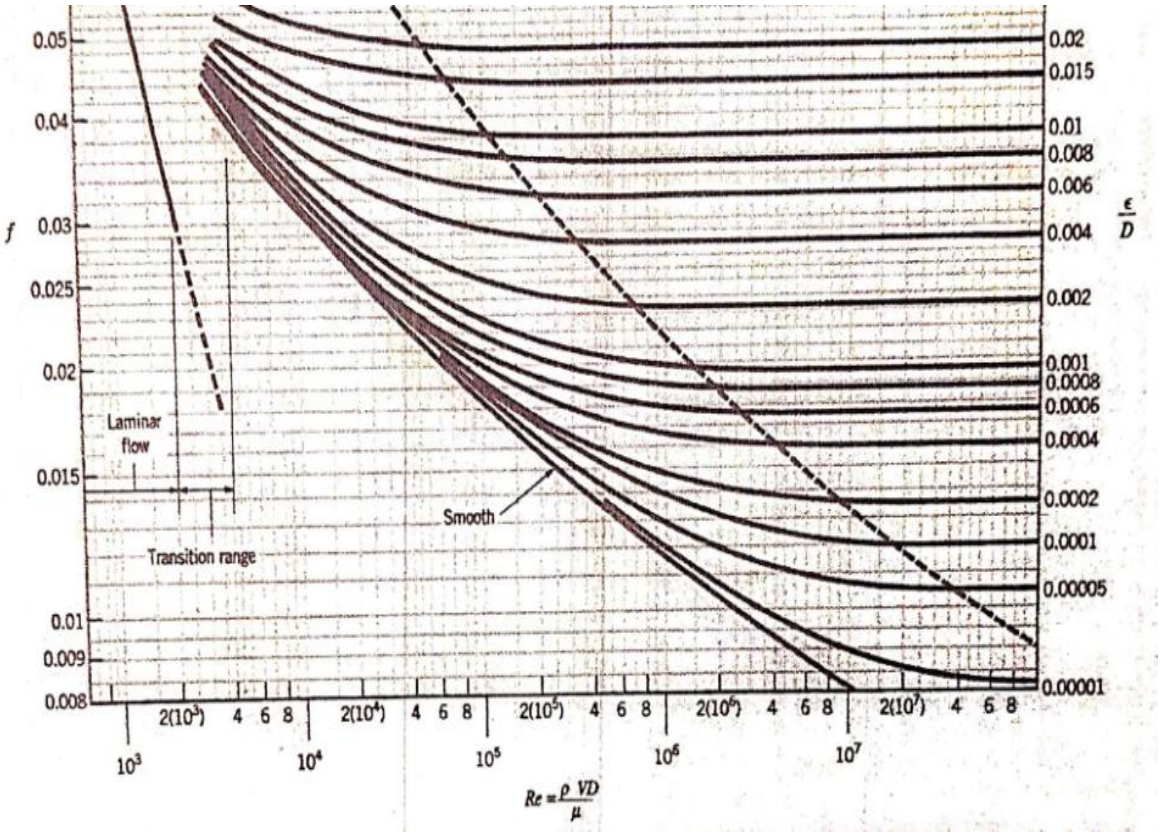

**Appendix C: $K_L$ Values of Different Fittings**

| | | |
|---|---|---|
| Elbows | | |
| Regular $90^0$, flanged | 0.3 | |
| Regular 900, threaded | 1.5 | |
| Long radius $90^0$, flanged | 0.2 | |
| Long radius $90^0$, threaded | 0.7 | |
| Long radius $45^0$, flanged | 0.2 | |
| regular $90^0$, flanged | 0.4 | |
| Valves | | |
| Glob, fully open | 10 | |
| Gate fully open | 0.15 | |
| Check, disk | 10 | |
| Foot, piston | 15 | |
| Foot, disk | 7 | |

## Appendix D: Atmospheric Pressure at Different Altitudes

| Altitude Above Sea Level | | | Temperature | | Barometric Pressure | | Atmospheric Pressure | | |
|---|---|---|---|---|---|---|---|---|---|
| Feet | Miles | Meters | F | C | In. Hg. Abs. | mm Hg. Abs. | PSIA | Kg / sq. cm | kPa A |
| 0 | | 0 | 59 | 15 | 29.92 | 760.0 | 14.696 | 1.0333 | 101.33 |
| 500 | | 153 | 57 | 14 | 29.38 | 746.3 | 14.43 | 1.015 | 99.49 |
| 1000 | | 305 | 55 | 13 | 28.86 | 733.0 | 14.16 | 0.956 | 97.63 |
| 1500 | | 458 | 54 | 12 | 28.33 | 719.6 | 13.91 | 0.978 | 95.91 |
| 2000 | | 610 | 52 | 11 | 27.82 | 706.6 | 13.66 | 0.960 | 94.19 |
| 2500 | | 763 | 50 | 10 | 27.32 | 693.9 | 13.41 | 0.943 | 92.46 |
| 3000 | | 915 | 48 | 9 | 26.82 | 681.2 | 13.17 | 0.926 | 90.81 |
| 3500 | | 1068 | 47 | 8 | 26.33 | 668.8 | 12.93 | 0.909 | 89.15 |
| 4000 | | 1220 | 45 | 7 | 25.84 | 656.3 | 12.69 | 0.892 | 87.49 |
| 4500 | | 1373 | 43 | 6 | 25.37 | 644.4 | 12.46 | 0.876 | 85.91 |
| 5000 | 0.95 | 1526 | 41 | 5 | 24.90 | 632.5 | 12.23 | 0.86 | 84.33 |
| 6000 | 1.1 | 1831 | 38 | 3 | 23.99 | 609.3 | 11.78 | 0.828 | 81.22 |
| 7000 | 1.3 | 2136 | 34 | 1 | 23.10 | 586.7 | 11.34 | 0.797 | 78.19 |
| 8000 | 1.5 | 2441 | 31 | -1 | 22.23 | 564.6 | 10.91 | 0.767 | 75.22 |
| 9000 | 1.7 | 2746 | 27 | -3 | 21.39 | 543.3 | 10.5 | 0.738 | 72.40 |
| 10,000 | 1.9 | 3050 | 23 | -5 | 20.58 | 522.7 | 10.1 | 0.71 | 69.64 |
| 15,000 | 2.8 | 4577 | 6 | -14 | 16.89 | 429.0 | 8.29 | 0.583 | 57.16 |
| 20,000 | 3.8 | 6102 | -12 | -24 | 13.76 | 349.5 | 6.76 | 0.475 | 46.61 |
| 25,000 | 4.7 | 7628 | -30 | -34 | 11.12 | 282.4 | 5.46 | 0.384 | 37.65 |
| 30,000 | 5.7 | 9153 | -48 | -44 | 8.903 | 226.1 | 4.37 | 0.307 | 30.13 |
| 35,000 | 6.6 | 10,679 | -66 | -54 | 7.06 | 179.3 | 3.47 | 0.244 | 23.93 |
| 40,000 | 7.6 | 12,204 | -70 | -57 | 5.558 | 141.2 | 2.73 | 0.192 | 18.82 |
| 45,000 | 8.5 | 13,730 | -70 | -57 | 4.375 | 111.1 | 2.15 | 0.151 | 14.82 |
| 50,000 | 9.5 | 15,255 | -70 | -57 | 3.444 | 87.5 | 1.69 | 0.119 | 11.65 |
| 55,000 | 10.4 | 16,781 | -70 | -57 | 2.712 | 68.9 | 1.33 | 0.0935 | 9.17 |
| 60,000 | 11.4 | 18,306 | -70 | -57 | 2.135 | 54.2 | 1.05 | 0.0738 | 7.24 |
| 70,000 | 13.3 | 21,357 | -67 | -55 | 1.325 | 33.7 | 0.651 | 0.651 | 4.49 |
| 80,000 | 15.2 | 24,408 | -62 | -52 | 0.8273 | 21.0 | 0.406 | 0.406 | 2.80 |
| 90,000 | 17.1 | 27,459 | -57 | -59 | 0.520 | 13.2 | 0.255 | 0.255 | 1.76 |
| 100,000 | 18.9 | 30,510 | -51 | -46 | 0.329 | 8.36 | 0.162 | 0.162 | 1.12 |
| 150,000 | 28.4 | 45720 | | | | 1.10 | $2.1 \times 10^{-3}$ | $1.4 \times 10^{-3}$ | 0.146 |
| 200,000 | 37.9 | 60960 | | | | 0.17 | $3.27 \times 10^{-3}$ | $2.0 \times 10^{-4}$ | $2.2 \times 10^{-2}$ |
| 300,000 | 56.8 | 91440 | | | | $8 \times 10^{-4}$ | $1.47 \times 10^{-5}$ | $1.06 \times 10^{-4}$ | $1.09 \times 10^{-6}$ |
| 500,000 | 94.7 | 152400 | | | | $3.73 \times 10^{-6}$ | $7.22 \times 10^{-8}$ | $5.07 \times 10^{-9}$ | $4.98 \times 10^{-7}$ |
| 2,000,000 | 378.8 | 609600 | | | | $3.6 \times 10^{-9}$ | $7.0 \times 10^{-11}$ | $4.9 \times 10^{-12}$ | $4.8 \times 10^{10}$ |
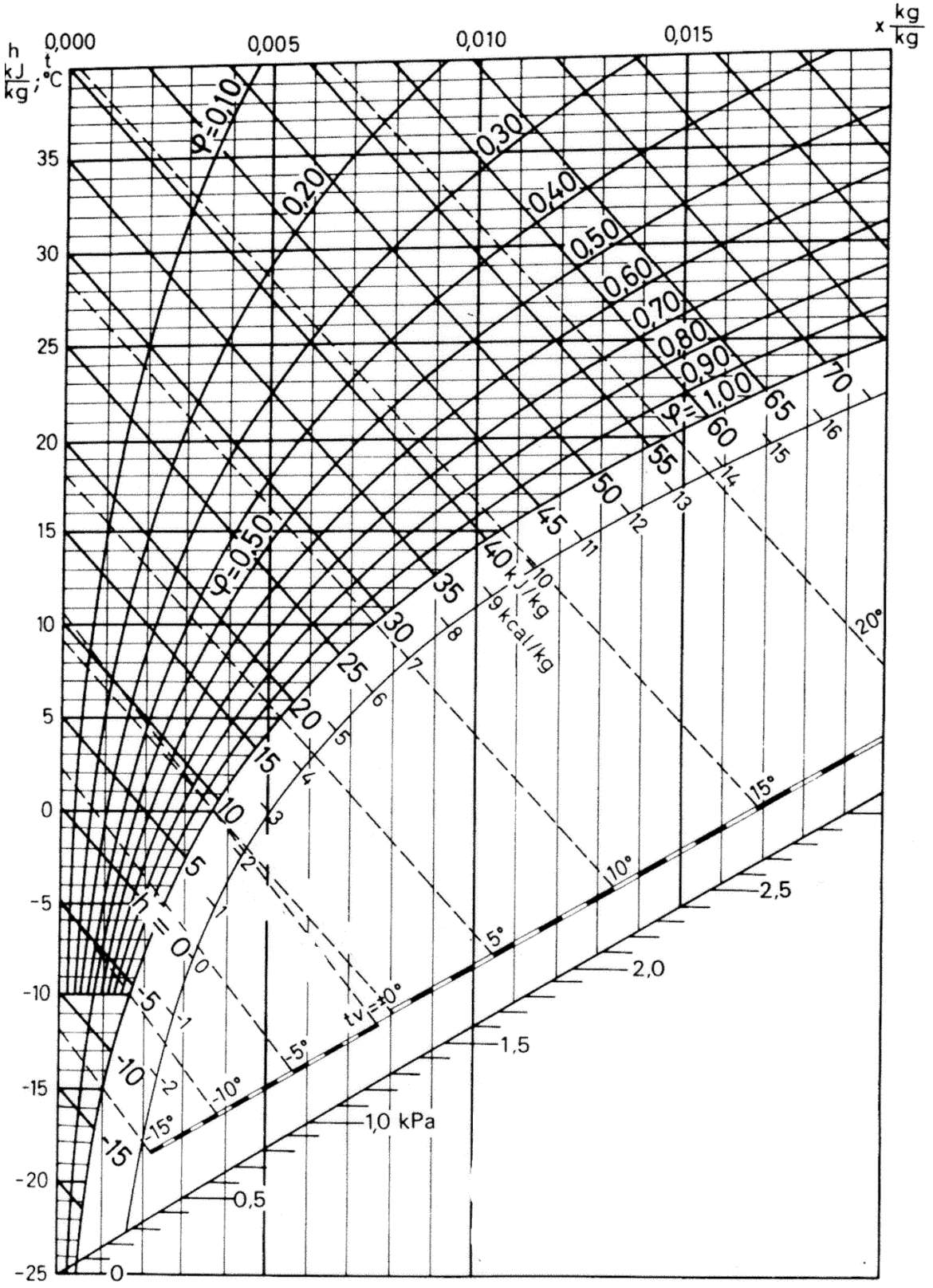
**Appendix E: Mollier Diagram**